ABSTRACT

SAJJADI, SOHEIL SEYYED. Investigating Impact of Sources of Non-recurrent Congestion on Freeway Facilities. (Under direction of Dr. Nagui Rouphail and Dr. Yahya Fathi).

Traffic congestion is a growing problem for the transportation system. From the user perspective, there is an increasing need for reliable travel time. Travel time unreliability is the direct result of the variable and often unpredictable events that occur in the transportation system. Different sources can contribute to travel time variability. Weather and environmental conditions, traffic incidents and work zones are important sources of non-recurrent congestion. The objective of this study is to evaluate the impact of non-recurrent sources of congestion on freeway operations using a fused database approach. Multiple models are evaluated under different operating conditions and recommendations are made based on their goodness of fit to empirical data. The research indicates that inclement weather conditions reduce both freeway capacity and free-flow speed. No evidence of reduction of free flow speed due to incidents was noted. From a traffic stream modeling perspective, the modified Greenshields model provided the best estimate of the freeway traffic stream behavior in almost all the tested conditions. The study recommends estimating free flow speed by fitting the modified Greenshields model and using an empirical threshold approach to estimate freeway capacity. The research findings have been incorporated into existing freeway practice in the Highway Capacity Manual. Finally by applying the recommended traffic stream parameters to an actual freeway facility, the resulting model fit is substantially improved.

. Investigating Impact of Sources of Non-recurrent Congestion on Freeway Facilities

by
Soheil Seyyed Sajjadi

A dissertation submitted to the Graduate Faculty of
North Carolina State University
in partial fulfillment of the
requirements for the degree of
Doctor of Philosophy

Civil Engineering

Raleigh, North Carolina

2013

APPROVED BY:

Dr. Nagui M. Rouphail Committee Co-Chair	Dr. Yahya Fathi Committee Co-Chair
Dr. Billy Williams	Dr. Bastian Schroeder

DEDICATION

This dissertation is dedicated to my parents (Hassan and Parvaneh) for their endless love, devotion, and sacrifice since I was born. Also, I want to express my gratitude to my brothers Sehra, Sahba, and Sepehr and my sister Samira for their encouragement and support in this hard path.

BIOGRAPHY

Soheil Sajjadi was born in Kuwait, Kuwait on March, 27th, 1980. Grow up in Tehran, Iran, and graduated from Alborz High School in 1997. He entered Tehran Polytechnic University in 1998 and received a B.S. Degree in Industrial Textile engineering in 2003. He continued his graduate study in Tehran Polytechnic in Industrial Engineering-System and Efficiency Management and earned a M.S. Degree in this field.

He entered North Carolina State University in Spring 2008 and received his Ph.D. in Transportation Systems (major degree) and Industrial Engineering (minor degree) in 2013. He is the lead developer of freeway facilities analysis computational engines of NCDOT FREEVAL-WZ and FREEVAL-RL.

ACKNOWLEDGMENTS

First and foremost, I want to express my deepest gratitude to my advisor, Dr. Nagui Rouphail for the invaluable lessons in life and science during past 4 years. He gave me a confidence which I had never experienced before. I will move forward with the knowledge he bestowed upon me.

I would also like to extend a special thank you to Dr. Yahya Fathi for his continuous support and guidance through the preparation of this dissertation. His helping attitude and devotion supported me all the time.

Dr. Bastian Schroeder deserves particular recognition for helping with the structure and the contents of this dissertation. I would also like to thank Dr. Billy Williams for the interesting courses he offered during my Ph.D. program and Dr. John Stone for acquainting me with the transportation science.

I would also like to thank my friends who helped me in preparing this dissertation specially Fatima Bateny and Thomas Chase.

TABLE OF CONTENTS

LIST OF FIGURES

LIST OF TABLES

1. INTRODUCTION

1.1 Background

The Federal Highway Administration (FHWA) notes that about half of system congestion is caused by temporary disruptions, or "non-recurrent" congestion, which takes away parts of the available roadway capacity. The three main causes of nonrecurring congestion are: incidents (25 percent of congestion), work zones (10 percent of congestion), and weather (15 percent of congestion). These effects can have a considerable impact on travel time variability, and therefore directly impact the reliability of the facility. (FHWA, 2012)

In an effort to define and isolate the sources of non-recurrent congestion, the Strategic Highway Research Program (SHRP, 2003) incepted by the US Department of Transportation, considers seven sources of non-recurrent congestion sources that affect day to day travel time variability. These sources are:

1- Traffic Incidents: These events that disrupt the normal flow of traffic include vehicular crashes, breakdowns, and debris in travel lanes as the most common form of incidents. Incidents can occur within one or more travel lanes, or be limited to the shoulder. All incidents impact capacity, as even shoulder incidents distract drivers and change driver behavior to where throughput is reduced.

2- Work Zones: Construction activities on the roadway result in reductions to capacity similar to incidents, but are generally planned and may be scheduled to avoid peak travel periods. Work zone can change the configuration of the facility by reducing the number of lanes, reducing lane widths, reducing available shoulder width and clear

zones, or shift traffic onto temporary pavement or even the opposite direction of travel. These changes have a considerable impact on the capacity of the facility and thus on travel time variability and reliability. Depending on the type and severity of work zones, as well as the level of public information campaigns, work zones may also have significant impacts on traffic demands on the facility, which may offset some of the capacity-reducing effects.

3- Weather: Weather events are a frequent source of non-recurrent traffic congestion, as environmental conditions can change driver behavior and affect traffic flow. Due to reduced visibility and precipitation, drivers will usually lower their speeds and increase headways, which translates to a drop in capacity. Also, rainfall or snow events often result in traffic impacts even after the precipitation has ended due to wet or icy pavement conditions. Clearly, travel demands may be impacted as a function of the severity and level of advanced warning of the weather event.

4- Fluctuations in Demand: Day-to-day variability in demand leads to some days with higher traffic volumes than others. Since the capacity of a typical freeway is roughly fixed, variation in demand can lead to variability in travel time.

5- Special Events: Large scheduled events, like a sporting event or state fair impose a sudden and temporary increase in demand on the transportation system. These events are generally predictable in time and also to some extent to the level of demand increase, but often result in significant disruptions in traffic flow nonetheless.

6- Traffic Control Devices: Disruption in continuous traffic flow by control devices such as railroad grade crossing, drawbridges, and poorly timed signals also can contribute to travel time variability. While traffic signals are often optimized based on an estimate of travel demands, their efficiency is often reduced as a result of fluctuations in demand. Similarly, signal malfunction including faulty traffic detectors result in reductions to the efficiency and capacity of traffic signal systems.

7- Inadequate Base Capacity: According to SHRP documentation "the physical capacity of the roadway does not contribute to travel time variability. However, the interaction of capacity with the six other sources of variability (above) does have an effect on variability. This is due to the nonlinear nature of the relationship between delay, volume, and capacity: when saturation levels are approached, small changes in volume or capacity lead to large changes in delay." (SHRP Final Report, 2003).

The objective of an ongoing national project, SHRP2-L08:"Incorporation of Travel Time Reliability into the HCM", is to determine how data and information on the impacts of different causes of noncurrent congestion (incidents, weather, work zone, special events etc.) can be incorporated into the performance measure estimation procedures contained in the Highway Capacity Manual (HCM 2010). The conceptual framework of the SHRP2-L08 Project is shown in Figure 1 (SHRP2-L08 Draft Final Report, 2012).

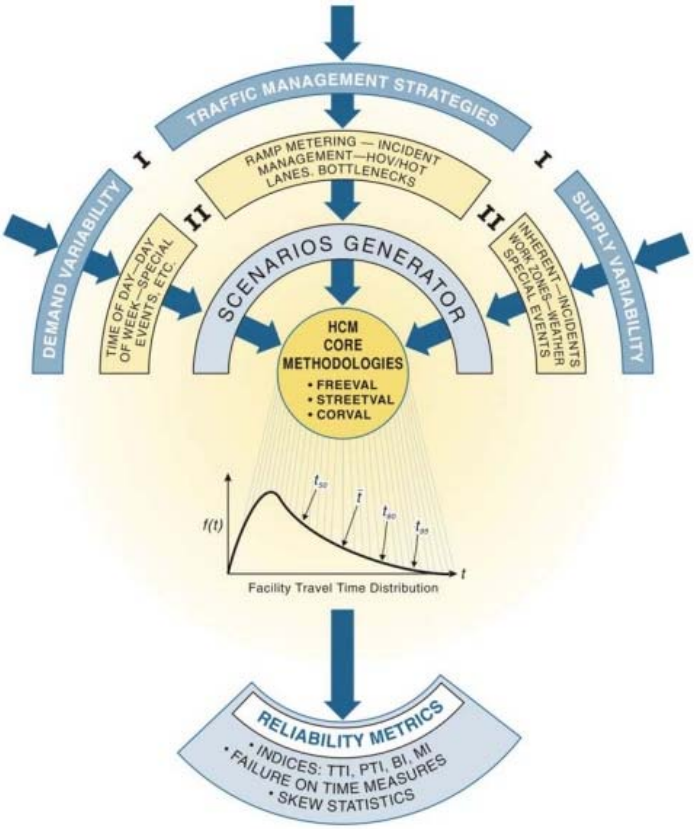

Figure 1 Conceptual Framework of SHRP2-L08 Project (Source: SHRP2 – L08 Proposal Final Draft)

As shown in Figure 1, the goal of the SHRP2-L08 project is to measure travel time reliability and calculate travel time reliability metrics from its distribution. The effect of non-recurrent congestion sources in addition to another freeway condition like demand level creates a unique set of conditions. A unique combination of demand and a non-recurrent congestion sources is defined as a scenario.

1.2 Problem Statement

There is strong evidence in the literature that inclement weather (Rakha, 2006) and incident events (Smith, 2003) impact the operations of a freeway facility significantly. Non-recurrent

congestion sources have varying impacts on different freeway facility, based on the characteristics of the study site. Although, multiple studies have tried to quantify the impact of the inclement weather and incidents on the traffic stream behavior, there is a lack of a rigorous framework which enables researchers to perform site specific analyses. One key challenge in the SHRP2-L08 framework and other reliability projects is to quantify (a) the frequency of non-recurring congestion events for a specific facility, and (b) the net impact of these events on facility operations and capacity. The analytical framework should thus possess clear and consistent methods to analyze the impact of multiple congestion sources on the freeway facility operations, as well as estimate the frequency of occurrence of different categories of non-recurring congestion.

For this purpose, this dissertation introduces a fused database approach and analysis framework to analyze the impact of the non-recurrent congestion sources. The framework enables researchers to isolate, assess and model the impact of different congestion sources, and provides a better understanding of impact on the transportation system.

1.3 Objectives and Tasks

The main objectives of this research are as follows:

1. Evaluate the operational impacts of non-recurring sources of congestion on freeway operations.
2. Develop or enhance predictive models and tools for estimating freeway performance based on the non-recurrent congestion source impact.

3. Enhance the existing freeway facilities practice with research findings and recommendations.

In order to fulfill the research objectives, a series of research tasks have been completed:

I. Use a fused database approach that considers the interaction between different non-recurrent congestion sources. The fused database approach provides categorized datasets which represent a unique condition of weather and incident status. The fused database approach should provide a robust platform to analyze the impact of various congestion sources on the freeway facility.

II. Select multiple predictive models and evaluate the predictive power of each model by testing models on datasets, which have been generated by the fused database approach.

III. Recommend ways to incorporate findings and models into existing freeway analysis practice (HCM).

IV. Demonstrate the implications of the enhanced existing practice for a real world case study. The enhanced model will be tested against a real world example. This task verifies that the enhanced model provides a better prediction of the freeway operation compared to the existing practice.

1.4 Organization

The dissertation manuscript is presented in eight chapters. Chapter 2 provides an extensive literature review covering previous research about the impact of non-recurring congestion sources such as inclement weather and incidents on the traffic stream behavior and other

related materials. Chapter 3 describes the research methodology and the database development process. Chapter 4 presents the modeling steps and results. Chapter 5 demonstrates the data analysis on the fused database. Chapter 6 proposes implementation of the results into the existing freeway facilities methods in the HCM 2010. Chapter 7 summarizes the research findings and provides future recommendations for additional research. References used in this study are presented in Chapter 8. Two appendices to the document provide additional details. Appendix A gives the software code developed in this dissertation and used for the database fusion task. Appendix B provides supplementary information on the study sites and more detail about the data collection efforts.

2. LITERATURE REVIEW

2.1 Overview

This chapter synthesizes previous research efforts. First, an overview of the HCM 2010 methodology is provided. In the following, past studies of the impact of weather, incidents, and work zones on the freeway traffic stream behavior is provided. At the end, research efforts which certify the drop of the capacity during the queue discharge mode are presented.

2.2 Existing HCM 2010 Methodology

This section discusses in detail how current HCM 2010 methodology can be applied to the analysis of non-recurrent congestion sources of weather, incidents, and work zones. This objective is fulfilled by looking at three important traffic stream components as follow:

1- Free Flow Speed (FFS)

2- Base Capacity and Capacity Adjustment Factor (CAF)

3- Speed-Flow Relationship

2.2.1 Free Flow Speed Estimation

HCM 2010 defines Free-Flow Speed (FFS) as "the theoretical speed when the density and flow rate of the study segment are both zero." It indicates that FFS on the freeway is expected to prevail at flow rates between 0 and 1,000 passenger cars per hour per lane (pc/h/ln). HCM 2010 notes that the FFS of the basic freeway segment is sensitive to three variables: lane width, lateral clearance, and total ramp density.

The following equation (*HCM 2010 Equation 10-1)* is used to estimate a basic segment FFS.

$$\boldsymbol{FFS = 75.4 - f_{LW} - f_{LC} - 3.22\, TRD^{\,0.84}} \quad (1)$$

Where,

FFS = free-flow speed

f_{LW} = adjustment for lane width (mi/h),

f_{LC} = adjustment for lateral clearance (mi/h), and

TRD = total ramp density (ramps/mi)

The FFS is an important characteristic for a freeway facility, as the base capacity, service flow rate, service volume, and daily service volumes all depend upon the FFS.

2.2.2 Capacity Estimation

One approach to define capacity of a directional freeway facility is to define it as "the minimum of the capacities of its component segments." This is a straightforward definition. However, HCM 2010 methodology indicates that individual segment capacities are not independent of each other. Thus, HCM 2010 provides two more freeway facility definitions as of "capacity of the component segment that breaks down first" and "maximum entering freeway demand flow that can be accommodated without any component segment breaking down." It should be noted that all of the freeway facility capacity options are arbitrary and require an assumption that may not be true.

Considering all the above definitions, HCM 2010 finalizes freeway facility capacity as "the capacity of the critical segment among those segments comprising the defined capacity. This capacity must, for analysis purposes, be compared to the demand flow rate on the critical

segment." The critical segment is defined as "the segment that will breakdown first, given that all traffic, roadway, and control conditions do not change, including the spatial distribution of demand on each component segment."

HCM 2010 method also uses base capacity in traffic stream models. Base capacity represents "the capacity of the facility, assuming that there are no heavy vehicles in the traffic stream and that all drivers are regular users of the segment. The base capacity for all freeway segments is a function of free-flow speed. Base capacity is expressed as flow rate for a 15-minute analysis period in (pc/h). The HCM 2010 base capacity measures can be found in Exhibit 10-5.

2.2.3 Segment Capacity Adjustments Due to Non-recurrent Congestion Sources

HCM 2010 considers capacity reduction in segment capacity due to different conditions. These conditions are as follow:

1- Capacity Reduction Due to Construction/Major Maintenance Operations:

HCM 2010 divides work capacity reductions due to construction activities into short-term work zone lane closure and long-term work zone lane closure. One important criterion for dividing work zone type is the nature of barriers used in work zones. The following equation for determining the adjusted mainline capacity (c_a):

$$\boldsymbol{c_a} = \{[(\mathbf{1,600} + \boldsymbol{I}) \times \boldsymbol{f_{HV}}] \times \boldsymbol{N}\} - \boldsymbol{R} \quad (2)$$

Where,

c_a = adjusted mainline capacity (veh/h);

I = adjustment factor for type, intensity, and proximity of work activity, (pc/h/lnn) (ranges between ±160 pc/h/lnn);

f_{HV} = heavy-vehicle adjustment factor;

N = number of lanes open through the work zone; and

R = manual adjustment for on-ramps (veh/h).

For long term work zones, HCM 2010 uses a table (Exhibit 10-14) to summarize findings of the previous research efforts for work zone capacity estimation. The table categorizes different work zone scenarios based on total number of lanes before the work zone in place and total number of lanes open while construction activities are going on. Some of the studies will be addressed in work zone analysis literature section.

2- Capacity Reduction due to Weather and Environmental Conditions:

Similar to work zone analysis, HCM 2010 uses literature to address the capacity reduction due to weather condition. (Exhibit 10-15) It covers weather conditions such as rain, snow, temperature, wind, and visibility. The impact of weather, for both segment capacity and FFS, is incorporated using CAF in the Equation 25-1. The methodology assumes the basic segment type for all the segments impacted by the inclement weather impact.

3- Capacity Reduction due to Traffic Accidents or Vehicular Breakdowns

Similar to work zone scenarios HCM 2010 uses certain configurations of incidents. Incidents are identified based on the facility number of lanes and number of lanes blocked. (Exhibit 10-17). Similar to weather scenario the impact of the incident on the freeway facility is incorporated using CAF in Equation 25-1.

2.2.4 Applying Capacity Reductions

The effect of capacity reduction can be described by applying appropriate CAF. This adjustment factor is reported in percentage, and is defined as the adjusted capacity divided by the base capacity. For example, if an adjusted capacity equals 1800 (pc/h/ln) while the base capacity at FFS= 75 is 2400 (pc/h/ln), the CAF of 0.75 should be used. The CAF will result in a shifted speed-flow curve that extends from the estimated scenario free-flow speed to the default density at a capacity value of 45 (pc/m/ln). The CAF is applied as shown in the HCM 2010: Equation 25-1:

$$\boldsymbol{S = FFS + \left[1 - e^{\ln\left(FFS+1-\frac{C*CAF}{45}\right)\frac{V_p}{C*CAF}}\right]} \quad (3)$$

Where,

S = segment speed (mi/h),

FFS = segment free-flow speed (mi/h),

C = original segment capacity (pc/h/ln),

CAF = capacity adjustment factor (≤ 1), and

v_p = segment flow rate (pc/h/ln).

As noted before, the accurate estimation of CAF relies heavily on accurate estimation of FFS and capacity. While FFS is usually easy to observe in field data the capacity estimation is challenging task and usually requires that the full speed-flow relationship domain be available.

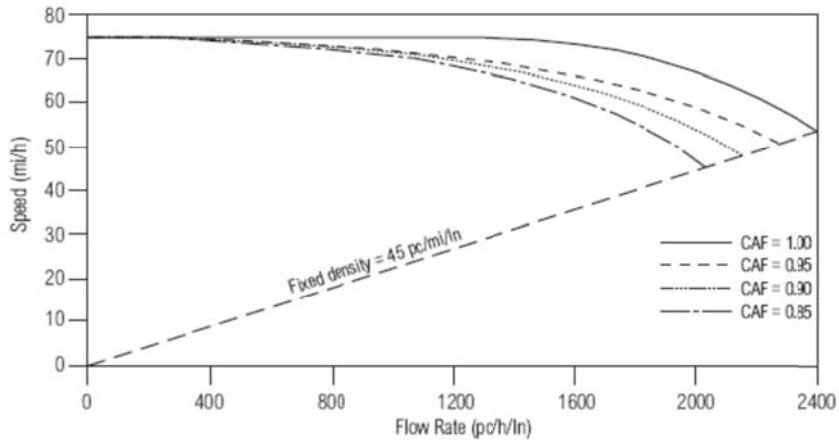

Figure 2 Illustration of Adjusted Speed-Flow Curves for Indicated Capacity Reductions

As a limitation in the HCM 2010 methodology, applying CAF using Equation (3) overwrites all the methodologies of existing HCM 2010 procedures for speed estimation based on the segment type. This may get problematic especially in non-basic segments. The problem arouses as the base capacity of a particular segment is calculated only from FFS. For example, in a typical weaving segment with FFS of 70 mph, the base capacity is assumed to be 2400 (pc/h/ln) and this results in overestimation of the actual segment capacity. Consequently, this may lead to overestimation of the segment speed.

Another drawback of this model is that it is not fully dependent on data. In order to estimate FFS and CAF to develop such speed-flow model, only start and end points of the curve will be estimated from field measurement. Thus, the model is independent from intermediate speed-flow data points.

The advantage of applying this model is that it provides a convenient lever for the analyst to incorporate different sources of capacity and FFS reduction.

2.3 Impact of Weather on Freeway Traffic Stream Behavior

The impact of weather on the traffic operation has been an interesting research area for numerous researchers during past decades.

Hall and Barrow (1988) investigated the effect on the relationship between flow and occupancy on freeways. They analyzed three possible effects on the function relating the two variables they found that capacity and speed reduce due to an inclement weather. The study findings also added that the intensity of the inclement weather condition is a determining factor in capacity and speed reduction. They proposed the following formula:

$flow = b_0 \times occupancy^{b_1}$

Or

$$\ln(\boldsymbol{flow}) = \boldsymbol{a} + \boldsymbol{b_1} \ln(\boldsymbol{occupancy}) \quad (4)$$

Where,

$a = \ln(b_0)$

The study investigated if the difference between different days in particular condition is significant and suggests that the weather type (for example: rain or snow) is more important than the difference in intensity of one weather condition. They tried to fit the model to 367 observations and came with the following model with R^2 = 0.946.

$$\ln(\boldsymbol{flow}) = \mathbf{4.9868} + \mathbf{0.8883} \ln(\boldsymbol{occupancy}) \quad (5)$$

Ibrahim and Hall (1994) conducted a study to monitor the effect of adverse weather conditions on the flow-occupancy and speed-flow relationships. They used regression analysis to select proper models representing the flow-occupancy and speed-flow relationship for uncongested operation. The study noted that the adverse weather conditions reduce the

maximum observed flow rates. They studied if a variation within each weather condition is significant and concluded that the speed-flow relationship is affected by the severity of the weather condition. The study used two terms of “light” and “heavy” for rainy and snowy days. They also added that the snow drastically impacts the speed - flow relationship.

The results of the study suggest that speed reduction is not significant under light rain conditions, but significant reductions happen in heavy rain. The research suggested that the free flow speed drops by 1.7% under light rain condition while for heavy rain the percent drop varies from 4.3% to 8.6%. Similar to light rain, light snow slightly reduces the free flow speed by near 2.5%, while heavy snow results in a 32% to 43% drop in the speed. The study notes that the changes in the free flow speed are statistically significant but they may not be of practical importance because of the high scatter of data. The maximum observed flows were reduced during high precipitation conditions. The research suggests 10% to 20 % maximum observed flow drop for heavy rain condition and 30% to 48% for heavy snow condition. The research also notes that these flows are not capacity flows but they are a good approximation of the capacity.

Rakha et.al. (2008) quantified the impact of inclement weather (precipitation and visibility) on traffic stream behavior and key traffic stream parameters including free-flow speed, speed-at-capacity, capacity, and jam density. The analysis conducted using weather (precipitation and visibility) and loop detector data (speed, flow, and density). The study showed that the snow results in a larger reduction in free-flow speed and capacity compared to rain. Data was collected in three different sites (Baltimore, Twin Cities, and Seattle) in two

different weather conditions of rain and snow. A regression analysis was utilized to build a model that predicts the weather adjustment factor (WAF) for a given precipitation type (rain and snow), intensity level, and visibility level for three key traffic stream parameters. These three key parameters are listed as follows:

1- Free-flow speed (u_f)
2- Speed at Capacity (u_c)
3- Flow at Capacity (q_c)

$$\boldsymbol{WAF = a_1 + a_2\, i + a_3\, i^2 + a_4\, v + a_5\, v^2 + a_6\, iv} \quad (6)$$

Where i is the precipitation intensity (cm/h), v is the visibility level (km), (iv) is the interaction term between precipitation and visibility, and $a_1, a_2, a_3, a_4, a_5,$ and $a_6$are calibrated model coefficients. In all the models the interaction term was found to be insignificant. Using MINITAB software the study developed 14 different models for each site and weather condition.

The study concluded that the traffic jam density is not sensitive to weather condition. Also, as the intensity of the weather condition increases the reduction in free-flow speed and speed at capacity increases similarly. It also notes that snow precipitation results in larger reductions in traffic stream free-flow speed and capacity when compared to rain. Visibility seems to have a larger impact on traffic stream parameters for snow precipitation when compared to rain. There are other research studies available in the literature focusing on the impact of the inclement weather on freeway facilities traffic behavior. A recent literature synthesis by Dowling et. al. (2013) gathered the speed reduction information from different research studies and presented them in a tabular format. Table 1 presents a more

comprehensive edition of the impact on the freeway facilities speed. Similarly, Table 2 demonstrates a summary of previous research efforts of the effect of different weather conditions on freeway capacity. The values in Table 2 correspond to the capacity before the breakdown unless distinguished by an asterisk as Queue Discharge flow.

Table 1 Review of Speed Reductions due to Inclement Weather Condition

Study	Location	Rain			Snow		
		Light	Heavy	Wet Pavement	Light	Heavy	Icy Pavement
Ibrahim and Hall (1994)	Mississauga, Ontario	1.7%	4.3%-8.6%		2.5%	32%-43%	
Rakha et. al (2008)	Baltimore, Minneapolis, Seattle	3-6% * 8-10% **	6-9% * 8-14% **		5-16% * 5-16%**	5-19% *	
Agarwal et.al. (2005)	Minneapolis	1-3% (trace) 5-10%(light)	10-17%		3-5% (trace) 6-11%(light)	7-13%	
Maze et. al. (2006)	Minneapolis	2-4%	6%		8-9%	13%	
Sabier et. al (2008)(a)	Netherlands		10-15%		7%		
Goodwin, L.C. (2002)(a)	N/A	10-25%		30-40%	10-25%		30-40%
Kilplainen & Summala (2007) (a)	Finland			6.7%			
Daniel et. al. (2009)	New Jersey	11-61%			15-50%		
Hernac et. al. (2006) (a)	United States	3%* 9%**			5% **		
Martin et. al. (2000) (a)	Utah (Arterials)	10%		13%	13%		30%

* FFS ** Speed at Capacity (a) Source: (Dowling et. al., 2012)

Table 2 Review of Capacity Reduction due to Inclement Weather Condition

Researches	Location	Rain		Snow	
		Light	Heavy	Light	Heavy
Ibrahim and Hall (1994)	Mississauga, Ontario		10-20%		30-48%
Smith et. al. (2004)		4-10%	25-30%		
Agarwal et. al. (2005)	Minneapolis /St. Paul	1-3%(trace) 5-10%(light)	10-17%	3-5%(trace) 6-11%(light)	7-13% 19-27%
Maze et. al. (2006)	Minneapolis /St. Paul	2-7%	14-15%	5-10%	25-30%
Rakha et. al (2008)	Baltimore, Minneapolis, Seattle	10-11%		12-20%	
Kim et. al. (2010)	Minneapolis	8.1-15.3%		7.8-12.7%	
Dehman (2012)	Milwaukee	2.1-5.4% 11.8%*	12.1%	3.4% 8.8%*	13.2% 22.3*

*Queue Discharge Flow (QDF)

2.4 Impact of Incidents on Freeway Facilities Traffic Stream

Smith and Qin (2003) conducted a study using Hampton Road region of Virginia in the Smart Travel Laboratory which provided a platform to model incident capacity reduction as a random variable. They used speed-flow or density-flow curve for a given highway to estimate capacity. The research focused on estimating accident capacity reductions with one lane and two lanes out of three lanes blocked, and modeled them as random variables based on the traffic flow and accident data. The results demonstrated that accident capacity reduction with one lane out of three lanes blocked can be modeled as Beta distribution with an average of 63 percent, and accident capacity reduction with two lanes out of three lanes blocked can be modeled as Beta distribution with an average of 77 percent.

Masinick and Teng (2004) analyzed the impact of incidents in the opposite direction of travel. An incident in the opposite direction may have a significant impact on the travel direction since drivers in the travel direction tend to slow down and look at the incident. This effect is referred to as "Rubbernecking Effect". From a traffic operations point of view, rubbernecking is a serious issue that can sometimes create traffic congestion and incidents. Figure 3 demonstrates the histogram of percent capacity drop of nearly 80 accidents.

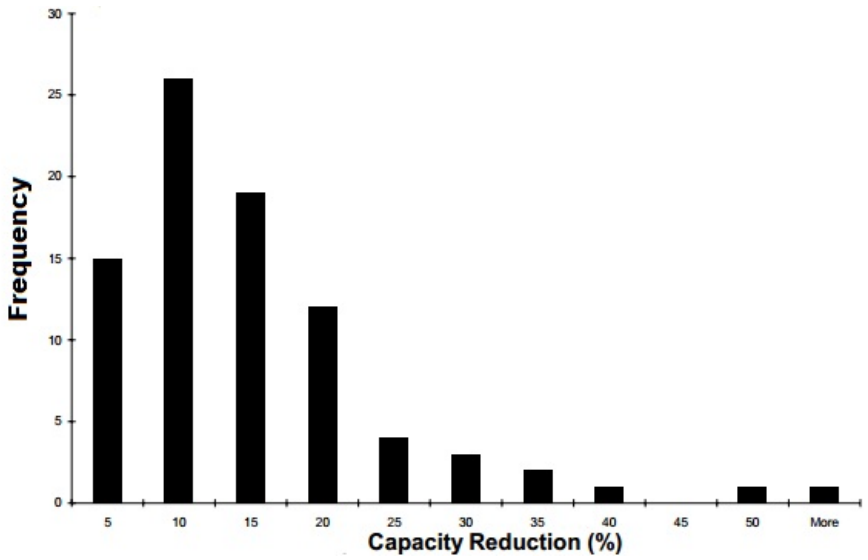

Figure 3 Histogram of Capacity Reduction Percentage as a Result of the Rubbernecking Effect Source: Masinick and Teng (2004).

Brilon et. al. (2007) proposed a stochastic concept for highway capacity analysis. They introduced a methodology for the estimation of the capacity distribution functions from empirical data based on statistical methods. The stochastic approach can be used to model capacity and flow interactions for reliability analysis. The proposed model also accounts for incident impacts on the freeway performance measures. Incidents (crashes and car

breakdowns) are randomly generated based on typical accident and car breakdown rates, respectively. The study used HCM 2000 values for percent capacity reduction in case of incidents.

The proposed method can be used for a variety of practical applications like the economic analysis on road construction projects, the estimation of the share of different congestion causes (high demand, incidents, work zones, and inclement weather conditions) to improve road management strategies or the evaluation of improved incident management.

Knoop et. al. (2008) used a helicopter to gather empirical data on two sites in the Netherlands. The research result showed that although in most analysis the capacity is only reduced in one direction, but the effects in the opposing direction could be of the same order. The HCM 2010 provides a comprehensive source of information for different incident scenarios. The proportion of freeway segment capacity available under each incident condition is presented in Exhibit 10-17.

The SHRP2-L03 project (2010) intended to develop predictive relationships between highway improvements and travel time reliability. As one of the important sources of non-recurrent congestion, the incident impact of delay and travel time was analyzed in 60 sites across the country. Incident data were available from three sources and were used to varying degrees, depending on the team's assessment of data sources for each city's situation which Incident data were available. First, the incident data were available from a private vendor, Traffic.com, for the research. The incident and even data were provided by Traffic.com at no cost from their Traveler Information Management System (TIMS). The TIMS data provided

a standardized source of information for traffic incidents, events, scheduled and unscheduled construction, and other events that could affect traffic conditions. Another important source of information was obtained from Traffic Management Centers (TMC) which includes work zones and special events data.

As part of the research study, the team found that incidents contribute between 1% and 48.2% with the average of 23.9% to total delay. The research team analyzed incidents with crashes separately. The study suggested that crashes contribute between 1.7% to 25.3% to the total delay with the average of 6.0%. They also estimated percent of delay for combinatorial scenarios of rain, incidents, and crashes. The average cumulative contribution of the combinatorial congestion sources was 18.2%.

An important result of the research was the finding that demands (volume) is an extremely important determination of reliability. Demand's interaction with capacity plays an important role in travel time reliability analysis.

The research team also investigated the effects of incidents and crashes on A.M. and P.M. peak periods travel time. The results indicated that non crash incidents increase travel times an average of 17 percent in the morning and 21 percent in the evening on corridors that have mean peak period travel rates over 1.10. However, mean travel time ranges from 9 to 75 percent in the morning. In the evening, travel times change from 6 to 119 percent. If only crashes are considered, the A.M. peak changes range from 14 to 90 percent, with an average of 40 percent while in the P.M. the range is between 9 to 176 percent, with an average of 41 percent.

In recent years with more emphasis on measuring travel time reliability, multiple researches have been conducted assessing the impact of incident on reliability of a travel time in freeway facilities. Kwon et.al. (2011) presented a method for quantifying the contribution of various factors such as traffic incidents, weather, work zones, and special events on the travel time reliability. The study concluded that traffic incidents contribute least during noon, more during AM and most during PM. They also added that a better incident management system can enhance travel time reliability. Also, another study by Tu et. al. in the Netherlands (2008) investigated the impact of traffic accidents on travel time reliability of freeway corridors near Rotterdam City. The study concluded that traffic accidents increase 10th, 50th, and 90th percentile travel times by an average of 3%, 15%, and 75% respectively.

2.5 Two-Capacity Phenomenon

The effect of capacity drop during queue discharge mode has been investigated in multiple past studies. Hall et. al. (1991) performed statistical tests on 20 different observations on the Queen Elizabeth Way in Mississauga to determine the significance of difference between the averages of pre-queue flow rate and queue discharge flow rates. In conclusion, this research suggested that the maximum observed flow rates reduced by 6% after the occurrence of congestion.

Banks' study (1991) showed less than 1% decrease in maximum flow rate. Using results of four case studies of metered bottlenecks in San Diego, the hypothesis was confirmed that maximum flow drops when a freeway breaks down, given the hypothesis applies to the

individual lanes. There was a 3% decrease in the maximum observed flow rate at one site but no significant drop was observed in other three sites.

Cassidy and Bertini's (1999) observations on two freeway segments located in metropolitan Toronto, Canada, showed that there is a significant drop in the capacity after the breakdown. They suggested a capacity drop of 8% and the possibility of a seasonal effect.

There exists more evidence in the literature that capacity drops in the queue discharge mode. Zhang and Levinson (2004) recommend a drop of 5% and similarly Agyemang-Duah (1991) study suggests a capacity drop of 4.3%. Chung et. al. (2007) study proposes a drop in capacity from 3% to 18%.

On the other hand, evidence against the two-capacity phenomenon is presented by Elefteriadou et al. (2003), whose test results showed that the maximum discharge flow could be either higher or lower than the maximum pre-breakdown flow in a research in Florida. The authors utilized the maximum pre and post breakdown flow values, which were not commonly adopted by the other researchers, and which are likely to be less stable than the pre-breakdown capacity or maximum sustainable flow rate.

A recent study by Hu et al. (2012) took a closer look on the impact of two-capacity consideration on the HCM freeway facilities methodology. They averaged the capacity percentage drop proposed by previous researches and suggested an average value of 7.1%. The research used 77 different sites for the average value calculations. The study also designed a sample experiment to account for the capacity drop in queue discharge mode in the HCM 2010 freeway facilities computational engine (FREEVAL). The study showed a

significant increase in travel time per vehicle (over 40%) even with 5% drop in the capacity. Therefore the research team upgraded FREEVAL engine to incorporate various measures of percent capacity drop in the freeway facilities analysis. Table 4 summarizes measurements of percent capacity derived from this study.

Table 3 Capacity Drop Observations from Past Studies

Location	**PBDF (pc/h/ln)**	**QDF**	**% Capacity Drop**
Mississauga Ontario	1917-2223	1967-2104	5.8%
San Diego	2100-2450	2100-2325	0-3%
Toronto	2040-2373	1660-2137	4-10%
Twin City	1772-2332	1895-2386	2-11%
Mississauga	2300	2200	4.3%
San Antonio and San Francisco Bay Area	1778-2079	1798-1934	3.6%
San Diego	2300-2683	2100-2320	5-18%
San Francisco	2035-2178	1930-2013	5.1-8.5%
Toronto	2050-2167	1910-2030	3-12%
London	1775-1920	1575-1750	6.7-10.7%
Average			**7.1%**

Source: Hu et. al. (2012)

3. METHODOLOGY

3.1 Overview

The following chapter lays out the methodology used in this research study for addressing the four main objectives of the study. These objectives are as follow:

1- Evaluate operational impacts of non-recurring sources of congestion on freeway operations using a fused database approach that considers the interaction of different sources of congestion.

2-Develop or enhance predictive models and tools for estimating freeway performance based on these impacts.

3-Recommend ways to incorporate findings and models into existing freeway analysis practice (HCM).

4- Demonstrate implications of the enhanced existing practice for real world case study (I-40 site near Raleigh, N.C.)

First, overall efforts to develop a fused database are summarized. Then different methods for estimating FFS and Capacity are analyzed. The FFS and Capacity estimation methods will be compared and appropriate suggestion will be made based on the observations.

3.2 Database Development

The recent advances in computer hardware technology have led to gigantic data storage devices. This enables researchers to store data in more details and higher quality than before. However, these databases only store data not information nor, in a higher level, knowledge. In order to extract information from databases, some well-defined processes are necessary.

This section aims to show how three main databases can be used to generate a single fused database with summarized yet sufficient information for facility analysis under various weather and incident conditions. These three main databases are traffic, weather, and incident. Another data source used in this research is Google Map and Google Earth ® for supplementary information regarding the sensor locations and facility geometrical information.

3.2.1 Fused Database Development Framework

This section aims to explain the integration process of traffic, weather, and incident databases. The goal of the proposed framework is to classify traffic data points (each 15-min observation) into appropriate weather and incident categories.

In order to provide a relation between different databases a common field should exist in all the databases. In this process, the "Time" field has been selected as the key field between all the databases. In order to provide a unique format between all the databases, the "Time" field has been reported in a uniform format which will be explained in detail later in this section. It should be noted that the time field has the date information embedded too. Following is the algorithm for this classification task:

1- Read traffic *record* (including Time Serial) in traffic database.

2- If no record is left in the traffic database go to Step 8.

3- Query the incident database if there has been an incident at this *record.*

4- If there was an incident in (3) then identify the *Incident Category*.

5- Associate incident information with the current traffic *record*.

6- Query the weather database for this *record* and associate appropriate *Weather Category* to the traffic record.

7- Goto Step 1.

8- End.

The following flowchart depicts the necessary steps to create an updated traffic database from weather and incident databases. (Figure 4)

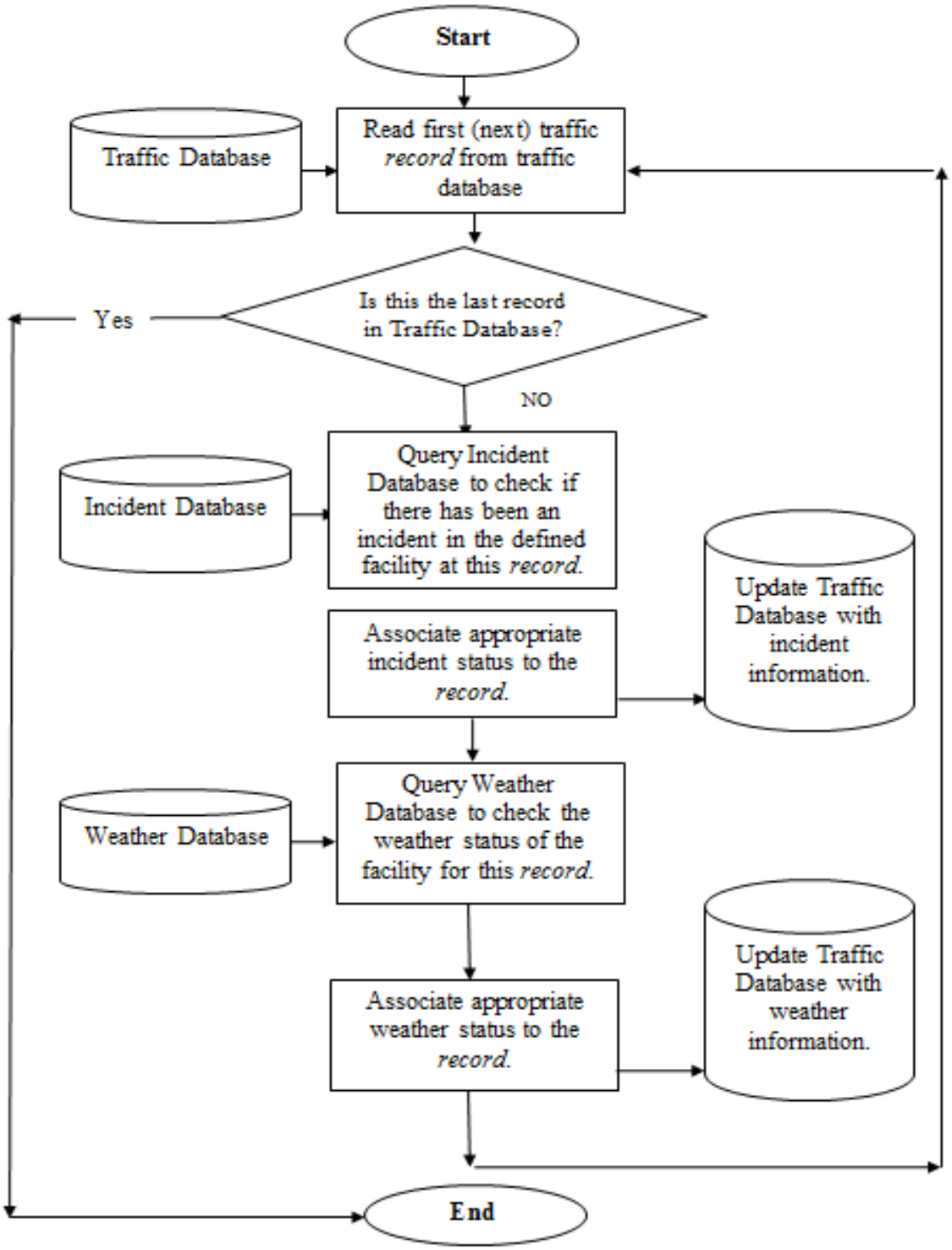

Figure 4 Flowchart for Updating Traffic Database with Weather and Incident Information

The weather category was identified easily. The real challenge was in labeling records (data points or observations) with the appropriate incident category. In this case, if an incident happens at certain times in the study facility, *distance* and *position* of an incident will be associated with the record. For example, a *record* in the traffic database will have two additional fields of *distance to incident (ft.)* and *position = (upstream or downstream).* The threshold of distance affecting a traffic sensor is 1 mile (either upstream or downstream). This distance between a typical incident and the sensor location can be named *effective incident distance.*

In order to run queries on weather and incident databases, two modules were developed. The first module links the weather information and the second module inserts the incident data in the traffic database. These modules can be invoked separately. After running both modules, the traffic database will be updated on weather and incident information. These modules are presented in Appendix A of this manuscript. Also, detailed information about traffic, weather, and incident sources and their respective fields are provided in Appendix B. Appendix B also contains complementary information about the study site and its sensors.

3.2.2 Integrated Database Characteristics

Traffic database has about 50,000 15-min observations which holidays and weekends are excluded. The data are available in both directions. The weather database has about 11,000 observations which the time intervals are not constant. The weather sensors record the weather condition every hour unless there is a change in the weather condition. In case of

immediate change in the weather condition, the weather database records another observation. The incident database has about 500 observations in both directions.

Each recorded incident has a start time and an end time. The location of the incident is also provided in latitude and longitude form. The distance of the incident to the sensor location is calculated using the great circle distance formula. The fused database has the following fields from left to right:

1-Time Serial: is a 10 digit serial number that includes all the time related information. This serial number is decoded as YYMMDDhhmm where it represents year (YY), month (MM), day (DD), hour (hh), and mm (minutes) of a particular observation. For example, a serial number of 1101022300 is interpreted as 15-min observation from 23:00 to 23:15 in January 2nd, 2011.

The challenge of integrating multiple databases is in finding a "Key Field" which is common between different databases. Traffic, weather, and incident data base represent their time of observations in different formats. Therefore, creating a common filed is a critical factor in merging the databases.

2-Date: Date of the observation for example "01/02/2011".

3-Month: month of the observation in two digit format.

4-Day: day of the observation.

5- DOW: day of the week of the observation, for example "Sunday".

6-Hour: hour of the observation

7-Min: minute of the observation

8-Time: time of the observation

9-Direction: traffic direction of the observation for example “South”

10-Volume: in vehicle per hour per lane.

11-Speed: average speed of the vehicles in 15-min time period presented in miles per hour.

12-Occupancy: occupancy percentage of the sensor.

13-Wather Start Time: weather event start time in Time Serial format (explained in item 1)

14-Weather End Time: weather event end time in Time serial format.

15-Percipitation: precipitation level at the time of observation.

16-Weather Type: weather condition at the observation time.

17-Visibility: visibility condition at the time of observation in scale from 0 to 10 in inches.

18-Temprature: temperature at the time of observation.

19-Incident Start Time: incident start time in Time Serial format.

20-Incident End Time: incident end time in Time Serial format.

21-Incident Duration: duration of the incident in text format. For example “2 hour and 7 minutes”

22-Incident Distance to the Sensor: distance in ft. Between the location of the incident and the sensor location using great circle distance formula.

23-Incident Type: type of the incident from the web based database.

24-If Downstream: Boolean value representing the relative location of the incident to the sensor assuming that current analysis direction is North Bound. The value of “True” depicts that the incident is downstream of the sensor when travel in north direction. The value of

“True” in south direction means that the incident is upstream of the sensor. More information regarding this parameter and relative measures is provided in incident analysis section

25- Vehicles Involved: total number of vehicles involved in an incident.

26- Max Number of Lanes Closed: maximum number of closed lanes in an incident.

3.3 FFS and Capacity Estimation Methods

FFS and capacity are two key parameters in the freeway traffic analysis. Using appropriate predictive models to estimate FFS and capacity has been a challenge for freeway engineers in the past. Multiple predictive approaches exist in the literature. This section compares and contrasts multiple approaches for FFS and capacity estimation to identify one recommended method for each.

Generally, there are two different types of methods to estimate FFS and capacity of a freeway facility: 1-Estimate FFS and capacity of fitting entire speed-flow domain and 2-Direct Methods. In the first methods, FFS and capacity values are estimated by fitting a model to the entire speed-flow domain and in the second type of models, direct methods are used to estimate FFS or capacity.

3.4. Fitting Entire Speed-Flow Domain

In this method, a speed-flow model is fitted to the data and the respective FFS and capacity values are estimated using the model parameters.

1- Northwestern Model

2- Van Aerde Model

3- Modified Greenshields Model

4. HCM 2010 Model

Each model is explained and the respective results are shown below:

3.4.1. Northwestern Model

This model was proposed by researchers at Northwestern University. The model is a single regime (S-shaped) statistical model The FFS is estimated by fitting the model to data. The formulation of this equation is provided below.

$$\boldsymbol{u = u_f e^{-\frac{1}{2}\left(k/k_o\right)^2}} \quad (7)$$

Where,
u = speed (mph)
u_f= free flow speed (mph)
k =density (vpmpln)
k_o= optimum density

This formulation requires the knowledge of the free flow speed and optimum density. Also, the speed does not go to zero when density reaches jam density. The model was fitted to each scenario data using a simple non-linear optimization model with the objective function of minimizing total error by changing the model parameters of FFS (u_f) and the jam density (k_o). A simplified non-linear model is as follow:

$$\boldsymbol{min \sum_{i=1}^{i=N} (Y_i^{obs} - Y_i^{pre})^2}$$

$$\textbf{s.t.: } \boldsymbol{K_o, u_f \geq 0}$$

Where,

Y_i^{obs}: Observed speed.
Y_i^{pre}: Predicted speed using the Northwestern model.
N: total number of observations.

3.4.2 Van Aerde and Rakha Model

In this section speed-flow-density model presented by Van Aerde and Rakha (1995) will be used to estimate FFS and capacity. The four-parameter traffic stream model is defined in the following equation:

$$\boldsymbol{k} = \frac{\mathbf{1}}{\boldsymbol{c_1} + \frac{\boldsymbol{c_2}}{\boldsymbol{u_f} - \boldsymbol{u}} + \boldsymbol{c_3 u}} \quad (8)$$

The calibration of the model requires estimating the parameters of c_1, c_2, and c_3. The calculation of these parameters requires estimating four parameters. These parameters include the free flow speed (u_f), the speed-at-capacity (u_c), the capacity (q_c), and the jam density (k_j) demonstrated below:

$$\boldsymbol{c_1} = \frac{\mathbf{1}}{\boldsymbol{k_j}} - \frac{\boldsymbol{c_2}}{\boldsymbol{u_f}} \quad \mathbf{(9)}$$

$$\boldsymbol{c_2} = \frac{\mathbf{1}}{\boldsymbol{k_j}\left(\boldsymbol{m} + \frac{\mathbf{1}}{\boldsymbol{u_f}}\right)} \quad \mathbf{(10)}$$

$$\boldsymbol{c_3} = \frac{-\boldsymbol{c_1} + \frac{\boldsymbol{u_c}}{\boldsymbol{q_c}} - \frac{\boldsymbol{c_2}}{\boldsymbol{u_f} - \boldsymbol{u_c}}}{\boldsymbol{u_c}} \quad \mathbf{(11)}$$

$$\boldsymbol{m} = \frac{\mathbf{2}\boldsymbol{u_c} - \boldsymbol{u_f}}{(\boldsymbol{u_f} - \boldsymbol{u_c})^{\mathbf{2}}} \quad \mathbf{(12)}$$

Where:

c_1: fixed distance headway constant (km).
c_2: first variable distance headway constant (km^2/h).
c_3: second variable distance headway constant (h).
m: is a constant used to solve for the three headway constants (h/km).

Using the basic traffic stream relationship that is shown in Equation (13) and incorporate it in Equation (8), the relationship between the traffic stream flow rate and speed is derived as in Equation (14).

$$\boldsymbol{q = ku} \quad (13)$$

$$\boldsymbol{q = \frac{u}{c_1 + \frac{c_2}{u_f - u} + c_3 u}} \quad (14)$$

The calibration of the Van Aerde model using each scenario was implemented using SPD_CAL software. The SPD_CAL software is an iterative heuristic procedure that was developed by Van Aerde and Rakha (1995) that fits the fundamental speed-flow-density relationship to data. The software uses the Van Aerde functional form. The functional form requires the calibration of four parameters; free-flow speed, speed at capacity, capacity, and jam density. Implementing the software requires that the dataset covers whole speed-flow diagram. In the other words, observations from both under-saturated and over-saturated conditions are available. If the dataset does not meet software minimum requirements, a caution message will inform the user.

3.4.3 Modified Greenshields Model

The dual-regime modified Greenshields model has two regimes of the free-flow and the congested-flow condition.

$$\boldsymbol{v_i = u_f} \qquad \boldsymbol{0 \leq k_i \leq k_{breakpoint}} \text{ (15)}$$

$$\boldsymbol{v_i - v_0 = (v_f - v_0).\left[1 - \frac{k_i}{k_{jam}}\right]^{\alpha}} \qquad \boldsymbol{k_{breakpoint} \leq k_i \leq k_{jam}} \text{ (16)}$$

Where,

v_i = speed on link *i*
v_f = speed-intercept
u_f = free-flow speed on link *i*
v_0= minimum speed on link *i*
k_i= density on link *i*
k_{jam}= jam density on link *i*
α = power term
$k_{breakpoint}$= break point density

This model uses FFS as an estimated speed for data points where the density is less than a certain threshold. In this model the lowest estimated speed is v_0 which is the minimum speed.

$$\boldsymbol{min \sum_{i=1}^{i=N} (Y_i^{obs} - Y_i^{pre})^2}$$

$$\boldsymbol{s.t.: v_i, v_f, u_f, v_0, k_i, k_{jam}, and\ k_{breakpoint} \geq 0}$$

Where,

Y_i^{obs}: Observed speed.
Y_i^{pre}: Predicted speed using the modified Greenshields model.
N: total number of observations.

3.4.4 HCM 2010 Method

The HCM 2010 speed-flow model is a three-regime model. The method uses two-step models presented in Exhibit 11-3 of HCM 2010 for the under-saturated regime. In the over-saturated regime, the method uses a linear relationship between flow and density and estimates the speed using this linear relationship. Figure 5 demonstrates the HCM 2010 two-regime model for under-saturated and over-saturated conditions.

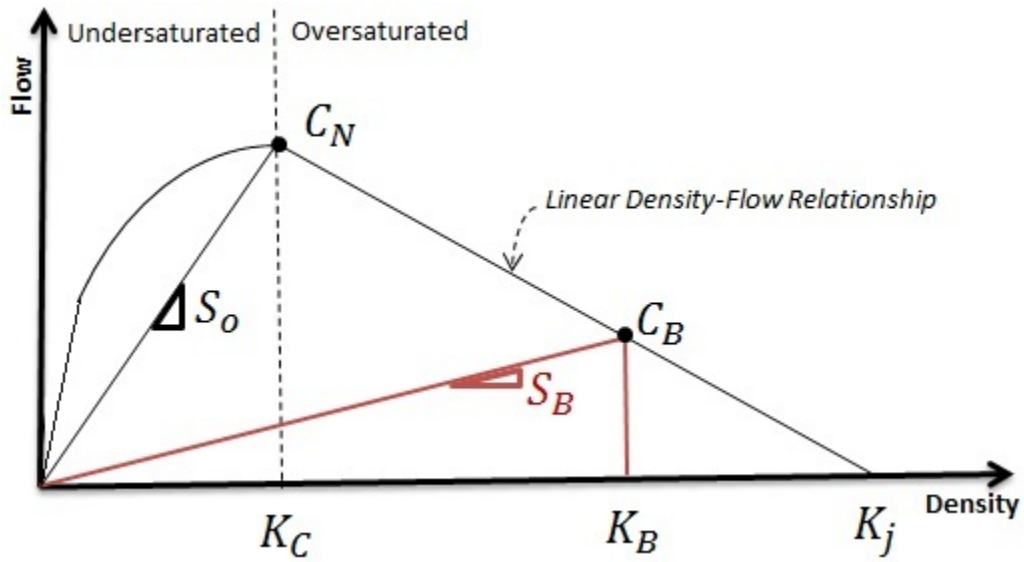

Figure 5 HCM 2010 Three-Regime Speed-Flow Relationship

The following equation is used to calculate speed in the over-saturated regime using linear density-flow relationship in HCM 2010.

$$\boldsymbol{S_B = \frac{S_o C_B}{C_B + S_o K_j (1 - \frac{C_B}{C_N})}} \qquad (17)$$

Where,

S_B: bottleneck speed

S_o: optimum speed (speed at capacity)
C_N: normal capacity
C_B: bottleneck capacity
K_j: jam density

In under-saturated regime one of the model parameters is FFS. This parameter estimates using HCM 2010 status-quo approach which is averaging all the speed observations which their respective flow rate is less than 1000 (pc/h/ln). This approach does not exclude congested observations and considers them in FFS estimation. This is a flaw in this approach since in scenarios where a large portion of the observations is in the congested regime (for example: snow and incidents), implementing this approach will underestimate the actual FFS.

3.5 Direct Methods

Direct methods are methods that do not necessarily require the entire speed-flow domain to be available to estimate FFS or capacity. These methods specifically estimate FFS or capacity and not both. Direct methods take advantage of the empirical threshold approach. The empirical threshold approach can be used for both FFS and capacity estimation. The direct methods are explained in the following:

3.5.1 Estimate FFS using Empirical Thresholds

In this approach thresholds for flow rate and density are considered. Observations are filtered based on the thresholds and the average speeds of observations are represented as FFS.

For volume, a threshold of 500 vph is suggested. The threshold for density is the density value which is a boundary of LOS A and LOS B in the HCM context. Therefore, the adjusted

HCM based, critical density threshold (LOS A/B boundary) is calculated for each scenario dataset. The process of calculating the equivalent density threshold of LOS A and LOS B is presented below:

First, the top 5 percentile minimum flow rate volumes (q) are *identified*. Then for each of the *identified* observations, density is calculated using the following equation:

$$\boldsymbol{k = q/\bar{u}} \quad (18)$$

Where,

k: density for each 15-min observation (veh/mi/lane)
q: 15-min flow rate for top flows as indicated in in (veh/h/lane)

$\bar{u}$: space mean speed (mph)

The equivalent density at capacity based on the HCM definition is calculated in the next step by the following equation:

$$\boldsymbol{k_{capacity} = \frac{1}{n}\sum k} \quad (19)$$

Where n is the number of *identified* 15-min observations in the top portion of the observed volumes. Therefore, the adjusted HCM-based, critical density threshold (LOS A/B boundary) is calculated by:

$$\boldsymbol{k_{A/B} = \frac{11(k_{capacity})}{45}}$$

Where 11 (pc/m/ln) represents the maximum density per lane passenger car equivalent density for LOS B segments, and 45 (pc/m/ln) is the default density at capacity in the HCM

method. The density of a typical observation should be less than $k_{A/B}$ to be considered for FFS estimation. The FFS is estimated using the following equation:

$$\boldsymbol{u_f = (\sum_{i=1}^{N} u_i)/N \quad u_i \, \varepsilon \{(u,k) | \, k \leq k_{A/B}\}} \quad (20)$$

Where,

u_f: free-flow speed
N: number of observations which are legitimate for free-flow speed calculation
(u,k): observation pair of speed and density
$k_{A/B}$: density threshold of LOS A and LOS B

3.5.2 Estimating Capacity Using Empirical Thresholds

Past researchers have used a simple yet appropriate approach to estimate the capacity using observed flow rates. The approach suggests estimating the capacity by averaging the top portion of the observed flow rates considering a certain threshold.

Multiple researchers have used the top first percentile or the top five percentile of the observed flow rates to estimate capacity.

Obviously, using the top five percentile flow rates to estimate capacity may underestimate the actual capacity compared to using the first top percentile but in scenarios with low number of observations, it is better to use the five percent threshold since the top first percentile observations may get limited only to 2,3 observations and this leads to poor capacity estimation.

3.6. Models Goodness of Fit Evaluation

The goodness of fit of each model is evaluated using two parameters of Root Mean Standard Error (RMSE) and R square (R^2). The definitions of these measures of fitness are provided in the following:

$$\boldsymbol{RMSE} = \sqrt{\frac{1}{N}\sum_{n=1}^{N}(Y_n^{obs} - Y_n^{pre})^2} \quad (21)$$

$$\boldsymbol{R^2} = \mathbf{1} - \frac{\sum_1^N (Y_n^{obs} - Y_n^{pre})^2}{\sum_1^N (Y_n^{obs} - \bar{Y})^2} \quad (22)$$

Where,

Y_n^{obs}: nth observed value
Y_n^{pre}: nth predicted value
$\bar{Y}$: average of observations.

Each model will be evaluated for goodness of fit using these two parameters.

3.7 Delay Analysis

In this section a method is used to estimate the incremental delay of different sources of congestion. The delay for each congestion source is estimated using a five step approach explained in the following:

A simple approach was used to estimate the delay for each time period. This approach is presented in the following:

$$\boldsymbol{VHD_i} = \mathbf{Max}(\mathbf{0}, \mathbf{0.25} * (\frac{x_i}{v_i} - \frac{x_i}{FFS}) * \boldsymbol{flow_i}) \quad (23)$$

Where,

FFS**:** free-flow speed (mph)

v_i: average speed at time period *i* (mph)
$\boldsymbol{x_i}$**:** the distance travelled in a time period *I* (mile)
$flow_i$: volume in time period *i* (vph)

Selecting a constant value of 1 mile for x_i, VHD_i equals veh hours of delay in 15-min time interval.

In order to calculate the incremental delay for each scenario the following steps should be taken:

1- Categorize each 15-min observations into different categories based on the congestion source they represent. For example: normal, light rain, and medium rain scenarios.

2- Calculate VHD_i for each 15-min time interval. Sum the values for each scenario and calculate Scenario Average Delay (SAD) for each vehicle by dividing the total calculated scenario delay by total number of observed vehicles in this particular scenario.

$$\boldsymbol{Scenario\ Average\ Delay\ (SAD)_j\ (hour)} = \frac{\sum_1^{n_j} VHD_i}{0.25 \sum_1^{n_j} flow_i} \quad j\ \varepsilon\ \{Scenarios\} \quad (24)$$

Where,

SAD_j: Average scenario delay in 15-minute time interval for scenario *j*
n_j: Total number of observations in scenario *j*

3- In this step, the incremental delay for each scenario is calculated using the following equation:

$$\boldsymbol{Scenario\ Specific\ Average\ Delay(SSAD)_j(hour) = SAD_j - SAD_{normal}} \quad (25)$$

4- The estimated Total Scenario Delay (TSD) is calculated by:

$$\boldsymbol{Total\ Scenario\ Delay_j}\ (hour) = \boldsymbol{SSAD_j \times n_j} \quad (26)$$

5- In the last step, Scenario Delay Contribution (SDC) is calculated in percentage using the following equation:

$$\boldsymbol{Scenario\ Delay\ Contribution_j}(\%) = \frac{\boldsymbol{TSD_j}}{\sum_1^j \boldsymbol{TSD_j}} \times \mathbf{100} \qquad j\ \varepsilon\ \{\ Scenarios\ \} \qquad (27)$$

4. MODELING RESULTS

4.1 Overview

The main objectives of this chapter are as follow:

1- Compare and contrast different models and methods for FFS and capacity estimation and recommend the best approach for each of the parameters.

2- Evaluate prediction power of each model described in the previous chapter on different traffic datasets. The model will be fitted on different datasets which each of them represent a unique combination of weather and incident situation. This unique combination of weather and incident are defined as *Scenario* herein. For example, normal scenario consists of 15-min observations when no incident has been reported and no inclement weather exists on the facility.

Different models have been fitted to five scenarios of: 1-Normal, 2- Light Rain, 3-Medium Rain, 4-Heavy Rain, and 5-Snow. Each scenario is described in the following:

1-Normal Scenario: this scenario consists of 15-min observations when no incident has been reported on the facility and also there are no sign of inclement weather or low visibility condition based on the weather database query. The reported precipitation rate in this scenario equals 0 in/hr. This is the base scenario when the 15-minute observation are free of any impact other than demand variability.

2- Light Rain Scenario: this scenario consists of 15-min observations when no incident has been reported and the reported weather condition is rain. The precipitation rate is greater than

0 and less than or equal to 0.1 inches/hour. This threshold matches the light rain condition in the HCM. Other parameters are similar to the normal condition.

3-Medium Rain: this scenario is similar to the light rain scenario except that the precipitation rate is higher compared to the light rain scenario. The precipitations rate is greater than or equal to 0.1 and less than 0.25 in/hour. This range matches HCM 2010 medium rain condition.

4. Heavy Rain: Similar to light medium rain scenarios, no incident has been reported and the reported weather condition indicates rain condition and the precipitation rate is greater than 0.25 in/hr.

5. Snow: this scenario contains 15-min observations when the weather database indicates that the weather condition is snowy. Also, no incident has been reported in 15-min time period.

In order to evaluate each model in under-saturated and over-saturated conditions in each scenario, the HCM threshold of 45 (pc/m/ln) was selected to bisect each scenario data to under-saturated and over-saturated conditions.

Four models are fitted to entire speed-flow domain as described in the previous chapter. These four models are:

1- Northwestern Model
2- Van Aerde Model
3- Modified Greenshields Model
4- HCM 2010 Model

Also, a couple of direct methods for FFS and capacity estimations are implemented on the data and the results are provided. Each model and method are compared and contrasted to select the best approach for FFS and capacity estimation.

4.2 Fitting Entire Speed-Flow Domain Modeling Results

In this section the result of fitting models on different weather scenario are presented.

4.2.1 Northwestern Model Fitting Result

Single regime statistical model proposed by researchers at Northwestern University was fitted to the data. The following figures demonstrate calibrated Northwestern model on each scenario.

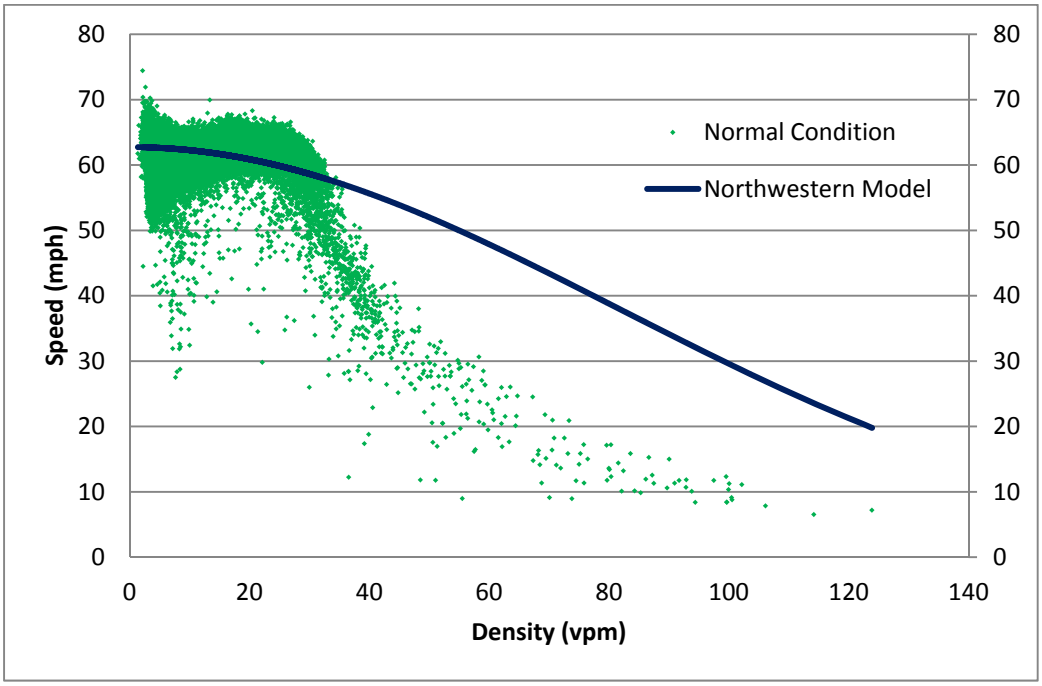

Figure 6 Normal Condition Speed-Density Relationship

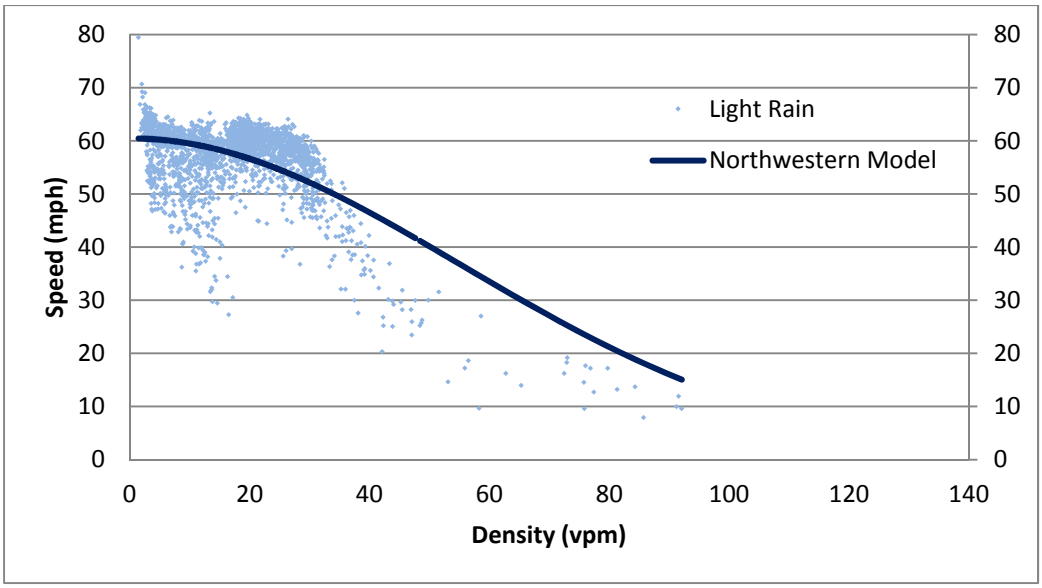

Figure 7 Light Rain Condition Speed-Density Relationship

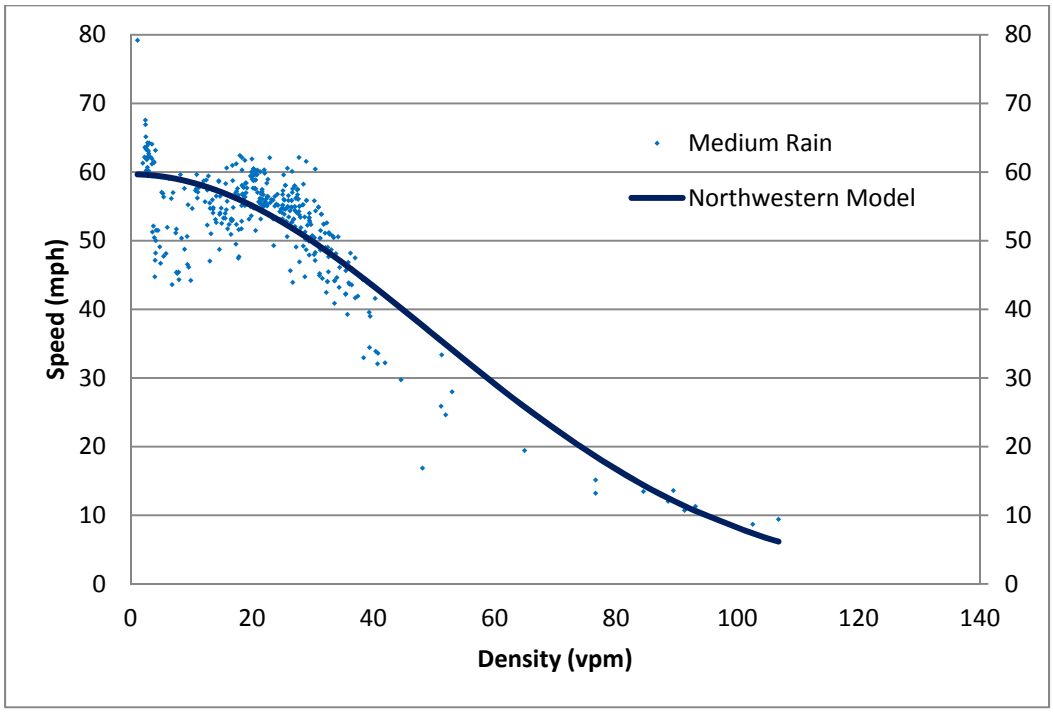

Figure 8 Medium Rain Condition Speed-Density Relationship

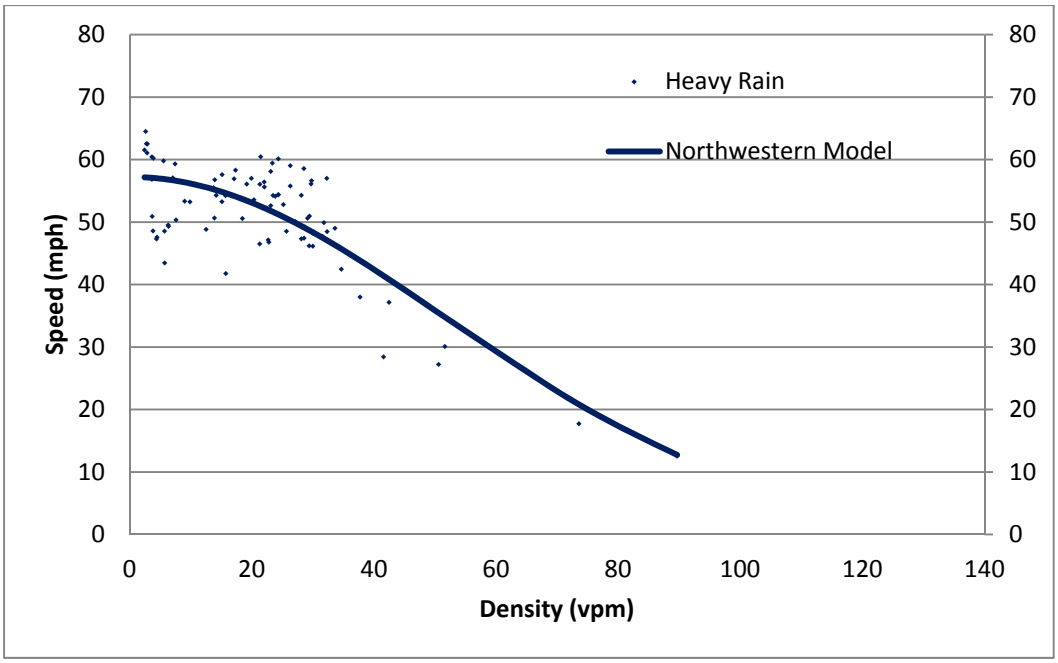

Figure 9 Heavy Rain Condition Speed-Density Relationship

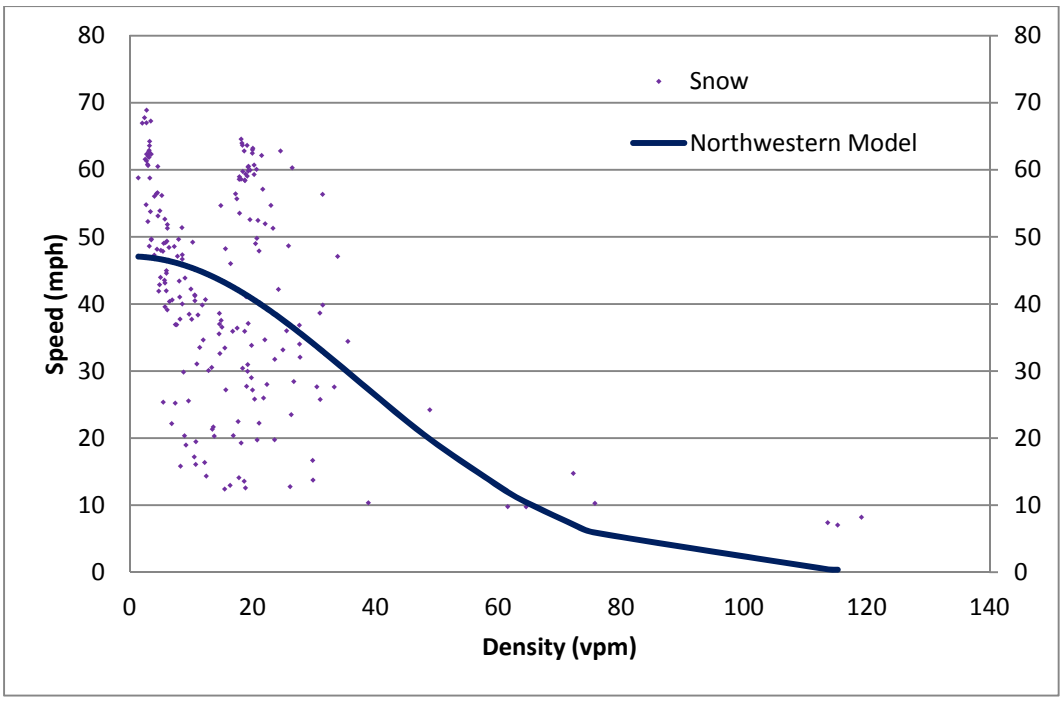

Figure 10 Snow Condition Speed-Density Relationship

Table 4 summarizes estimated FFS (u_f) and Capacity (q_m) values using the Northwestern model. The maximum flow or capacity (q_m) occurs at optimum density (k_o) and using Equation (7), we have the following equation:

$$\boldsymbol{q_m} = \frac{\boldsymbol{u_f K_o}}{\sqrt{\boldsymbol{e}}} \quad (28)$$

Table 4 Northwestern Model Parameters for each Scenario

	u_f (mph)	K_o (vpm)	q_m (vph)
Normal Condition	62.7	81.6	3,104
Light Rain Scenario	60.4	55.2	2,026
Medium Rain Scenario	59.7	50.1	1,814
Heavy Rain Scenario	57.2	51.7	1,794
Snow	47.1	1062	1,147

It seems that there is a reasonable reduction in estimated FFS value; however the estimated capacity under normal condition seems odd. This was expectable since the model does not fit well to the normal scenario dataset. The model does not fit the over-saturated regime well. The odd number of normal condition capacity estimation was expectable since the Northwestern model does not fit well in the normal condition scenario. (Figure 6)

4.2.2 Van Aerde Model

The calibration of the Van Aerde model using each scenario was implemented using SPD_CAL software. The SPD_CAL software is an iterative heuristic procedure that was

developed by Van Aerde and Rakha (1995) that fits the fundamental speed-flow-density relationship to data.

The following figures demonstrate calibrated Van Aerde speed-flow model on each scenario dataset.

The following figures demonstrate calibrated Van Aerde Model and the scenario data points.

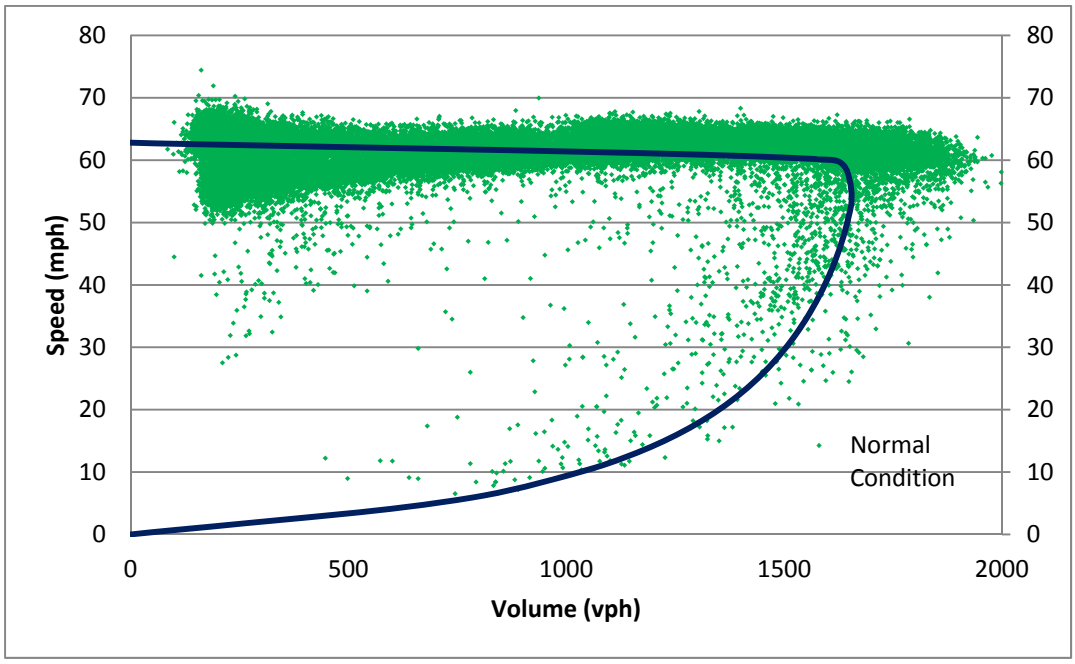

Figure 11 Calibrated Van Aerde Model on Normal Condition Scenario

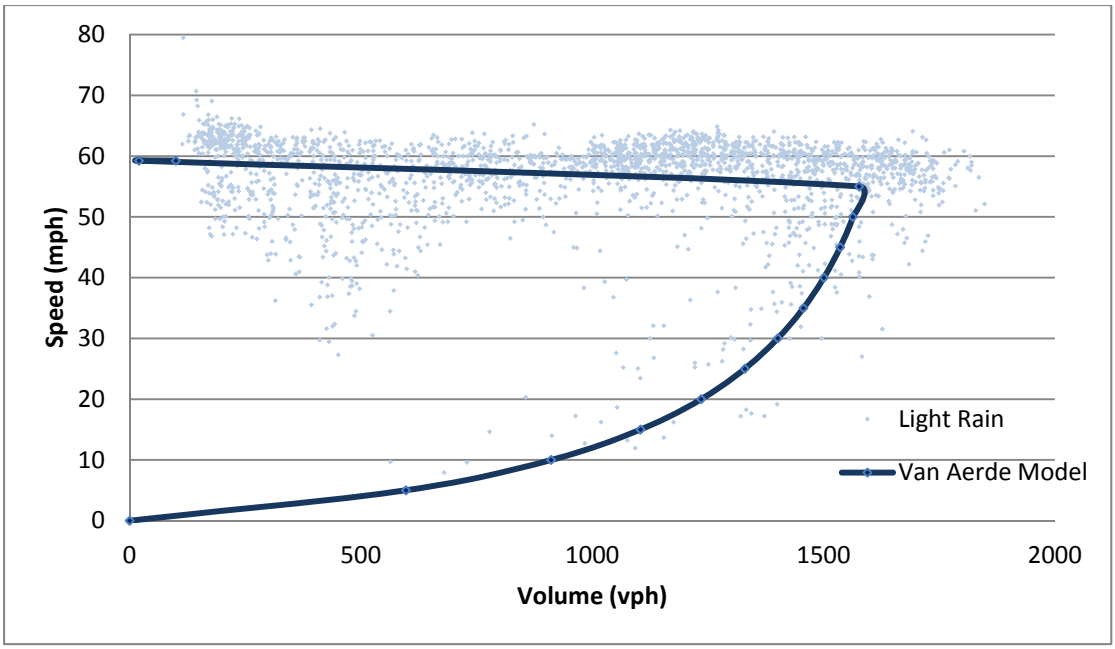

Figure 12 Calibrated Van Aerde Model on Light Rain Condition Scenario

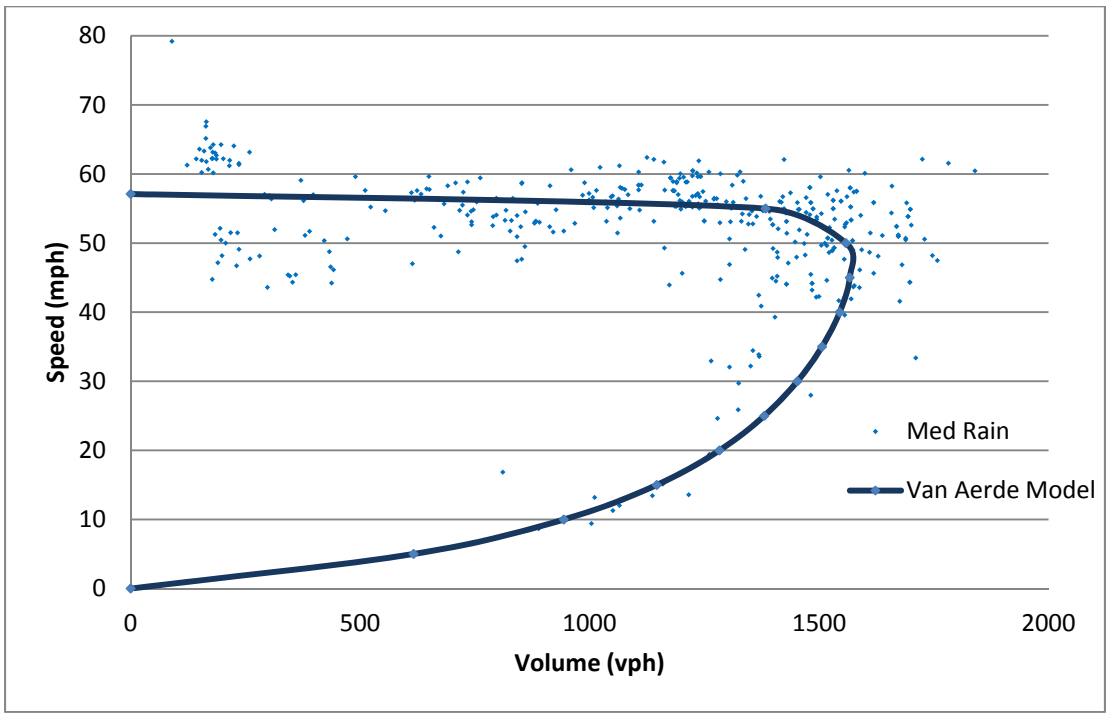

Figure 13 Calibrated Van Aerde Model on Medium Rain Condition Scenario

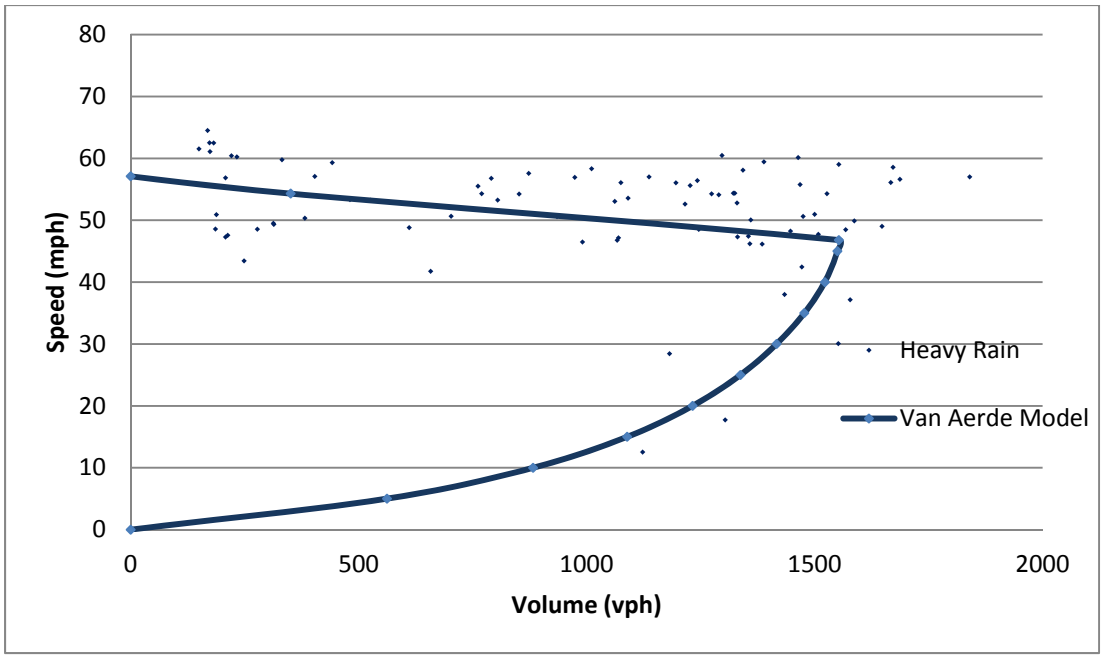

Figure 14 Calibrated Van Aerde Model on Heavy Rain Condition Scenario

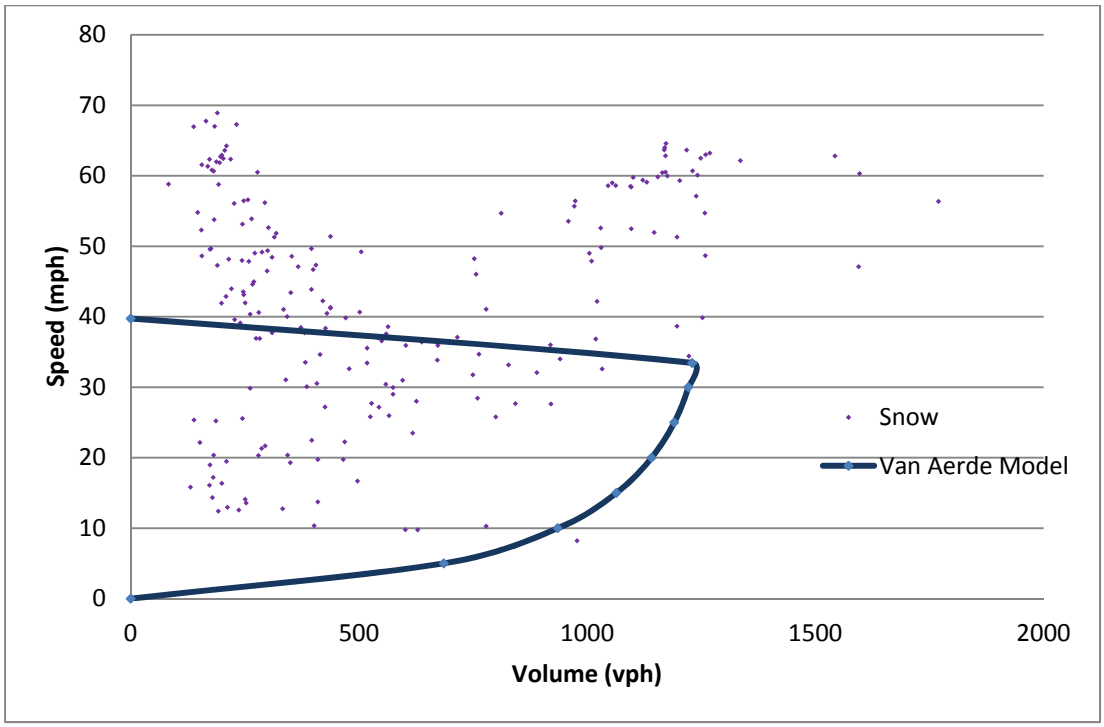

Figure 15 Calibrated Van Aerde Model on Snow Condition Scenario

As it was expected the Van Aerde Model does not fit well in the snow condition. Table 5 depicts four main parameters of the Van Aerde model calibrated for different scenarios:

Table 5 Van Aerde Model Parameters for Different Scenario

	FFS (mph)	Speed at Capacity (mph)	Capacity (vph)	Jam Density (vpm)
Normal	62.8	57.2	1654	217.6
Light Rain	59.3	54.8	1577	173.4
Medium Rain	57.1	46.8	1569	177.6
Heavy Rain	54.4	46.8	1553	154.9
Snow	39.8	33.4	1230	256.8

It seems that this approach does a good job in estimating FFS (mph) and the reasonable reduction trend exists. However, the model seems to underestimate capacity based on the result shown in Table 5 and the speed-flow diagrams. The model does not cover high volume values well. It seems the model tries to provide the best fit for entire speed-flow domain by sacrificing estimation of the pre-breakdown flow rates. These pre-breakdown volumes are used to estimate capacity.

The reasonable reduction in capacity exists when the weather condition worsens. It should be considered that in order to use this approach, the full shape of the speed-flow diagram should exist. Therefore, this approach may not be used in some scenarios with a low number of observations.

4.2.3 Modified Greenshields Model

The dual regime modified Greenshields model was calibrated on each scenario data. The following figures depict the calibrated model for each scenario.

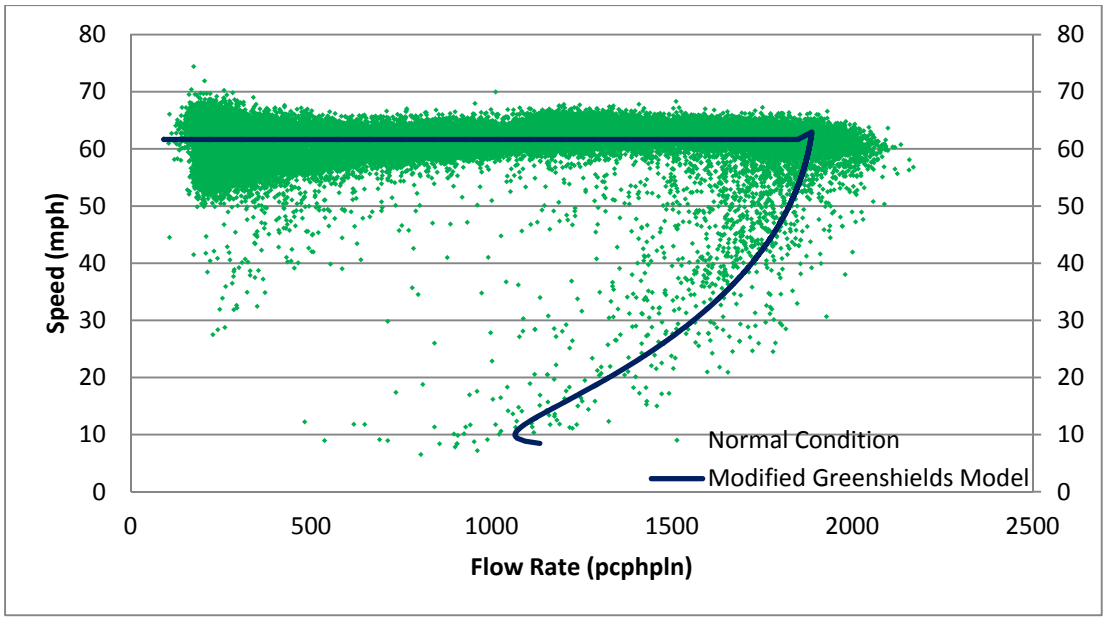

Figure 16 Calibrated Modified Greenshields Model on Normal Condition Data

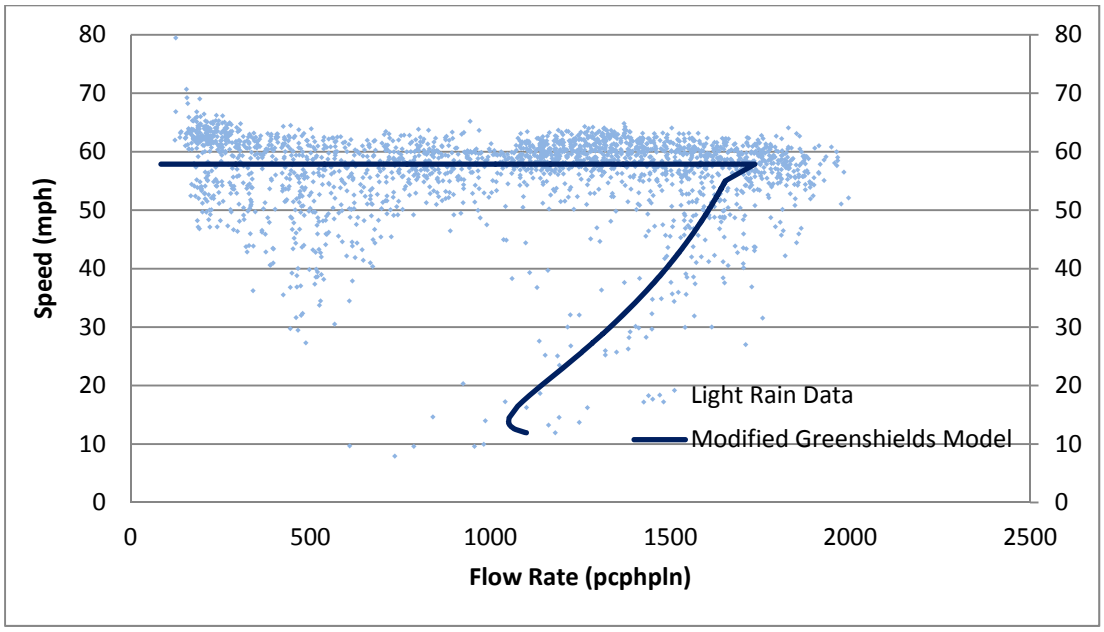

Figure 17 Calibrated Modified Greenshields Model on Light Rain Data

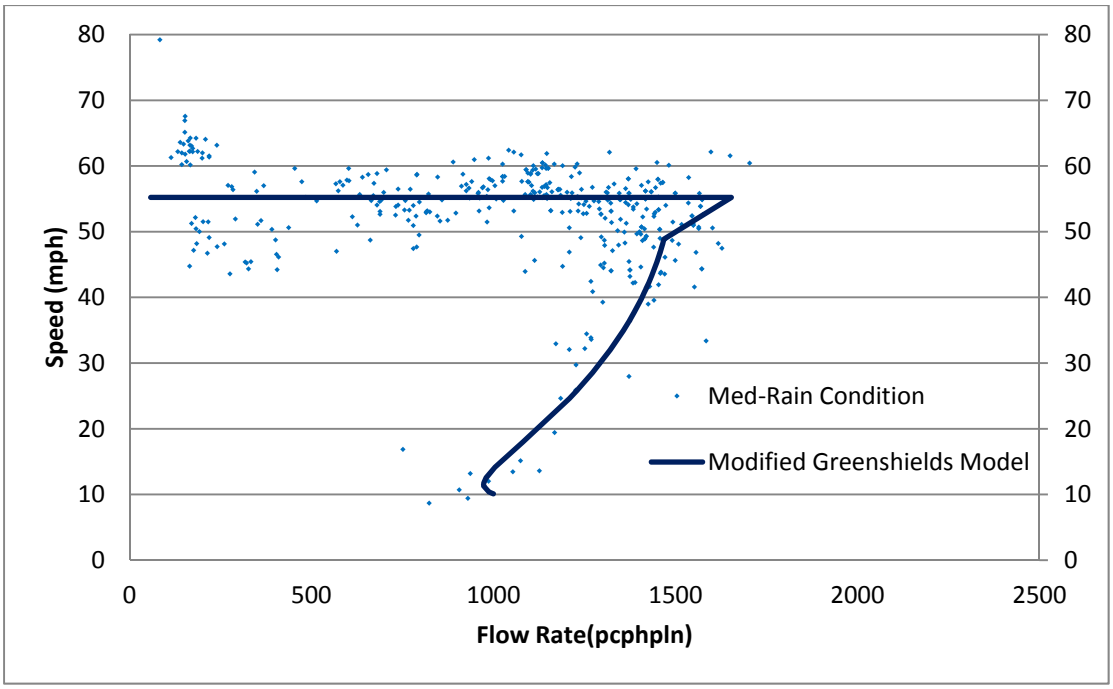

Figure 18 Calibrated Modified Greenshields Model on Medium Rain Scenario

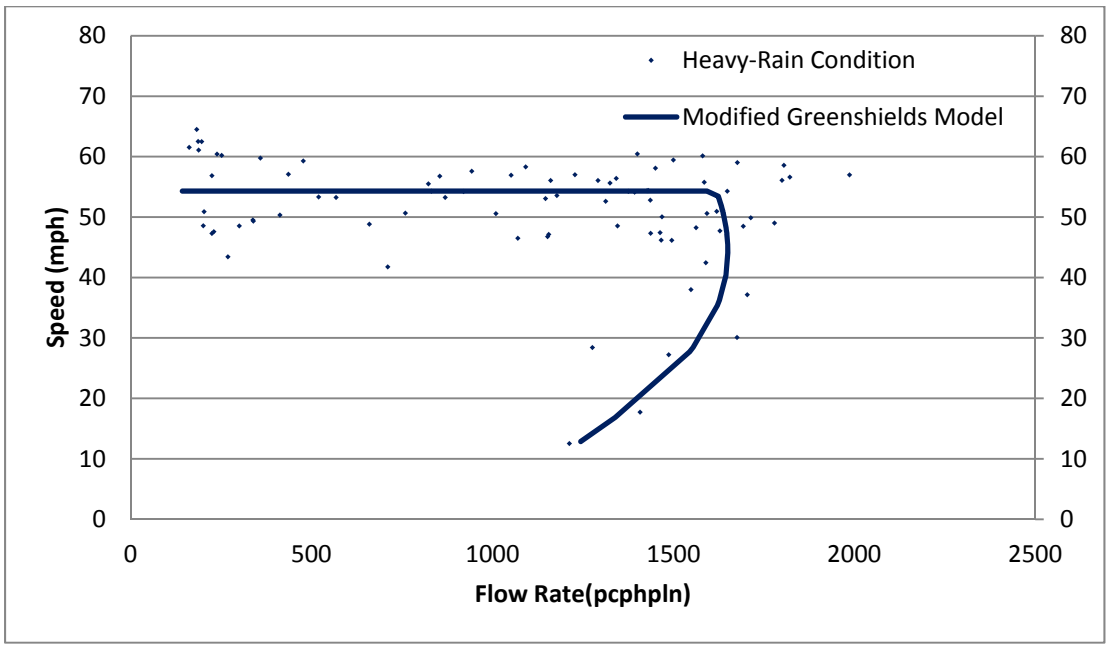

Figure 19 Calibrated Modified Greenshields Model on Heavy Rain Scenario

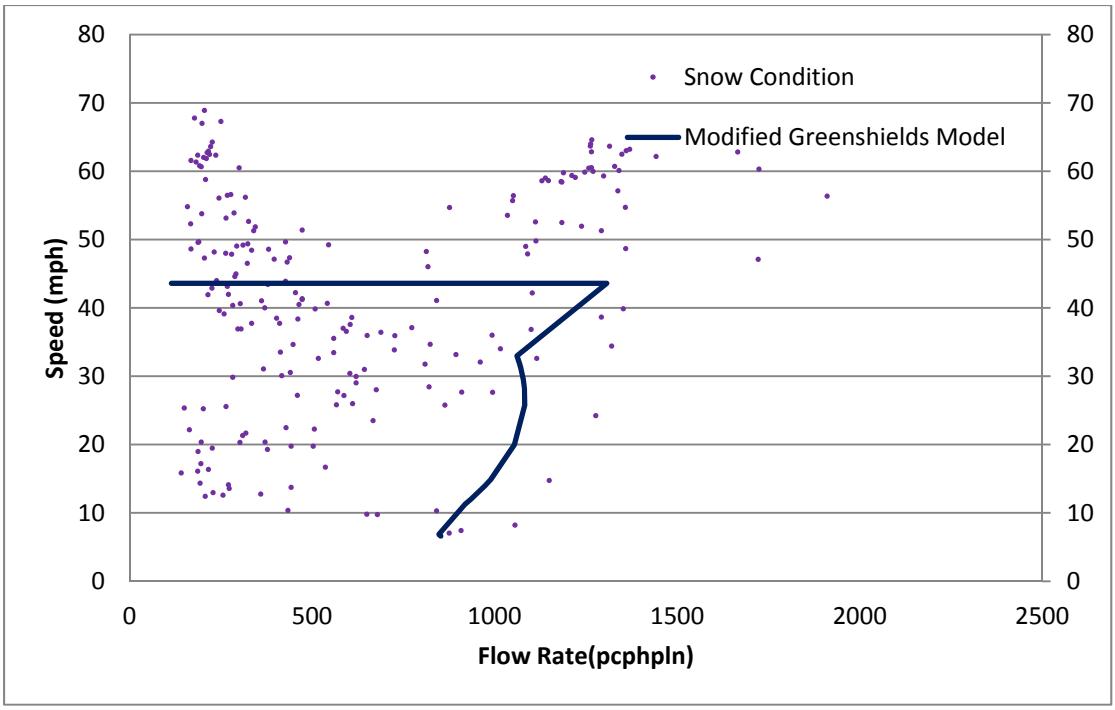

Figure 20 Calibrated Modified Greenshields Model on Snow Scenario

Table 6 summarizes critical model parameters after fitting the Modified Greenshields Model.

Table 6 Estimated FFS and Capacity Values Using Modified Greenshields Model

Scenario	# Observations	$K_{breakpoint}$ (pc/m/ln)	$u_{capacity}$ (mph)	u_f(mph)	Capacity (pc/h/lnn)
Normal	41,844	32.5	61.6	61.6	2,000
Light Rain	2,212	30	57.9	57.9	1,735
Medium Rain	400	27.5	55.2	55.2	1,510
Heavy Rain	80	30	54.3	54.3	1,651
Snow	208	27.5	43.6	43.6	1,107

It seems reasonable that the reduction in estimated FFS exists. In terms of capacity estimation, there is a counterintuitive observation on the heavy rain capacity estimation. Note that FFS and estimated speed at capacity are equal since this model assumes a linear relationship for under-saturated condition and the speed drops when density reaches the break point value.

4.2.4 HCM 2010 Model

In under-saturated regime one of the model parameters is FFS. This parameter estimates using HCM 2010 status-quo approach which is averaging all the speed observations which their respective flow rate is less than 1000 (pc/h/ln).

The capacity (as an end point of under-saturated regime), is estimated using empirical threshold approach. In order to make sure those observations which are used in capacity estimation are in *sustainable mode* (HCM definition) in all the scenarios; the top five percentile observed flow rate is selected for capacity estimation. In the HCM 2010 method the density at capacity (K_c) is assumed to be at 45 (pc/m/ln) and jam density (K_j) equals 180 (pc/m/ln). Please note that incidents and work zone observations are excluded from each data set. The speed-flow diagram for normal, light rain, medium rain, and heavy rain scenarios are represented below:

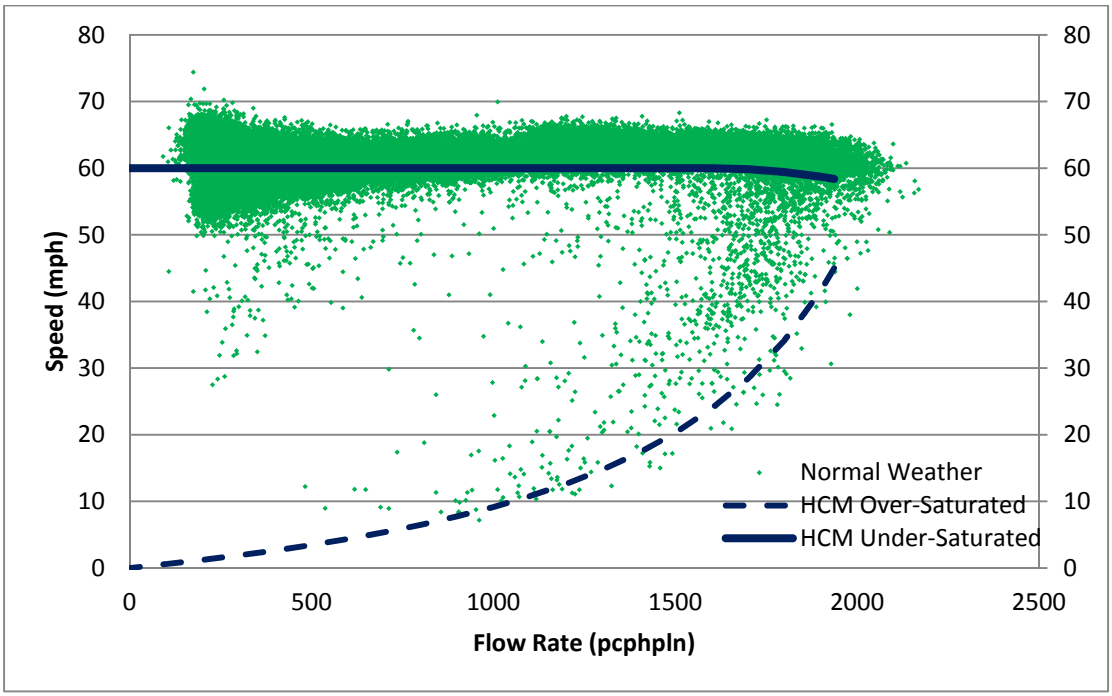

Figure 21 Calibrated HCM 2010 Model on Normal Data

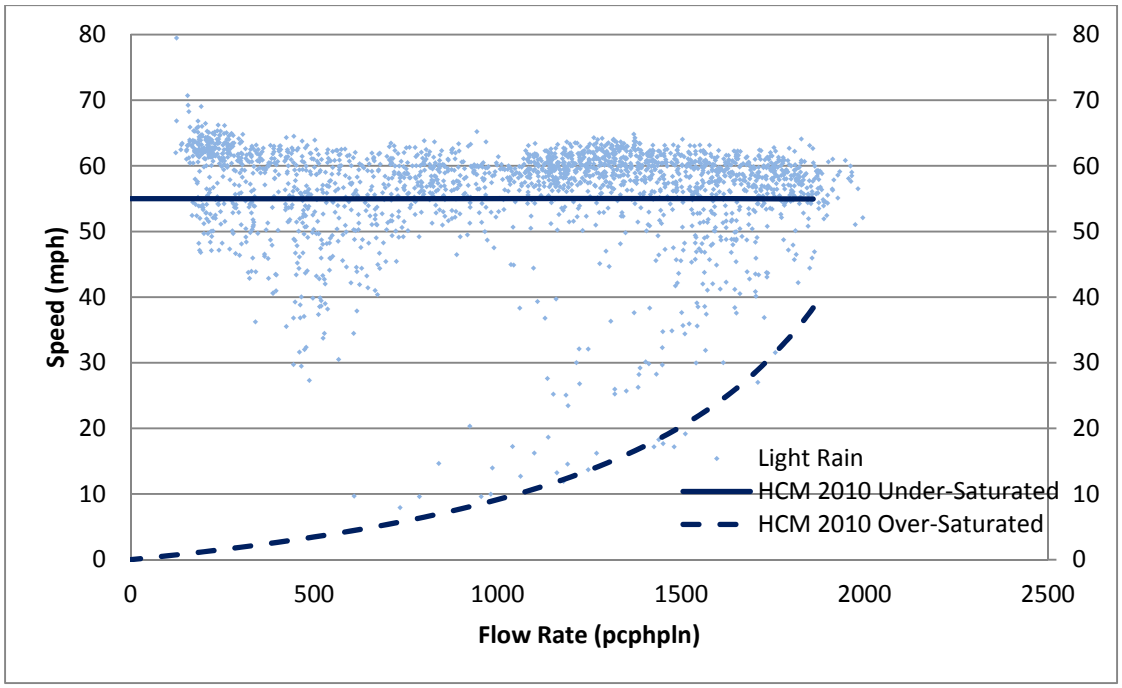

Figure 22 Calibrated HCM 2010 Model on Light Rain Data

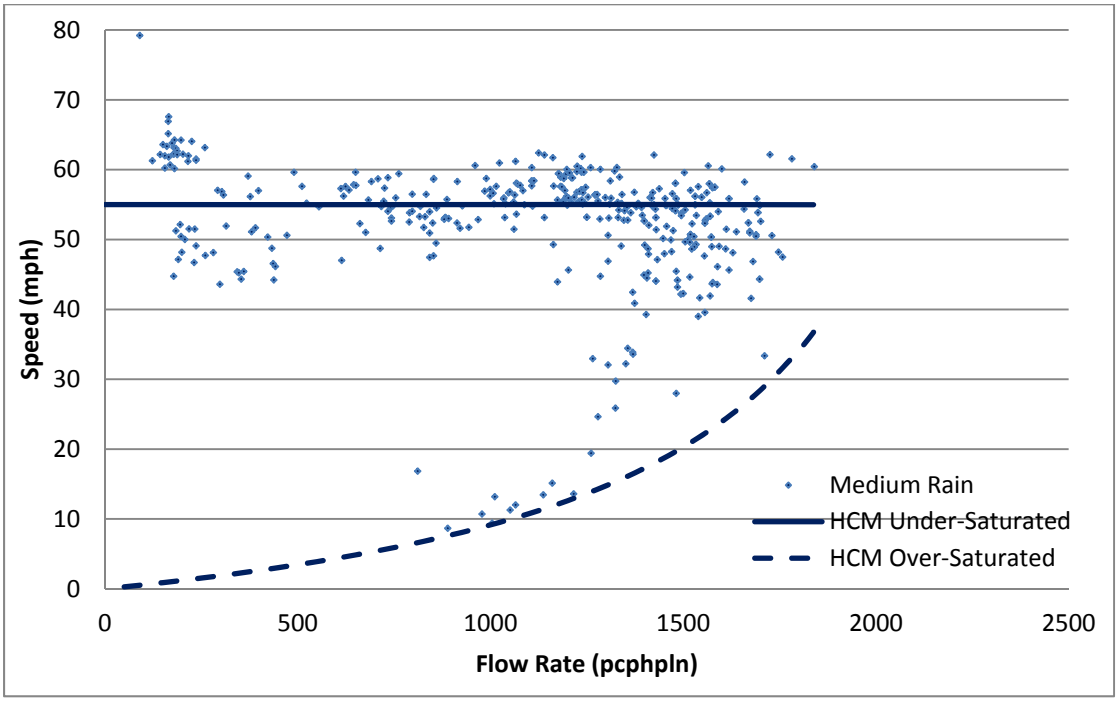

Figure 23 Calibrated HCM 2010 Model on Medium Rain Scenario

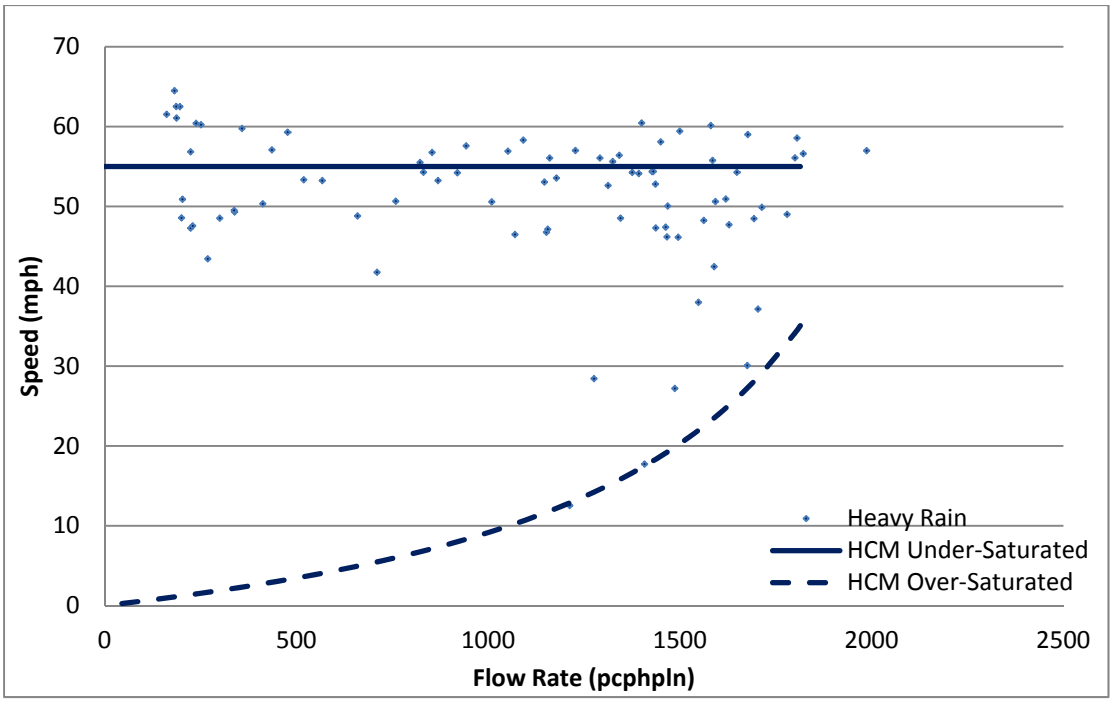

Figure 24 Calibrated HCM 2010 Model on Heavy Rain Scenario

Table 7 summarizes estimated FFS using HCM 2010 approach (status quo). In order to use HCM 2010 under-saturated model, the estimated FFS is rounded to the nearest 5 increment (shown in the parenthesis). The table also demonstrates estimated capacity values for each scenario using the five percent threshold value.

Table 7 Estimated FFS Using HCM 2010 Approach (Status Quo)

Scenario	FFS (Rounded to the Nearest 5) (mph)	Capacity (pc/h/ln)
1. Normal	60.5 (60)	1,935
2. Light Rain	56.5 (55)	1,860
3. Medium Rain	53.5 (55)	1,838
4. Heavy Rain	54.2 (55)	1,814
5. Snow	38.5(40)	1,436

4.3 Direct Methods

Individual methods are methods that specifically estimate FFS or capacity and not both. The empirical threshold approach also can be used for capacity estimation. These approaches are explained in the following:

4.3.1 Estimate FFS using Empirical Thresholds

The empirical threshold approach is implemented in different scenarios and the result of this analysis is summarized in Table 8. The table also provides the dispersion of the estimated FFS in each scenario using the standard deviation parameter.

Table 8 Estimated FFS Values Using Empirical Thresholds Approach

	Estimated FFS (mph)	Standard Deviation
Normal Weather	60.4	1.7
Light Rain	59.5	2.5
Medium Rain	57.0	4.6
Heavy Rain	55	2.6
Snow	57.3	7.3

The estimated FFS in the snow scenario is unrealistically high. This might be due to low number of observations in this scenario. It seems that this approach may not provide a good estimate in scenarios with low number of observations.

4.3.2 Estimating Capacity Using Empirical Thresholds

Past researchers have used a simple yet appropriate approach to estimate the capacity using observed flow rates. The approach suggests estimating the capacity by averaging the top portion of the observed flow rates by certain threshold. Multiple researchers have used the top first percentile or the top five percentile of the observed flow rates to estimate capacity. Table 9 demonstrates capacity values using the empirical capacity threshold approach.

Table 9 Estimated Capacity Values using Empirical Thresholds Approach

	Estimated Capacity (pc/h/ln)			
	Top First Percentile		Top Five Percentile	
	# Obs.	Value	# Obs.	Value
Normal Weather	418	2021	2092	1935
Light Rain	22	1937	111	1860
Medium Rain	4	1924	20	1838
Heavy Rain	1	1987	4	1814
Snow	2	1962	10	1436

4.4. Models Goodness of Fit Evaluation

In this section the combined methods are evaluated for goodness of fit. Three scenarios with adequate number of observations (normal, light rain, and medium rain) were selected for this purpose. Also two measures of goodness of fit were selected for this purpose. These measures are Root Mean Square Error (RMSE) and R^2.

Each model was evaluated in normal, light rain, and medium rain scenario using goodness of fit performance measures mentioned above. These scenarios have been selected since there is adequate number of observations in each scenario. Each scenario is divided into three conditions of under-saturated, over-saturated, and overall. The HCM 2010 density threshold of 45 (pc/m/ln) was used to bisect each scenario dataset.

Table 10 Number of Observation in Each Scenario Condition

	Number of Observations			K >45 Ratio
Scenario	**K <= 45**	**K >45**	**Overall**	**(%)**
Normal	41,640	202	41,842	0.5
Light Rain	2,178	34	2,212	1.6
Medium Rain	344	56	400	16.3
Heavy Rain	54	36	80	66.7
Snow	178	30	208	16.9

Table 10 demonstrates each number of observations in each scenario condition. Since, all the incidents and inclement weather conditions have been excluded from the normal scenario, only a very small portion (0.5%) of observation have density greater than 45 (pc/h/ln). The portion of observation with density greater than 45 (pc/m/ln) seem to increase monotonically in rain scenarios as the rain intensity increases. However, in the snow scenario the portion of observation with density greater than 45 (pc/m/ln) drops significantly compared to the heavy rain scenario. This phenomenon can be explained by the fact that drivers tend to keep a longer safety distance from the following car in an adverse weather condition such as snow and this reduces overall density. Also, conservative drivers may avoid travelling during snow, thus, the density of traveling vehicles reduces.

4.4.1 Normal Condition Scenario

Table 11 summarizes the model's goodness of fit evaluation for the normal condition scenario.

Table 11 Models Goodness of Fit Evaluation for Normal Condition Scenario

Row Number	Model	Normal					
		Test Statistic					
		k=<45		K>45		Overall	
		RMSE	R^2	RMSE	R^2	RMSE	R^2
1	Northwestern	3.6	0.17	23.9	*	3.96	*
2	Van Aerde	3.44	0.01	8.17	0.19	3.63	0.33
3	Modified Greenshields	2.95	0.27	4.24	0.78	2.96	0.54
4	HCM 2010	3.77	*	7.22	0.92	3.79	0.25

(*) due to weak model fitness, the R^2 value is not shown.

It seems that the Modified Greenshields model fits better in all the possible cases (under-saturated, over-saturated, and overall condition) compared to other models. As it was expected from the speed-density diagram (Figure 6) the North Western model does not fit well in the normal condition scenario especially in the over-saturated condition with a very high RMSE. The Van Aerde model work well in the under-saturated condition, however, it does not provide a good prediction in the over-saturated condition. The HCM 2010 method works better in the over-saturated condition compared to the under-saturated condition.

4.4.2 Light Rain Condition Scenario

Table 12 summarizes models goodness of fit evaluation for light rain condition scenario.

Table 12 Model Goodness of Fit Evaluation for Light Rain Condition Scenario

Row Number	Model	Light Rain					
		Test Statistic					
		k=<45		K>45		Overall	
		RMSE	R^2	RMSE	R^2	RMSE	R^2
1	Northwestern	5.77	*	11.54	*	6.02	*
2	Van Aerde	5.69	0.45	2.47	0.90	5.69	0.46
3	Modified Greenshields	5.19	0.29	3.84	0.72	5.17	0.55
4	HCM 2010	6.53	0.47	9.46	0.86	6.54	0.47

(*) due to weak model fitness, the R^2 value is not shown.

In under-saturated condition, almost all the models are in a same range, the modified Greenshields models shows slightly lower RMSE compared to other scenarios and HCM 2010 approach looks to have a better fit in terms of R^2. In the over-saturated condition the Van Aerde model seems to fit better than any other model. In the overall condition, similar to normal condition, the modified Greenshields model looks to have the best fit in both measures. Similar to the normal scenario, the Northwestern model does not fit the over-saturated condition well.

4.4.3 Medium Rain Condition Scenario

Similar to normal condition scenario and light rain scenario, each model goodness of fit was evaluated on the medium rain condition scenario. Table 13 summarizes the results of this analysis.

Table 13 Model Goodness of Fit Evaluation for Medium Rain Condition Scenario

Row Number	Model	Med Rain					
		Test Statistic					
		k=<45		K>45		Overall	
		RMSE	R^2	RMSE	R^2	RMSE	R^2
1	Northwestern	5.12	*	4.17	*	5.0	*
2	Van Aerde	7.56	0.22	3.36	0.47	7.6	0.34
3	Modified Greenshields	4.89	0.48	1.19	0.99	4.5	0.76
4	HCM 2010	9.47	0.19	3.83	0.83	8.89	0.51

(*) due to weak model fitness, the R^2 value is not shown.

The modified Greenshields model dominates all other models in terms of prediction accuracy in all the conditions (under-saturated, over-saturated, and overall). It should be noted that the medium rain scenario has lower number of observations (400) when compared to normal condition scenario (about 41,000) and light rain scenario (about 2,200). This fact might explain the drop in the prediction power of the Van Aerde and HCM 2010 models.

4.5 SUMMARY OF RESULTS AND CONCLUSION

Table 14 summarizes estimated FFS and the consequent Table 15 summarizes estimated capacity values using different approaches.

Table 14 Summary of Estimated FFS for Different Scenarios (mph)

	Normal	Light Rain		Medium Rain		Heavy Rain		Snow	
		FFS	SAF	FFS	SAF	FFS	SAF	FFS	SAF
Northwestern Model	62.7	60.4	0.963	59.7	0.952	57.2	0.912	47.1	0.751
Van Aerde Model	62.8	59.3	0.943	57.1	0.909	54.4	0.866	39.8	0.633
Modified Greenshields Model	61.6	57.9	0.940	55.2	0.896	54.3	0.882	43.6	0.708
Empirical Thresholds	60.4	59.5	0.985	57.0	0.944	55	0.911	57.3	0.949
HCM	60.5	56.5	0.934	53.5	0.884	54.2	0.896	38.5	0.636

Table 15 Estimated Capacity Values using Different Approaches (pc/h/ln)

	Normal	Light Rain		Medium Rain		Heavy Rain		Snow	
		Capacity	CAF	Capacity	CAF	Capacity	CAF	Capacity	CAF
Northwestern Model	3352	2188	0.65	1959	0.58	1794	0.53	1146	0.34
Van Aerde Model	1786	1703	0.95	1694	0.95	1553	0.87	1328	0.74
Modified Greenshields Model	2000	1735	0.87	1510	0.76	1651	0.83	1107	0.55
Average of Top 1% Flow Rate Values	2021	1937	0.96	1924	0.95	1987	0.98	1962	0.97
Average of Top 5% Flow Rate Values	1935	1860	0.96	1838	0.95	1814	0.94	1436	0.74

Important findings in using different approaches to estimate FFS and capacity are summarized as follow:

1 – The Northwestern Model:

- The reasonable reduction in the FFS exists in this model.
- In the under-saturated condition, the RMSE of this model is in a range of other models.
- The RMSE of this model in over-saturated condition is very high in normal (23.9) and light rain (11.54) scenarios but reduces to an acceptable range in the medium rain scenario (5.0).

- The model overestimates the capacity in the normal and light rain scenarios and underestimates capacity in the snow scenario; therefore, it is not suggested to use this model for capacity estimation.

2- Van Aerde Model

- The reduction in estimated FFS and capacity values exists when using this model.
- The model fits well to all the scenarios when considering model RMSE and R^2 values. It seems that this model provides the best prediction in the over-saturated condition of the light rain scenario compared to other models.
- The model tends to underestimate capacity values compared to the empirical threshold method but the estimated CAFs seem reasonable.

3- Modified Greenshields Model

- This model dominates all other models when comparing the goodness of fit performance measures in overall condition.
- The reasonable reduction in FFS and capacity is observed using this model in different scenarios.
- The model does not provide a good estimate for capacity measures when there are few numbers of observations in a particular scenario. In order to use the modified Greenshields model, a full shape of the speed-flow model should be available. This is not a case in the low volume scenarios like heavy rain and snow.

4- HCM 2010 Model

- The model offers the lowest estimated FFS in inclement weather conditions because this approach considers congested observations in FFS estimation.
- The model prediction power reduces when inclement weather conditions occur. The RMSE value almost doubles up in the light rain scenario and triples up in the medium rain scenario. It seems that the model does not have enough flexibility to fit inclement weather conditions data.
- A drawback of the model in the under-saturated condition is that it uses a breakpoint of 1800 (pc/h/ln) for comparably low FFS of 55 mph. In scenarios which capacity reduces due to non-recurrent congestion sources, the under-saturated part of the model changes into a straight horizontal line of the estimated FFS.

5- Empirical Thresholds

- The empirical threshold used for FFS estimation seems to overestimate the actual value. This approach excludes all the observations in the congested condition. The FFS overestimation is more considerable in the snow scenarios where the suggested FFS is higher compared to all other approaches.
- The empirical threshold approach used for capacity estimation provides reasonable results when using the average of the top five percent observed flow rates. The reasonable reduction in capacity exists and the estimated CAFs look reasonable too. However, using the top first percent threshold for estimating the capacity value seems problematic in scenarios with comparably few numbers of observations. For example,

the estimated capacity value used in snow condition is a result of only two observations. This results in unrealistic capacity estimation in the snow scenario.

Considering all the findings mentioned above, it seems that the best combination for FFS and capacity estimation is to use the modified Greenshields model to estimate FFS and the empirical threshold approach with 5% threshold for capacity.

The Greenshields model is recommended for FFS estimation since the model fits the data better than any other model (especially in the under-saturated regime). The empirical threshold approach is recommended for capacity estimation since it provides reasonable predictions in all the scenarios especially with scenarios with few numbers of observations. (Table 15)

5. DATA ANALYSIS

5.1 Overview

This chapter demonstrates data analysis efforts of this study. In the first section of the chapter, operational analysis of each scenario is provided. The database is categorized into multiple categories which each category represents a unique scenario. In order to provide better understandings of the operational impacts of non-recurring congestion sources on the freeway facilities in different conditions, each scenario data are divided into peak and off-peak conditions. For each weather category, basic statistics like average and standard deviation of observed speed and volumes are calculated. Using the conclusion of the previous chapter, FFS and capacity for each scenario is estimated. FFS are estimated by fitting the modified Greenshields model and Capacity is estimated using an empirical threshold approach which averages the top five percentile values of observed flow rates and represents it as estimated capacity. The speed-flow diagram for each scenario is also provided.

In the second section of the chapter, scenario delay analysis is provided. The delay analysis provides an overview of the contributing factors to overall freeway delay.

In the third and last section of the chapter, an analysis is conducted on observations with low observed flow rates to provide explanations for the trumpet shape speed-flow diagram.

5.2 Scenarios Description

The fused database contains records which each have multiple fields. These fields provide information regarding traffic, weather, and incidents. In order to analyze the impact of each non-recurrent congestion source, the database is divided into different datasets based on the

weather and incident condition that each 15-min observation represent. It should be noted that all the scenarios are mutually exclusive. The definition of each scenario is provided in the following:

1-Normal Scenario: this scenario consists 15-min observations where no incident has been reported on the facility and also there are no sign of inclement weather or low visibility condition based on the weather database query. The reported precipitation rate in this scenario equals 0 in/hr.

2-Wet Pavement: This scenario contains of observations which the reported weather condition is rainy but the precipitation rate is at zero value. This is a condition when the pavement is wet due to the prior rain but there is no pouring. Based on the literature review results in the second chapter, there are evidences that wet pavement impacts freeway facility FFS and capacity.

3- Light Rain Scenario: this scenario consists of 15-min observations when no incident has been reported and the weather condition is reported as rain condition. The precipitation rate is greater than 0 in/hr and less than or equal to 0.1 in/hr. This threshold matches the light rain condition in the HCM. Other parameters are similar to the normal condition.

4-Medium Rain: this scenario is similar to the light rain scenario except that the precipitation rate is higher compared to the light rain scenario. The precipitation rate is greater than or equal to 0.1 and less than 0.25 in/hour. This range matches HCM 2010 medium rain condition.

5- Heavy Rain: Similar to light rain and medium rain scenarios, no incident has been reported and the reported weather condition is rainy. The precipitation rate is greater than 0.25 in/hr.

6- Snow: this scenario contains 15-min observations when the weather database indicates that the weather condition is snowy. Also, no incident has been reported.

7-Downstream Incident: an incident has occurred downstream of the travel direction. There is no evidence of inclement weather conditions on the freeway.

8-Opposite Direction Incident: an incident has occurred in the opposite direction of the travelling direction but no incident is being reported in the direction of travel. There is no report of snow or rain on the facility. The rubberneck impact analysis will be implemented on this data set.

9-Upstream Incident: An incident has been occurring in the upstream of the direction of travel. There is no report of inclement weather condition of the facility. An upstream incident usually meters the traffic and the metered vehicles will travel the segment at a higher speed.

5.2.1 Normal Weather Condition Analysis

The normal condition has the highest number of observations among all the scenarios. The estimated free flow speed is 61.6 mph. Segment capacity is estimated as 1792 vphpln. These values will be used as the denominator for estimating other scenario's capacity and speed adjustment factors (CAF and SAF). Table 16 summarizes capacity and FFS findings for the normal condition and Figure 25 illustrates the speed - flow relationship for the normal condition scenario. In this figure and other following scenario speed-flow diagrams, the peak period observations are shown in red and the off-peak observations are demonstrated in gray.

Table 16 Normal Condition Scenario Estimated Capacity and FFS

	Average	StdDev
Capacity (pc/h/ln)	1935	46.1
FFS (mph)	61.6	n/a

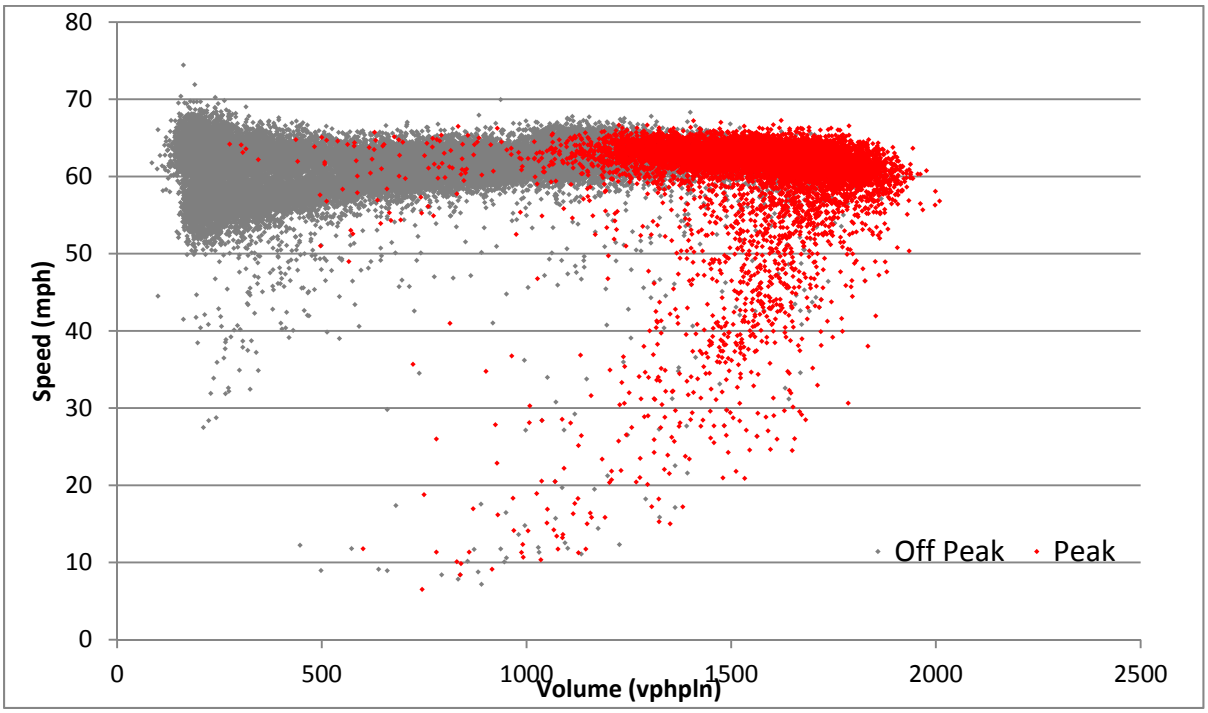

Figure 25 Speed-Flow Relationship for Normal Condition Scenario

In order to have an estimate of the peak traffic periods in the facility under study, a moving average method was used on the average 15-min observed volume data. The peak period is calculated in three different time spans of 1-hour, 2 hours, and 3 hours.

Figure 26 shows the applied moving average method to estimate AM/PM peak periods and the following Figure 26 summarizes the result of this analysis for north, south, and both

directions of the facility. Figure 27 shows the demand level does not significantly change during different days of the week.

AM PEAK			
	North	South	Both Directions
5:00	106	170	276
5:15	135	217	352
5:30	170	259	429
5:45	189	295	484
6:00	209	307	516
6:15	259	340	599
6:30	306	365	671
6:45	327	372	699
7:00	345	365	710
7:15	401	389	790
7:30	431	412	843
7:45	428	421	849
8:00	415	406	821
8:15	421	404	825
8:30	409	379	788
8:45	385	364	750
9:00	351	330	680
9:15	344	317	661
9:30	337	307	643
9:45	317	297	615
10:00	299	280	580
10:15	306	278	584
10:30	312	274	587
10:45	312	274	587
11:00	305	271	576
11:15	309	275	584
11:30	312	280	591
11:45	311	280	591

PM PEAK			
	North	South	Both Directions
15:00	391	321	713
15:15	404	338	741
15:30	407	348	756
15:45	405	359	765
16:00	412	363	775
16:15	426	377	803
16:30	422	384	806
16:45	426	391	818
17:00	431	394	826
17:15	452	407	859
17:30	432	400	832
17:45	418	388	805
18:00	401	368	769
18:15	395	347	743
18:30	374	322	695
18:45	349	297	646
19:00	326	274	600
19:15	309	260	569
19:30	281	244	525
19:45	264	232	496
20:00	251	217	468
20:15	243	211	454
20:30	223	204	428
20:45	211	196	407
21:00	204	191	396
21:15	203	194	397
21:30	186	186	371
21:45	177	176	353

Figure 26 AM/PM Peak Period Calculation using the Moving Average Method (the numbers in the cells represent average observed flow rate volume (vphpln) in normal condition data, the boxed values show the maximum)

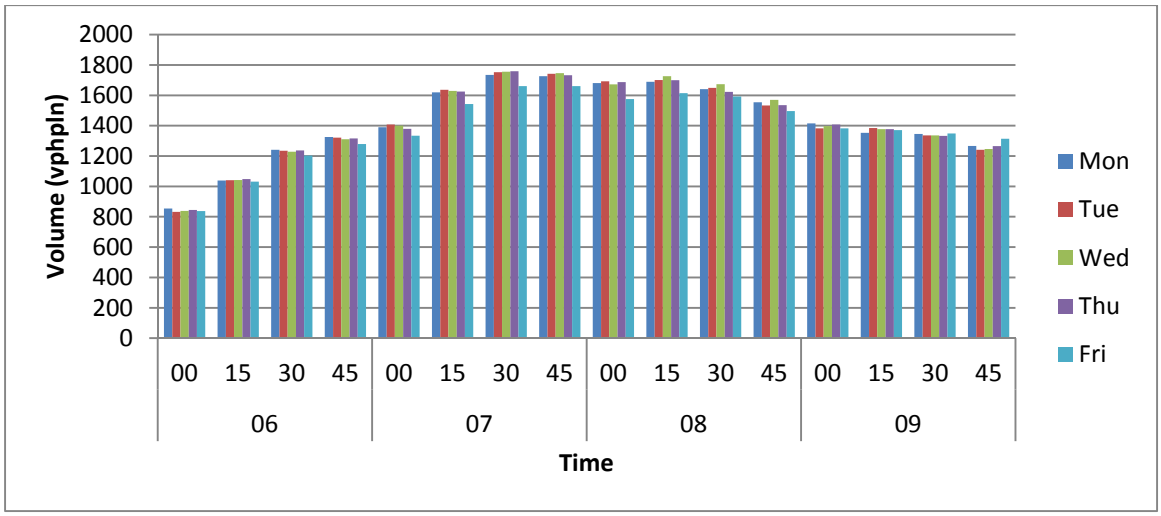

Figure 27 AM Peak Period Day of the Week Observed Flow-Rate Analysis

Table 17 Peak Periods

	AM Period					
	North		**South**		**Both Directions**	
1 Hour	7:30	8:30	7:30	8:30	7:30	8:30
2 Hours	7:15	9:15	6:45	8:45	7:00	9:00
3 Hours	6:45	9:45	6:15	9:15	6:30	9:30
	PM Period					
1 Hour	16:45	17:45	16:45	17:45	16:45	17:45
2 Hours	16:00	18:00	16:15	18:15	16:00	18:00
3 Hours	15:15	18:15	15:30	18:30	15:30	18:30

In order to provide a better understanding of the operational characteristics of the freeway facility, the data is divided into sub-categories of peak, off-peak, and over all data point.

Using three hour peak period for both AM and PM from the previous step, the average observed flow rate volumes and speeds are calculated. Table 18 demonstrates the average observed flow rate volume and speed for peak and off-peak periods alongside an overall overview of the facility under this condition. The average speed slightly differs in peak and off-peak periods but the average observed flow rate during the off-peak period is almost half of the peak period. This seems reasonable since the facility is almost congested in the peak period and the observed flow rate volume drops significantly during off-peak period. Also, the demand in the off-peak time period is more dispersed compared to the peak period.

Table 18 Normal Condition Scenario Peak and Off-Peak Comparison

	# Observations	Volume (vphpln)		Speed (mph)	
		Avg.	**StdDev**	**Avg.**	**StdDev**
Peak	10075	1563	196	60.7	6.2
Off-Peak	31767	800	447	61.3	3.6
All	41842	983	517	61.1	4.4

The 15-min observed volume distribution is calculated by dividing the average observed volume of each 15-min by the sum average observed volumes for all of the 15-min periods and reported in percentage format. Figure 13 illustrates 15-Min observed volume distribution factors. The data used in this analysis is from the normal condition scenario.

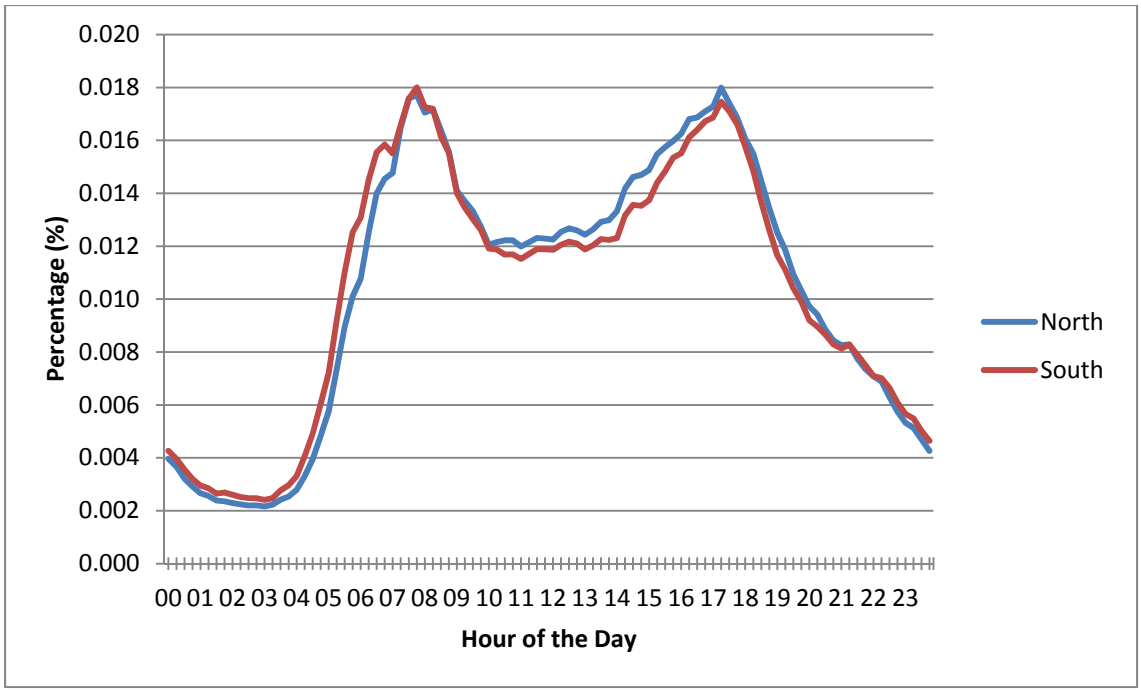

Figure 28 Observed 15-Min Distribution Factors

It is clear that there exist two peak periods of AM and PM and the hourly volume distributions between two directions are almost the same.

The observed volume distribution factor in 15-min resolution is provided to check that the facility has two peak periods**.** (Figure 28)

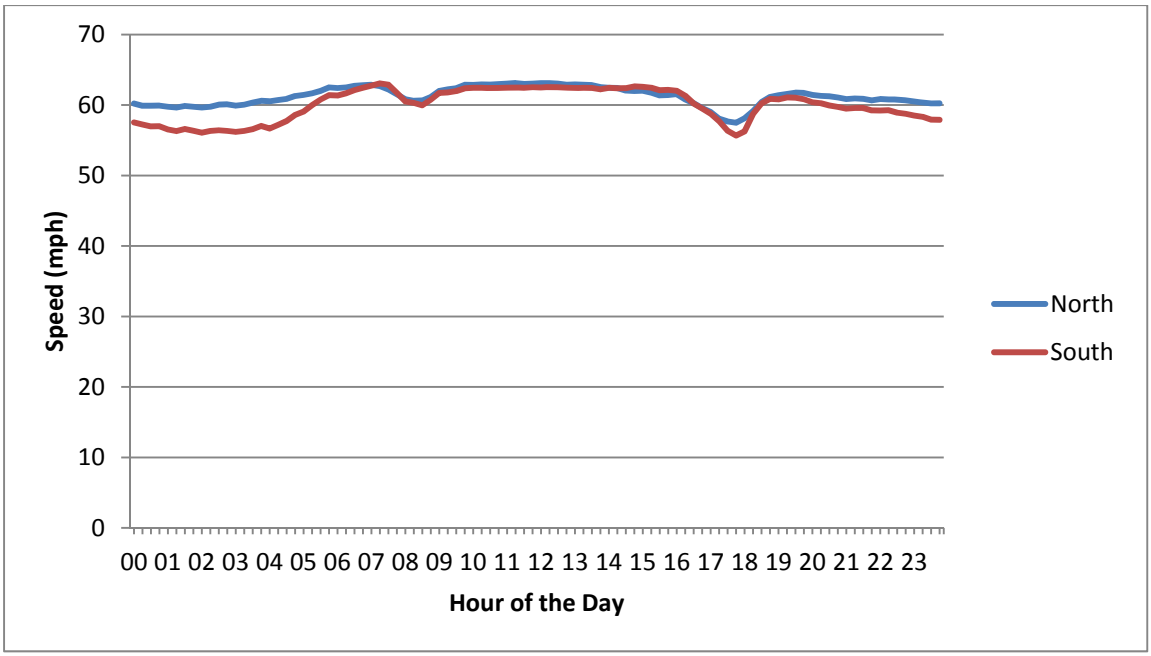

Figure 29 Average Speed of 15-Min Time Intervals

The average speed is almost the same during different times of the day with slight reduction during the peak hours. (Figure 29)

5.2.2 Wet Pavement Scenario

There are 2,227 observations in this scenario. The data analysis in different time periods (peak vs. off-peak) reveals that the average speed and volume during the peak hour drop by 4% compared to the normal scenario. In the off-peak period, the average volume does not drop significantly but the average speed drops by 3%.

Table 19 Wet Pavement Scenario Capacity and FFS Estimation

	#Observations	Average	Std. Dev.	CAF/SAF
Capacity	111	1860	47.5	0.961
FFS	n/a	57.9	n/a	0.940

Table 20 Average Volume and Speed at Different Time Periods under Light Rain Scenario

Period:	#Observations	Volume				Speed			
		Avg.	Compare to Normal Scenario	StdDev	Compare to Normal Scenario	Avg.	Compare to Normal Scenario	Std Dev	Compare d to Normal Scenario
Peak	578	1504	0.962	197	1.01	58.0	0.956	7.4	1.94
Off-Peak	1649	809	1.01	454	1.02	59.6	0.972	5.3	1.472
All	2227	989	1.01	505	0.977	59.2	0.969	6.0	1.364

The volume dispersion does not change significantly from the normal scenario in all time periods but there is considerable increase in observed speed during different time periods.

5.2.3 Light Rain Scenario

The light rain scenario consists of 2,212 observations. The precipitation level of light rain scenario is between 0 and 0.10 inch./hour. The estimated capacity and FFS for this scenario is summarized in Table 21. Figure 30 demonstrates the speed-flow diagram under light rain condition. Similar to the normal condition scenario, there are three restrictive lines for FFS estimation. The peak period observations are shown in red.

Table 21 Light Rain Scenario Capacity and FFS Estimation

	#Observations	Average	Std. Dev.	CAF/SAF
Capacity	111	1860	47.5	0.961
FFS	n/a	57.9	n/a	0.940

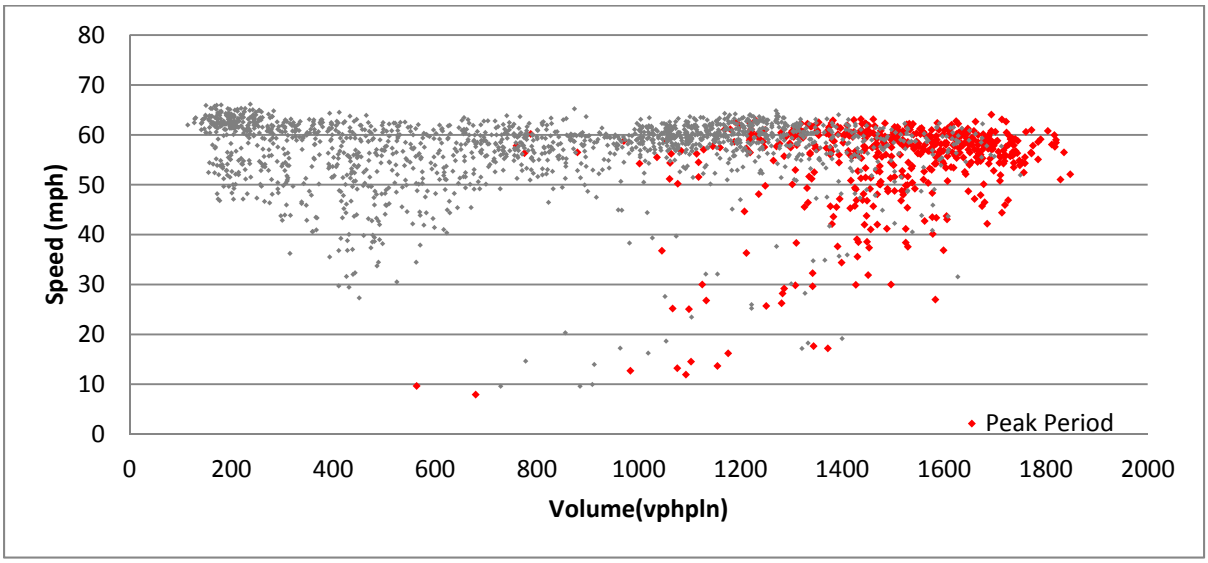

Figure 30 Light Rain Scenario Speed-Flow Diagram

The impact of the light rain on the traffic is more sever in the peak period compared to the off-peak period both in average volumes and speed.

Table 22 Average Volume and Speed at Different Time Periods under Light Rain Scenario

Period:	#Observations	Volume				Speed			
		Avg.	Compare to Normal Scenario	StdDev	Compare to Normal Scenario	Avg.	Compare to Normal Scenario	Std Dev	Compared to Normal Scenario
Peak	525	1496	0.957	192	0.980	54.5	0.898	9.2	1.484
Off-Peak	1687	797	0.996	431	0.964	57.1	0.931	7.1	1.972
All	2212	962.5	0.979	489	0.946	56.5	0.925	7.7	1.750

The average speed drops by 10.2% in the peak period compared to 7.5% drop in the off-peak period. The dispersion of the speed increases significantly compared to the normal scenario. Light rain reduces the average observed flow rate volume by 4.3% in the peak period but only reduces it by 0.04% during off-peak period. It seems that the magnitude of the impact increases significantly when accompanied by high flow rate volumes (congestion).

Also, in order to provide a better overview of the impact of light rain on observed volume and speed of the facility, hourly distribution analysis is conducted. Referring to Figure 31 and Figure 32 it seems that light rain impact on speed increases during peak hours compared to off-peak periods.

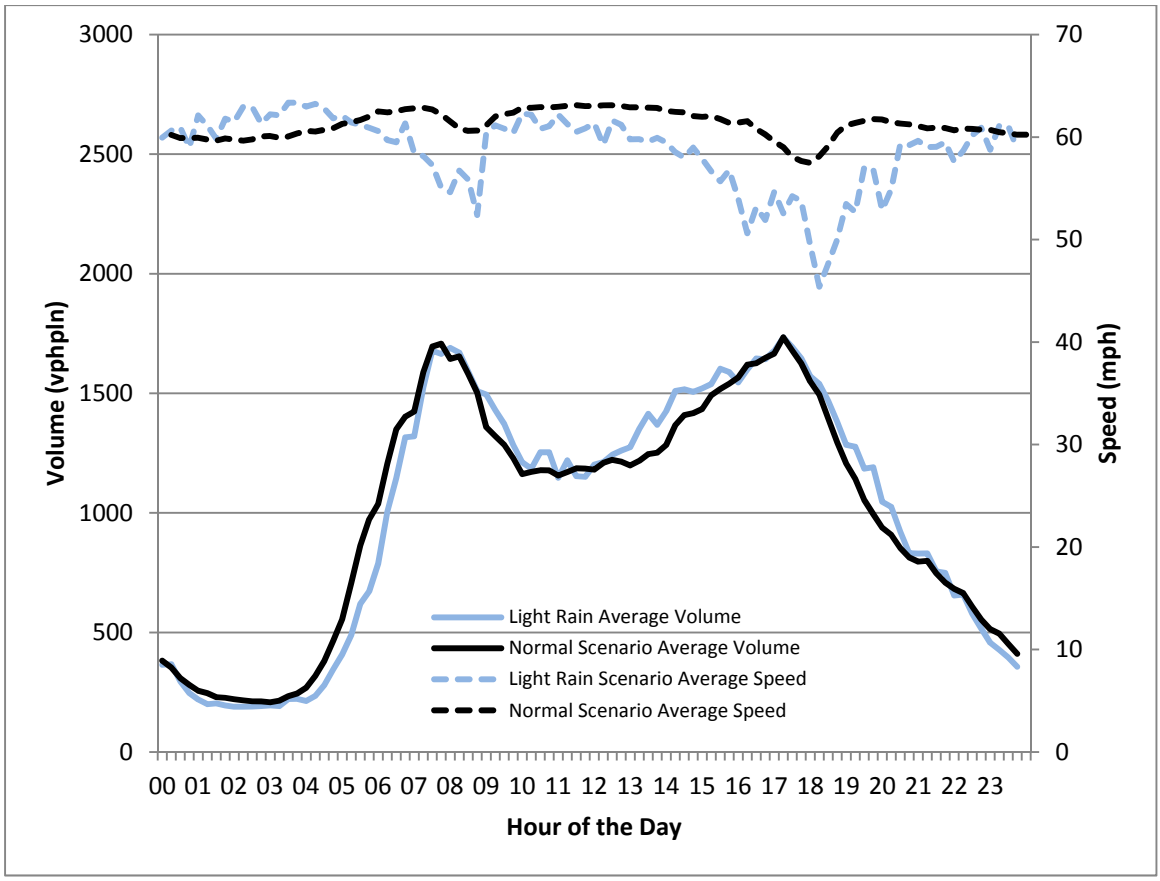

Figure 31 Light Rain and Normal Scenarios Speed and Volume Hourly Distribution (North Direction)

Also in the south direct (Figure 32) light rain reduces flow rate volumes during peak period but it does seem that have a significant impact on the demand level. It is obvious that, the magnitude of the inclement weather on speed increases when it is accompanied with heavy traffic. There are average of 11 observations in each 15-min bin for light rain scenario analysis with maximum of 19 observations and minimum of 4 observations.

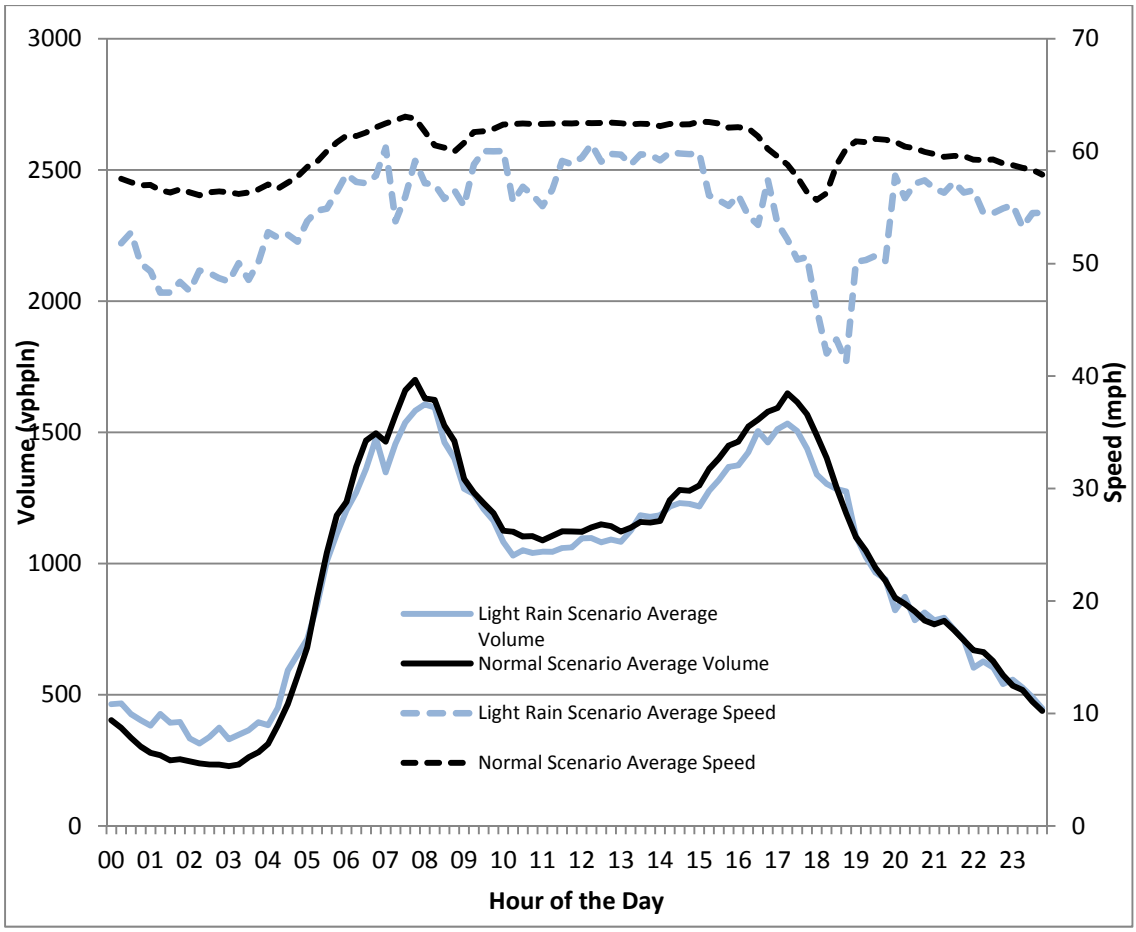

Figure 32 Light Rain and Normal Scenarios Speed and Volume Hourly Distribution (South Direction)

5.2.4 Medium Rain Scenario Analysis

Medium rain scenario has 400 observation points where 130 of them are in the peak period and 270 are in the off-peak period. Table 23 summarizes medium rain scenario capacity and FFS estimation results. Medium rain drops the capacity by 5.1% and reduces the FFS by 10.4%.

Table 23 Medium Rain Scenario Capacity and FFS Estimation

	# Observations	Value	Std. Dev.	CAF/SAF
Capacity	20	1,838	46.4	0.949
FFS	n/a	55.2	n/a	0.896

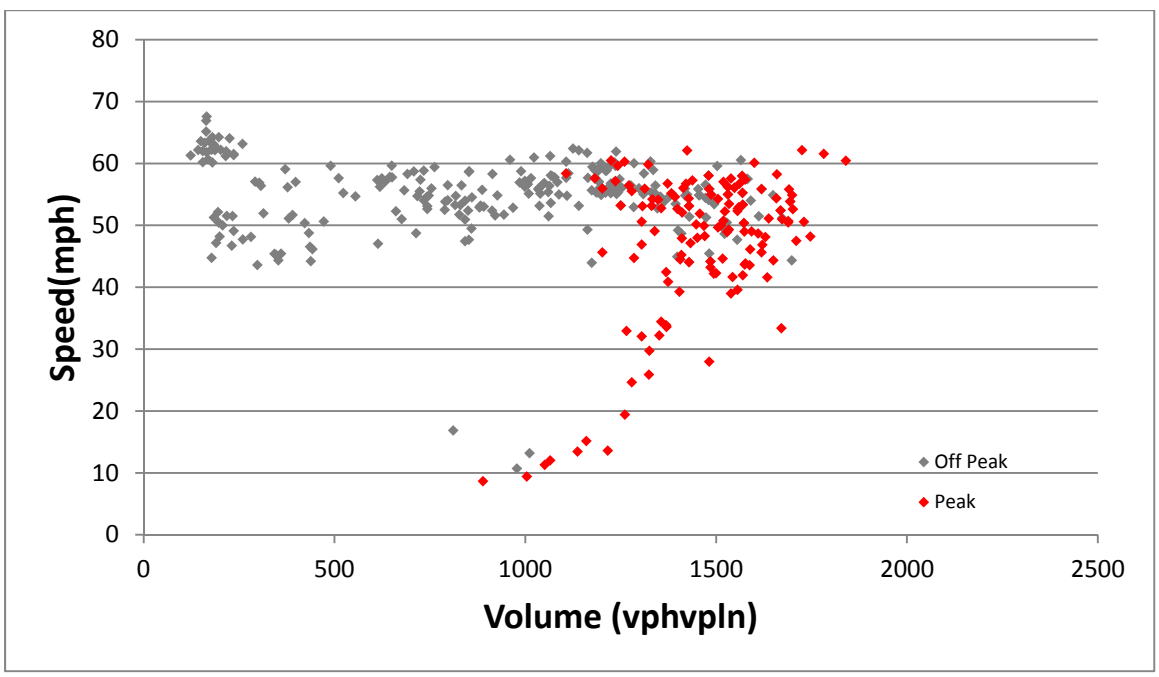

Figure 33 Medium Rain Scenario Speed Flow Diagram

Figure 33 demonstrates the speed flow diagram of the medium rain scenario observations. The majority of the congested observations belong to the peak period and drop in average speed is obvious in the diagram.

Table 24 Average Volume and Speed at Different Time Periods under Medium Rain Scenario

Time Period:	#Observations	Volume				Speed			
		Avg.	Compare to Normal Scenario	StdDev	Compare to Normal Scenario	Avg.	Compare to Normal Scenario	StdDev	Compare d to Normal Scenario
Peak	130	1457	0.932	173	0.883	48.3	0.779	11.9	1.919
Off-Peak	270	942	1.178	457	1.022	54.9	0.896	6.4	1.778
All	400	1110	1.120	459	0.888	52.2	0.854	9.3	2.114

Table 24 represents average volume and speed at different time periods under medium rain condition. The average speed reduces by 22.1% and 10.4% during peak period and off-peak period respectively. The speed dispersion almost doubles in all time periods. The average observed volume during the peak hour reduces by 6.8% which is reasonable compared to the reduction in volume under light rain condition of 4.3%.

However, the average observed volume in off-peak periods and overall increase of 17.8% and 12.0%. This phenomenon can be explained by the fact that off-peak period observed flow rate volume has a high Coefficient of Variation (COV) of 0.49 which means there is a high variability in the data. In other words, there needs to be more observant during the off-

peak period to provide a reliable estimation. It should be noted that off-peak observation is very diverse.

For more illustration, the medium rain scenario includes observations right before and after the peak periods (which are very similar to the peak period observations) alongside midnight and early morning observations which are very light traffic. It seems that average speed during an off-peak time period is more statistically reliable since their respective COV is between 18% to 24%.

5.2.5 Heavy Rain Scenario

The Heavy Rain Scenario has the lowest number of observations among rainy scenarios with total of 80 observation which 25 of them are in the peak period and 55 of them are in the off peak period. The precipitation rate should be higher than 0.25 in/hour to be considered as heavy rain.

Table 25 Heavy Rain Scenario Capacity and FFS Estimation

	# Observations	**Value**	**Std. Dev.**	**CAF/SAF**
Capacity	5	1814	81	0.936
FFS	n/a	58.4	2.6	0.881

Table 25 summarizes the capacity and FFS estimation for the heavy rain scenario. The capacity is reduced by 6.4% and FFS is reduced by 11.9% as a result of heavy rain. Figure 34 demonstrates the speed-flow relationship diagram of heavy rain scenario.

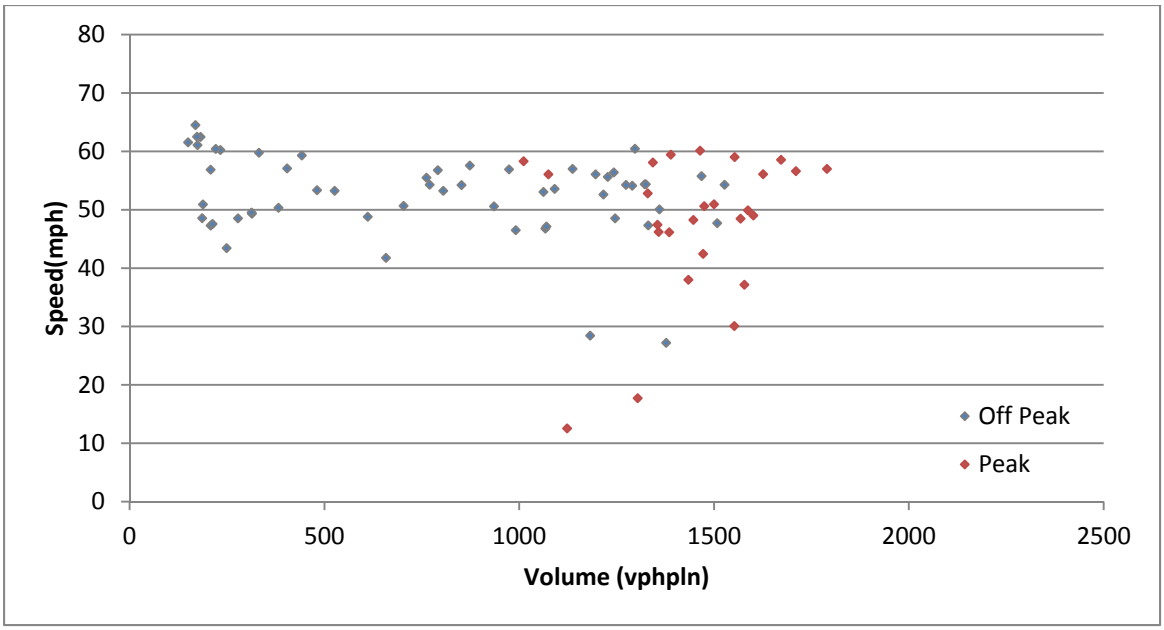

Figure 34 Heavy Rain Scenario Speed-Flow Diagram

Table 26 demonstrates average volume and speed at different time periods under heavy rain condition.

Table 26 Average Volume and Speed at Different Time Periods under Heavy Rain Scenario

Time Period:	#Observations	Volume				Speed			
		Avg.	Compare to Normal Scenario	StdDev	Compare to Normal Scenario	Avg.	Compare to Normal Scenario	Std Dev	Compared to Normal Scenario
Peak	25	1454	0.930	193	0.984	46.2	0.759	12.3	1.98
Off-Peak	55	777	0.971	459	1.02	52.7	0.860	7.0	1.94
All	80	992	1.01	505	0.977	51.2	0.838	9.2	2.09

The average flow rate volumes during the peak period drops by 7.0% compared to the normal scenario. The average speed in the peak period drops by 24.1%. As it was expected, this drop is the highest among all the rain scenarios. Similar to other rain scenarios, the speed dispersion almost doubles compared to normal scenario.

5.2.6 Snow Analysis

There are total of 208 observations in the snow scenario. All the snow observations are categorized in a single category as "Snow Scenario". The following Table 27 summarizes estimated capacity and FFS under snow condition.

In snow condition drivers tend to increase the safety distance with the following vehicle. In result, the density at capacity will decrease significantly compared to the normal condition. Table 27 summarizes FFS and capacity estimation in the snow scenario.

Table 27 Snow Condition Capacity and FFS Estimation

	# Observations	**Value**	**Std. Dev.**	**CAF/SAF**
Capacity	9	1436	23.4	0.741
FFS*	n/a	43.6	n/a	0.904

* FFS has been estimated relaxing the critical speed constraint.

Table 27 summarizes capacity and FFS estimation under snow condition. Note that capacity has dropped by 26.9% and there is a 9.6% percent drop in the estimated FFS. It should be noted that the average of top five percent observed flow rate volumes may not represent the

capacity as some drivers may detour the freeway and use the alternative routes in the snowy weather. Also, there is a possibility of a significant demand drop in the snowy weather.

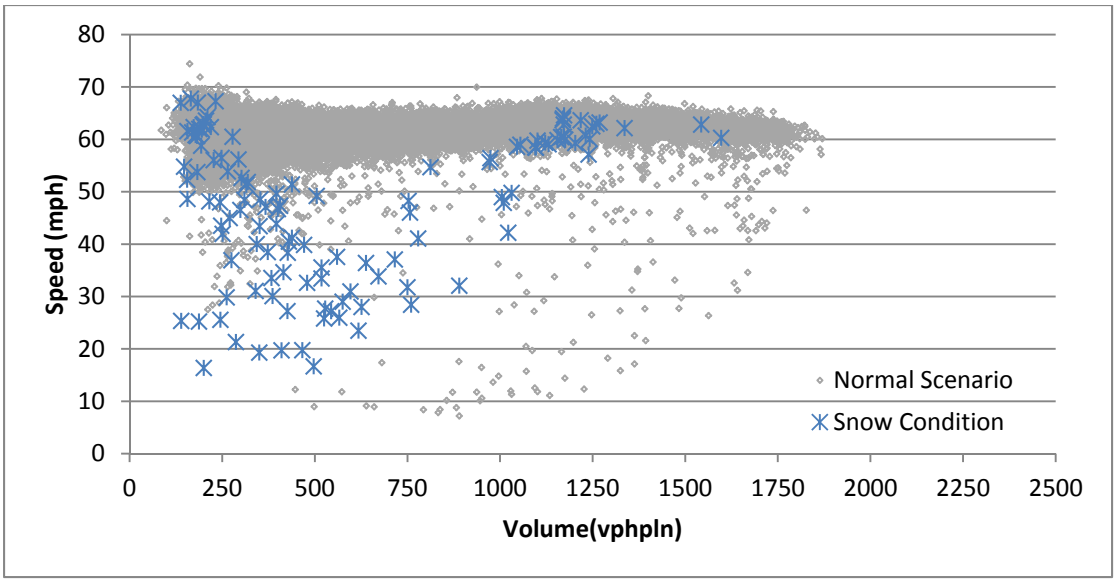

Figure 35 Snow Weather Scenario Speed-Flow Diagram in the Off-Peak Period

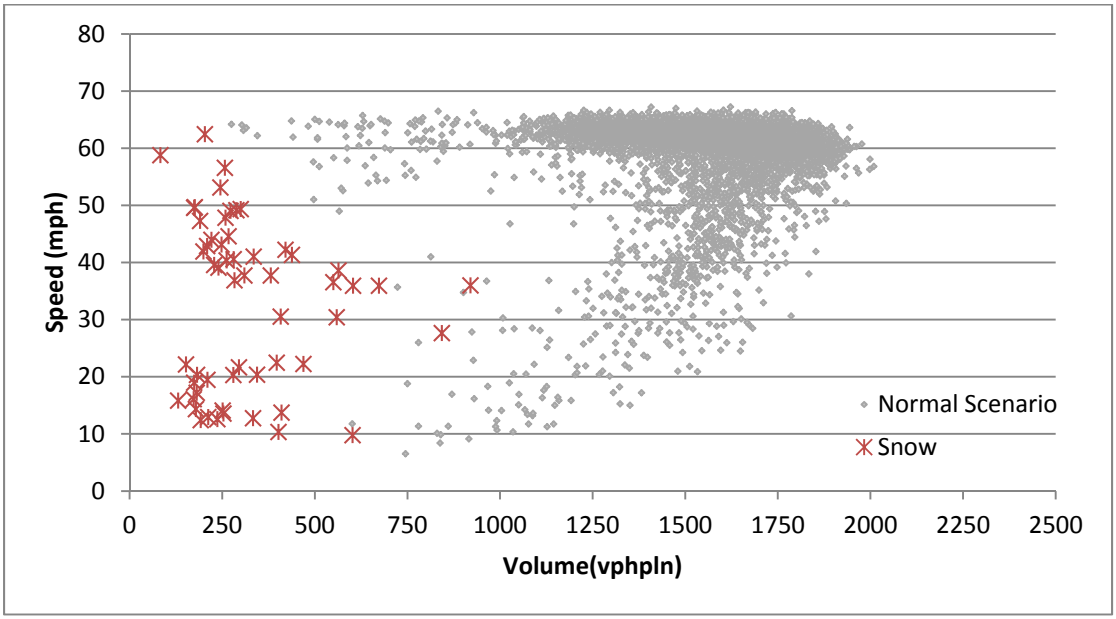

Figure 36 Snow Weather Scenario Speed-Flow diagram in the Peak Period

The speed-flow relationship under snow condition has been illustrated in Figure 35 and Figure 36. The majority of the observations is in the congested regime especially in the peak period.

Table 28 Average Volume and Speed at Different Time Periods under Snow Scenario

Time Period:	#Observations	Volume				Speed			
		Avg.	Compare to Normal Scenario	StdDev	Compare to Normal Scenario	Avg.	Compare to Normal Scenario	StdDev	Compare to Normal Scenario
Peak	30	1009	0.646	286	1.46.	35.1	0.578	16.1	2.59
Off-Peak	178	500	0.625	360	0.805	42.9	0.700	15.9	4.41
All	208	573	0.583	393	0.760	41.8	0.684	16.1	3.65

Table 28 demonstrates average observed flow rate volumes and speed for different time periods. The average observed speed and volumes in different time periods reduce significantly compared to the normal scenario. The average observed flow rate volume in the peak hour drops by 36.4% and the average speed drops by 42.2% during peak hour. Also, the dispersion in both average flow rate volume and speed increases significantly compared to the normal scenario.

5.2.7 Downstream Incident Analysis

The incident database has recorded 436 events including road maintenance operations or work zone events. The duration of the events ranges from 1 minute to eight hours. The events cover 944 15-min observations which 378 are road maintenance observations (work zones)

and 84 observations are combination of weather and incidents. There are four traffic lanes and two shoulder lanes in each direction.

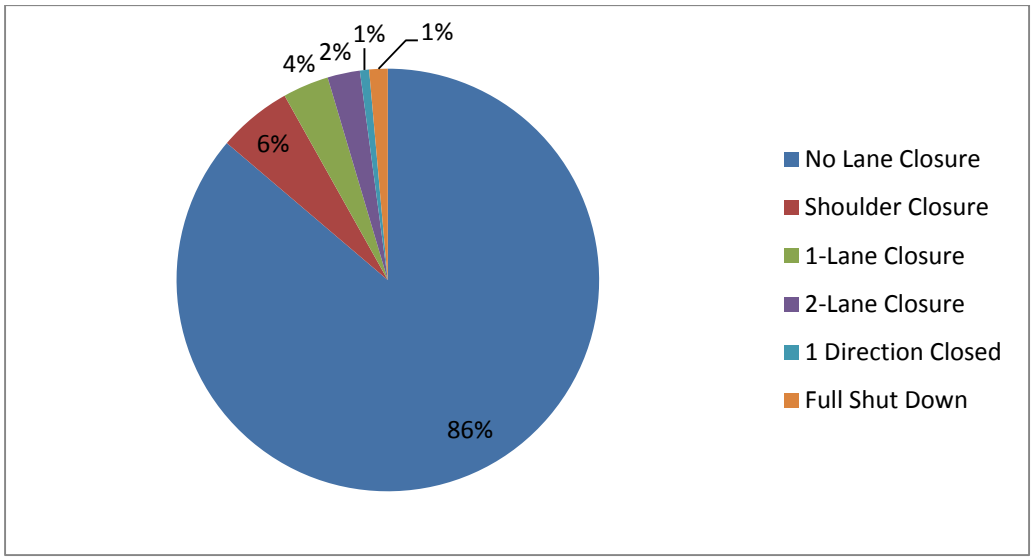

Figure 37 Number of Closed Lane(s) As a Result of an Incident

Figure 37 depicts different types of incident scenario and their relative frequencies in percentages. Note that a majority of incidents do not cause a lane closure and most of the incidents are resolved in a short amount of time. It seems that the incident database only reports documented lane closures by the police enforcement and ignores temporary lane closures because of the incident and blocking vehicles. Most of the incidents with no lane closures are “Disabled Vehicles” which is 51.1%.Collision and accidents account for about 27% of no lane closure incidents. The rest of the incidents with no lane closure include “Obstructions” and “Debris on the roadway”.

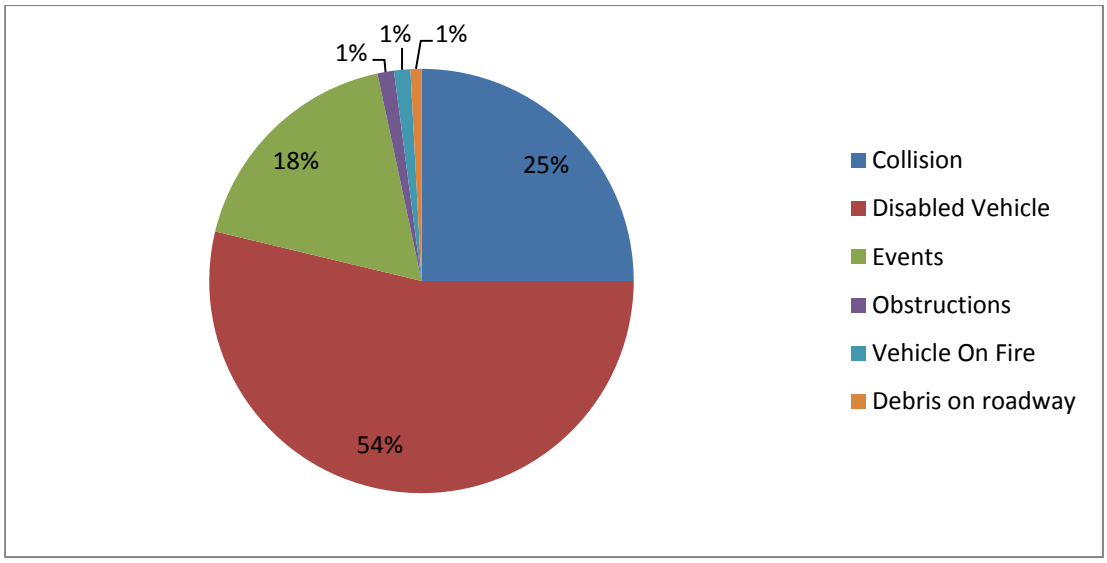

Figure 38 Overall Incident Types

Figure 38 demonstrates different incident types based on total number of 15-min observations they possess in the incident database. While, collisions and accidents account for 25% of the incidents, the majority of incidents have occurred because of "Disabled Vehicles" on the freeway. The final figure in this section demonstrates the distribution of incidents in different days of the week. Note that holidays and weekends are excluded from the incident database.

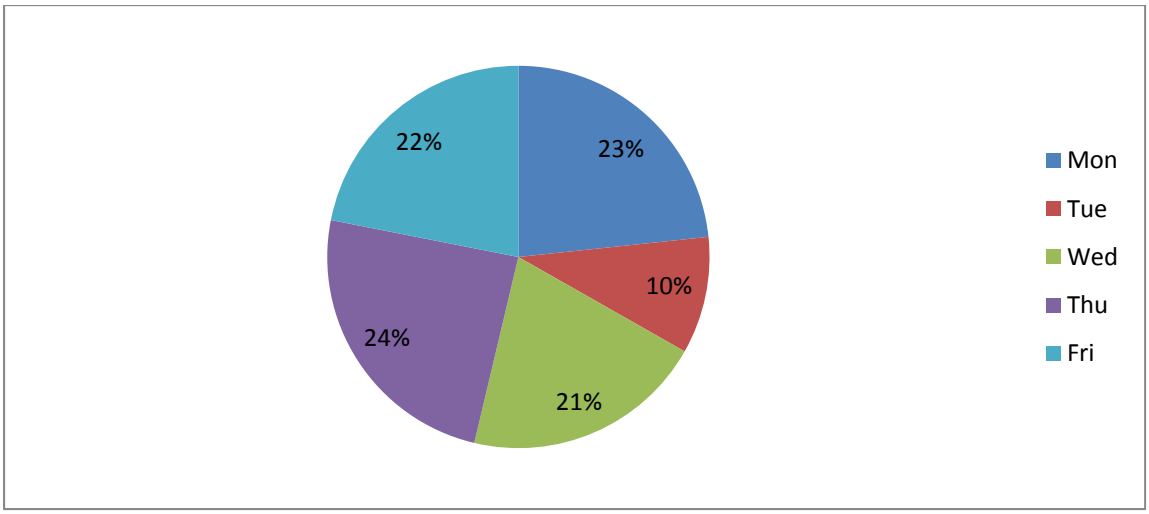

Figure 39 Incidents Distribution over Days of the Week

Referring to Figure 39, it seems that incidents are almost evenly distributed between days of the week except for Tuesdays.

There are total of 488 observations in "No Lane Closure" incident category and number of incidents with shoulder closure is limited to 32 observations. The rest of the lane closure scenarios sum up to 46 observations. It should also be noted that almost half of the incidents are in the upstream position of the sensor. In this case, an incident meters the traffic and results in higher speed observations compared to a downstream incident. Therefore, it is better to combine all the incident scenarios together (except for the relative position to the sensor) and look at the overall impact on the traffic behavior. The downstream incidents also will be analyzed under rain condition. There are total of 50 observations in this combinatorial condition.

The data are also adequate for analyzing the "Rubberneck" effect. The rubberneck effect happens when an incident happens in the other direction of the travel and drivers tend to slow down and look at the other direction incident for their curiosity.

If travel direction and incidents are in the same direction then the observations will be considered in "Downstream Incident Scenario" (Same Direction/Downstream condition in Figure 40) and if they are not in the same travel direction as of the traffic they are considered for the rubberneck effect analysis (Opposite Direction/Downstream and Opposite Direction/Upstream conditions in Figure 40).

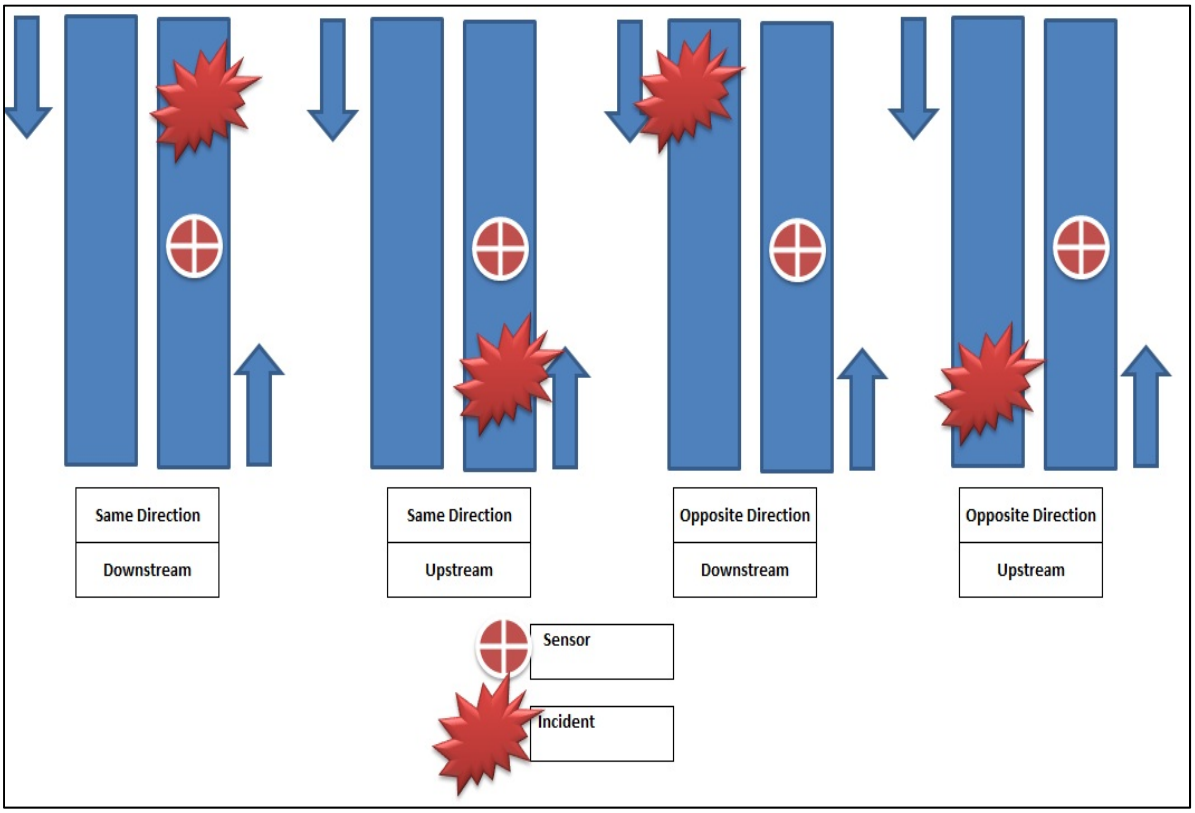

Figure 40 Relative Location of the Incidents to Sensors

The downstream incident scenario can be categorized into two different categories based on the weather type: normal weather and rainy weather. There are 185 observations in normal weather condition and 46 observations in rainy weather condition. Figure 41 demonstrates speed flow diagram for downstream incident scenario under both normal and rainy weather conditions.

Using the modified Greenshields approach to estimate the FFS in the downstream incident scenario, the estimated FFS equals 61.9 mph which does not differ significantly from the normal scenario estimated FFS of 61.6 mph.

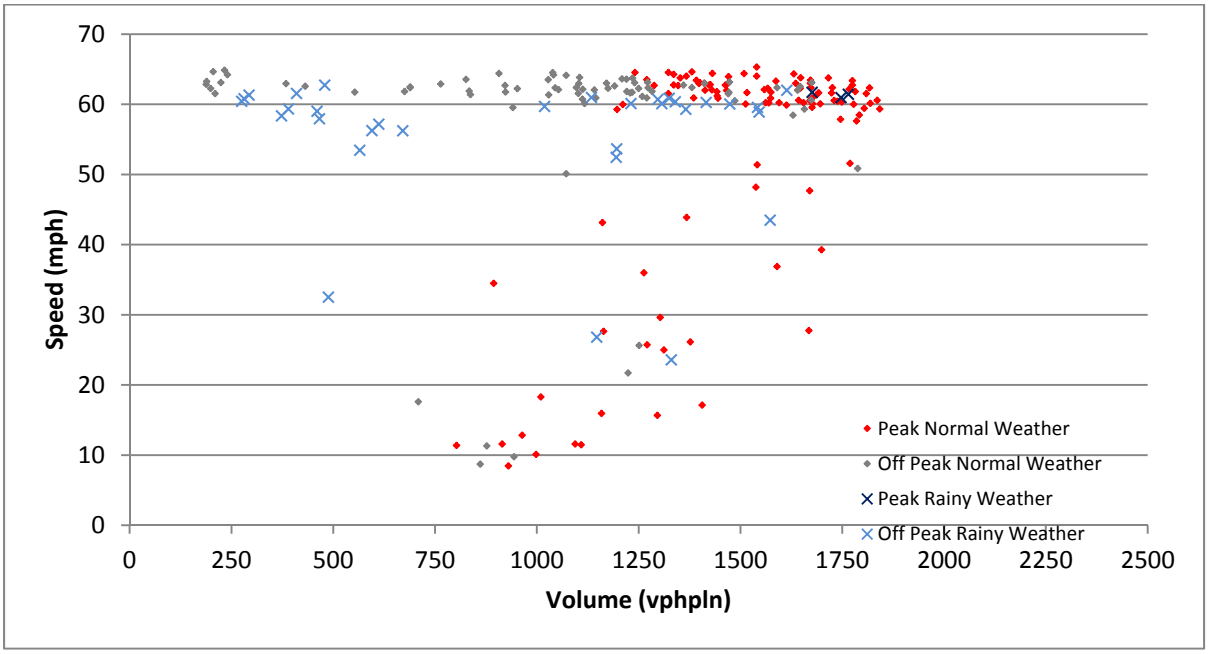

Figure 41 Downstream Incident Scenario Speed-Flow Diagram

Table 29 Downstream Incident Scenario under Normal Weather

Time Period:	#Observations	Volume				Speed			
		Avg.	Compare to Normal Scenario	StdDev	Compare to Normal Scenario	Avg.	Compare to Normal Scenario	StdDev	Compared to Normal Scenario
Peak	108	**1492**	0.955	239	1.219	**53.3**	0.878	16.6	2.677
Off-Peak	77	**1044**	1.305	403	0.902	**58.4**	0.953	12.8	3.556
All	185	**1306**	1.329	540	1.044	**55.4**	0.907	15.3	3.477

Table 29 presents average flow rate volumes and speed in different time periods. This is the only scenario which total number of observations in the peak period are higher than the off peak period. This phenomenon can be explained by the fact that the probability of incident occurrence increases with increase in the total number of vehicles on the freeway (flow rate volume). Since majority of observation in this scenario has occurred in the peak period, therefore overall average observed flow rate volume shows an increase of 32.9% compared to the normal scenario.

The average speed in the peak period decreases by 12.2% and its dispersion almost triples up compared to the normal scenario. This table summarizes a wide variety of incident types and severity and creates only a general image of incidents impact on the traffic stream behavior.

5.2.8 Downstream Incident in Rain Condition

The combinatorial condition of rain and incidents are analyzed in this section. There are 46 observations in this combinatorial scenario which most of them happen in the off-peak period. The rainy weather observations in the under-saturated regime have lower speed compared to the normal weather scenario observations. Figure 42 demonstrates this scenario speed flow diagram.

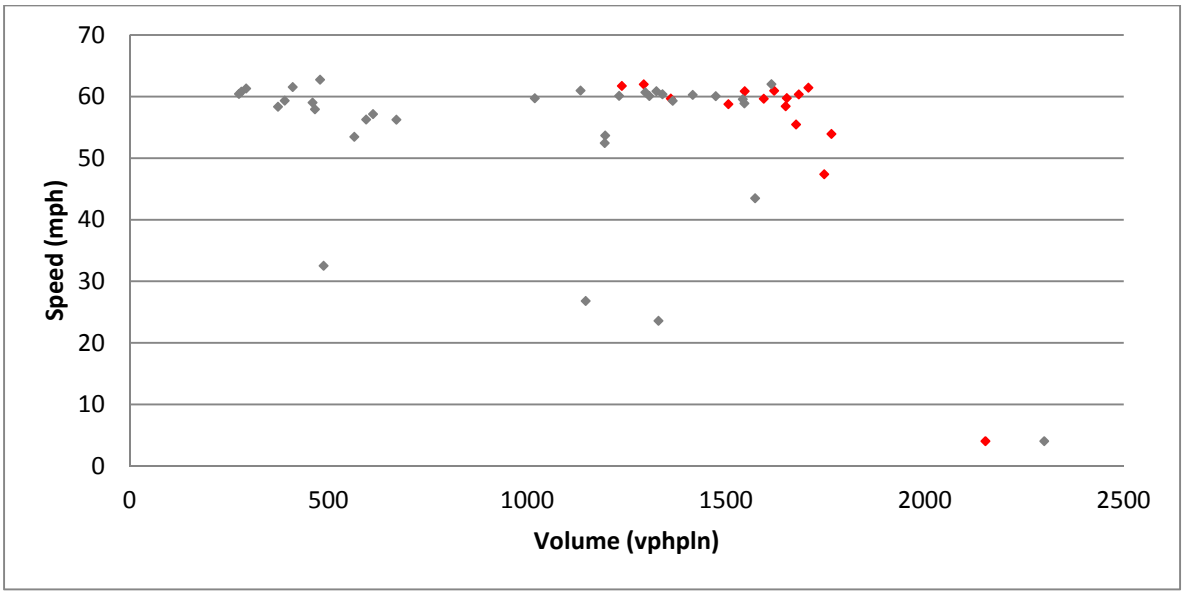

Figure 42 Downstream Incident Scenario Speed-Flow Diagram

There are not enough rainy observations in the congested regime even in the peak period. In the off peak period, there is a 4.8% reduction in average speed and 9.0% reduction in average observed flow rate volumes compared to "Downstream Incident in Normal Condition" scenario. Table 30 summarizes traffic characteristics in this scenario in different time periods.

Table 30 Downstream Incident Scenario under Rain Condition

Time Period:	#Observations	Volume				Speed			
		Avg.	Compare to Normal Scenario	StdDev	Compare to Normal Scenario	Avg.	Compare to Normal Scenario	StdDev	Compare d to Normal Scenario
Peak	14	**1574**	1.00	167	0.85	**58.6**	0.97	16.6	2.68
Off-Peak	32	**950**	1.19	403	0.90	**55.6**	0.91	12.8	3.56
All	46	**1140**	1.15	540	1.04	**56.5**	0.92	15.3	3.48

Similar to the previous scenario the observed volumes are higher compared to normal scenario since the probability of incident occurrence is higher in the high volume conditions. The average observed speed drops in the off peak by 9%.

Although, the methodology is capable of analyzing combinatorial scenario, using the full potential of this capability depends on available data sources.

5.2.9 Opposite Direction Incident (Rubbernecking Effect Analysis)

The observations which an incident occurs in the opposite direction and there is no sign of rain or snow in the facility are considered for rubbernecking effect analysis. This incident situation is represented as “Opposite Direction/Downstream” and “Opposite Direction/Upstream” combinations in Figure 40. Also, Figure 43 demonstrates the speed-flow diagram of the rubberneck effect.

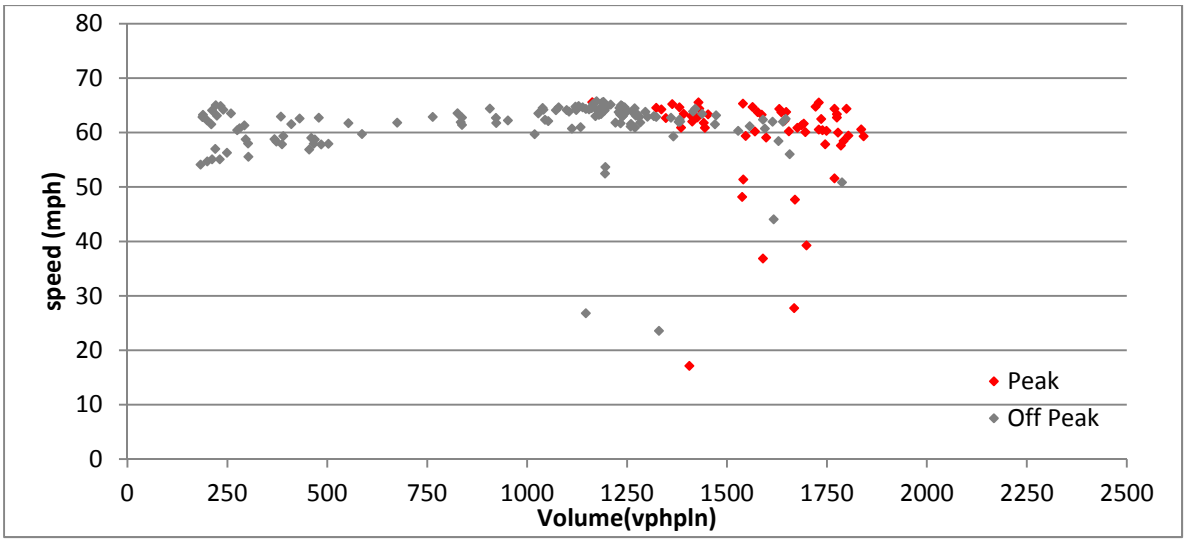

Figure 43 Rubberneck Effect Speed Flow diagram

Table 31 demonstrates the estimated capacity and FFS under this incident condition. It seems that capacity and FFS are not impacted by an incident in the opposite direction in this site. The rubberneck impact is a function of the freeway geometrical characteristics. In the freeways where median is so wide there is no rubberneck effect. The length of the median in the study site is about 30 ft. which a wire barrier separates two directions of travel. This result may change significantly in another site with different geometrical characteristics.

Table 31 Rubberneck Condition Capacity and FFS Estimation

	# Observations	Average	Std. Dev.	CAF/SAF
Capacity	10	1941	26	1.00
FFS	n/a	62.2	n/a	1.00

Table 32 presents average observed volume and speed during different time periods. The average volume during the peak hour increases by few percentages and this increase in the off peak period reaches about 22%.

This phenomenon can be explained considering these are the observations which an incident has been reported and we know that incidents are more likely to occur when there is a high traffic volume on the freeway facility. Therefor the results are biased toward higher observed volumes.

Table 32 Average Flow Rate Volumes and Speed in Rubberneck Impact Analysis

Time Period:	#Observations	Volume				Speed			
		Avg.	Compare to Normal Scenario	StdDev	Compare to Normal Scenario	Avg.	Compare to Normal Scenario	StdDev	Compared to Normal Scenario
Peak	91	**1592**	1.019	168	0.857	**59.2**	0.975	16.6	2.678
Off-Peak	169	**974**	1.218	445	0.996	**61.3**	1.000	12.8	3.556
All	260	**1159**	1.179	477	0.923	**60.7**	0.993	16.9	2.950

While the average speed during the peak period drops by only 2.5%, the dispersion of the average speed increases significantly by 268% and 356% in peak and off-peak periods. This tremendous increase in average speed dispersion is explained by the diversity in the incident types. Incidents severity ranges from a “vehicle with flat tire” to “vehicles on fire” and considering this range, the magnitude of the incident impact varies significantly.

5.2.10 Upstream Incident Scenario

Analyzing the impact of the upstream incidents are as important as downstream incidents since the probability of an incident occurring in the upstream of a sensor is equal to the probability of an incident occurring in the downstream of a sensor. The upstream incident meters the traffic and certainly impacts the traffic stream behavior of the freeway facility.

The efforts to estimate capacity and FFS in this scenario resulted in capacity higher than the capacity measured in the normal scenario. (Figure 44)

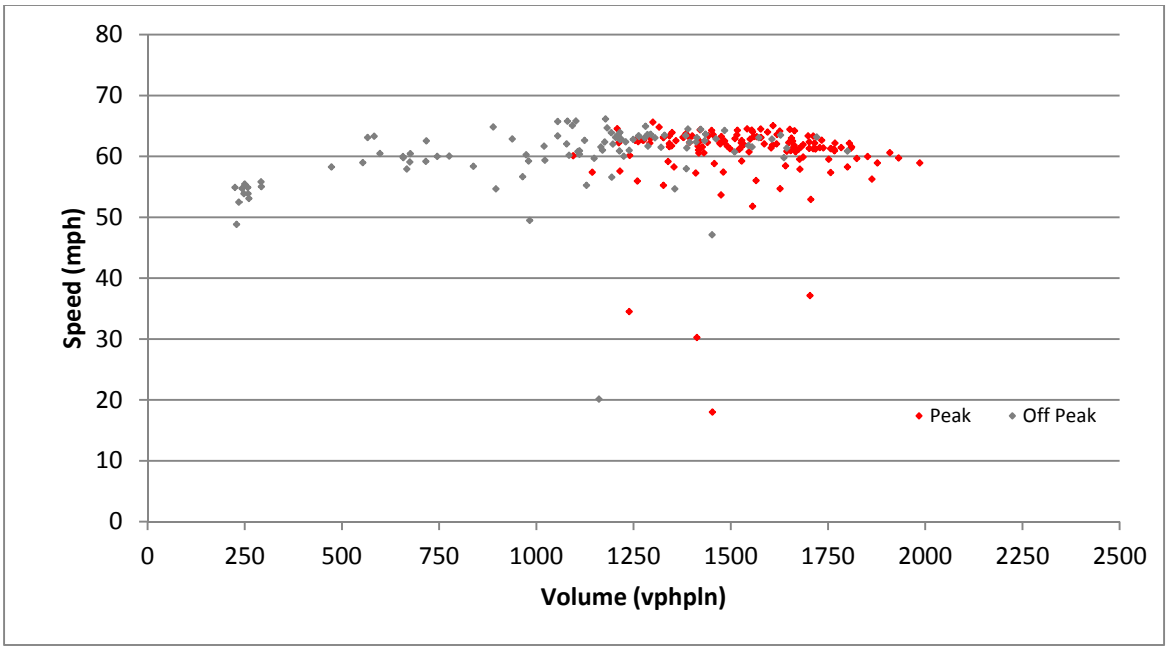

Figure 44 Upstream Incident Scenario Speed Flow Diagram

Table 33 summarizes estimated capacity and FFS findings in this scenario. It seems that the upstream incidents do not impose a significant change in the estimated FFS and capacity of the freeway system.

Table 33 Upstream Incident Scenario Capacity and FFS Estimation

	# Observations	Average	Std. Dev.	CAF/SAF
Capacity	12	1856	60	0.96
FFS	n/a	61.3	n/a	1.00

Table 34 shows the average volume and speed in different time periods in the upstream incident scenario.

Table 34 Average Flow Rate Volumes and Speed in Upstream Incident Scenario

Time Period:	#Observations	Volume				Speed			
		Avg.	Compare to Normal Scenario	StdDev	Compare to Normal Scenario	Avg.	Compare to Normal Scenario	StdDev	Compared to Normal Scenario
Peak	135	1539	0.985	185	0.944	60.5	0.997	16.6	0.968
Off-Peak	102	1065	1.331	395	0.884	60.1	0.980	12.8	1.528
All	237	1335	1.358	376	0.727	60.3	0.987	6.9	1.318

The average flow rate volume drops by 15% in the peak period but the speed almost remains the same. In the off peak period there are relatively higher observed flow rates (33.1%). Obviously, this increase in average flow rates is due to backed up vehicles in the queue upstream of the sensor. This phenomenon obviously is more noticeable during the off peak period. The average flow rate volumes in the off peak and overall time periods are the highest observed flow rates among all the scenarios.

5.3 Delay Analysis

In this section a method is used to estimate incremental delays of different sources of congestion. The delay for each congestion source is estimated using a five step approach. A simple approach was used to estimate the delay for each time period. This approach is presented in the following:

$$VHD_i = \text{Max}(0, 0.25 * (\frac{x_i}{v_i} - \frac{x_i}{FFS}) * flow_i)$$

Where,

FFS**:** free-flow speed (mph)
v_i: average speed at time period *i* (mph)
$\boldsymbol{x_i}$**:** distance travelled in time period *i* (mile)
$flow_i$*:* volume in time period *i* (vph)

Selecting a constant value of 1 mile for x_i, VHD_i equals veh hours of delay in 15-min time interval.

In order to calculate the incremental delay for each scenario the following steps should be taken:

1- Categorize each 15-min observations into different categories based on the congestion source they represent. For example normal, light rain, and medium rain condition.

2- Calculate VHD_i for each 15-min time interval. Sum the values for each scenario and calculate Scenario Average Delay (SAD) for each vehicle by dividing the total calculated scenario delay by total number of observed vehicles in this particular scenario.

$$Scenario\ Average\ Delay\ (SAD)_j\ (hour) = \frac{\sum_1^{n_j} VHD_i}{0.25 \sum_1^{n_j} flow_i} \qquad j\ \varepsilon\ \{Scenarios\}$$

Where,

SAD_j: Average scenario delay in 15-minute time interval for scenario j
n_j: Total number of observations in scenario j

3- In this step, the incremental delay for each scenario is calculated using the following equation:

$$Scenario\ Specific\ Average\ Delay(SSAD)_j(hour) = SAD_j - SAD_{normal}$$

4- The estimated Total Scenario Delay (TSD) is calculated by:

$$Total\ Scenario\ Delay_j\ (hour) = SSAD_j \times n_j$$

5- In the last step, Scenario Delay Contribution (SDC) is calculated in percentage using the following equation:

$$Scenario\ Delay\ Contribution_j(\%) = \frac{TSD_j}{\sum_1^j TSD_j} \times 100 \qquad j\ \varepsilon\ \{\ Scenarios\ \}$$

Table 35 demonstrates step by step analysis of the proposed delay analysis framework.

Table 35 Step by Step Delay Analysis Result Summary

	Step 0		Step 1	Step 2	Step 3	Step 4	Step 5
j	# Obs.	$0.25\sum_{1}^{n_j} flow_i$	$\sum_{1}^{n_j} VHD_i$ (veh-hrs)	SAD_j (min)	$SSAD_j$ (min)	TSD_j (min)	SDC_j (%)
Normal Condition	41,842	10,287,357	5,637	0.033	0	0	0.0
Wet Pavement	2,227	550,767	568	0.0619	0.0290	15,963	10.2
Light Rain	2,212	532,639	1,290	0.145	0.1124	59,883	38.2
Medium Rain	400	110,791	531	0.287	0.2544	29,188	18.0
Heavy Rain	80	20,720	123	0.355	0.3224	6,680	4.3
Snow	208	29,812	388	0.781	0.7484	22,313	14.2
Light Rain Incident	35	10,302	46	0.269	0.2363	2,434	1.6
Down. Incident	185	60,390	343	0.341	0.3081	18,604	11.9
Upstream Incident	237	79,113	67	0.0510	0.0181	1,431	0.9
WZ	186	37,468	42	0.0671	0.0342	1,281	0.8
Sum	47,618	11,719,358	9,034	2.392	2.063	156,77	100.0

In order to calculate percent contribution of recurrent vs. non-recurrent congestion, total delay in normal scenario (5,637 veh-hrs.) was considered as recurrent delay and delay in all other scenarios was summed up as non-recurrent delay (3,397 veh-hrs.). It was found that 62% of delay are due to recurrent congestion sources and remaining 38% is due to non-recurrent congestion sources.

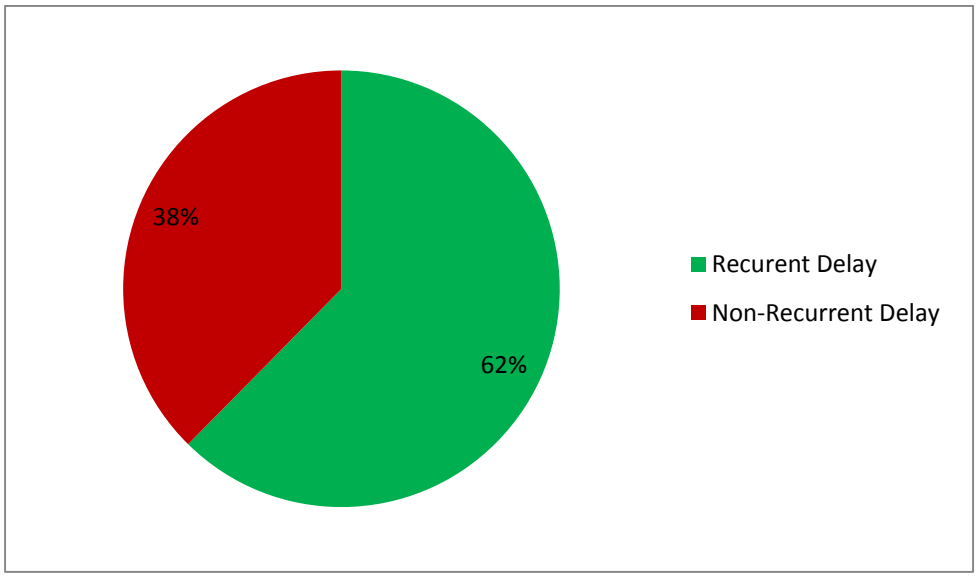

Figure 45 Non-Recurrent vs. Recurrent Congestion Sources

The deeper analysis of non-recurrent congestion sources revealed than light rain scenario has the highest contribution rate with 38% of overall non-recurrent delay. Medium rain and wet pavement scenario are next two contributors with 18% and 10% respectively. Incidents account for near 15% of non-recurrent delay while snow condition contributes 8%. Figure 46 demonstrates breakdown of the non-recurrent congestion sources total delay (38% in Figure 45). Figure 47 demonstrates a pie chart of number of observations in each non-recurrent congestion scenario.

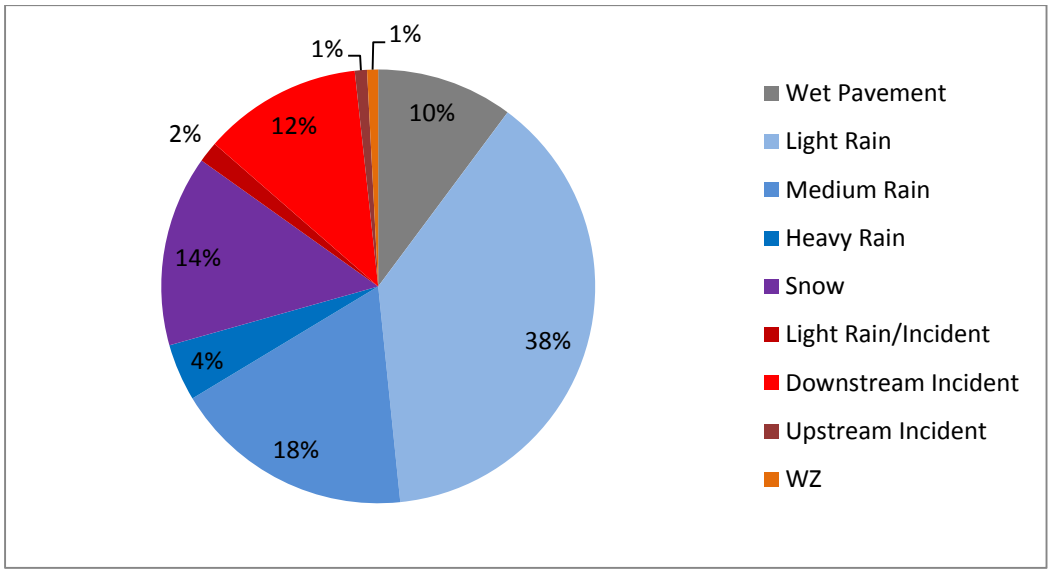

Figure 46 Breakdown of Non-Recurrent Congestion Sources

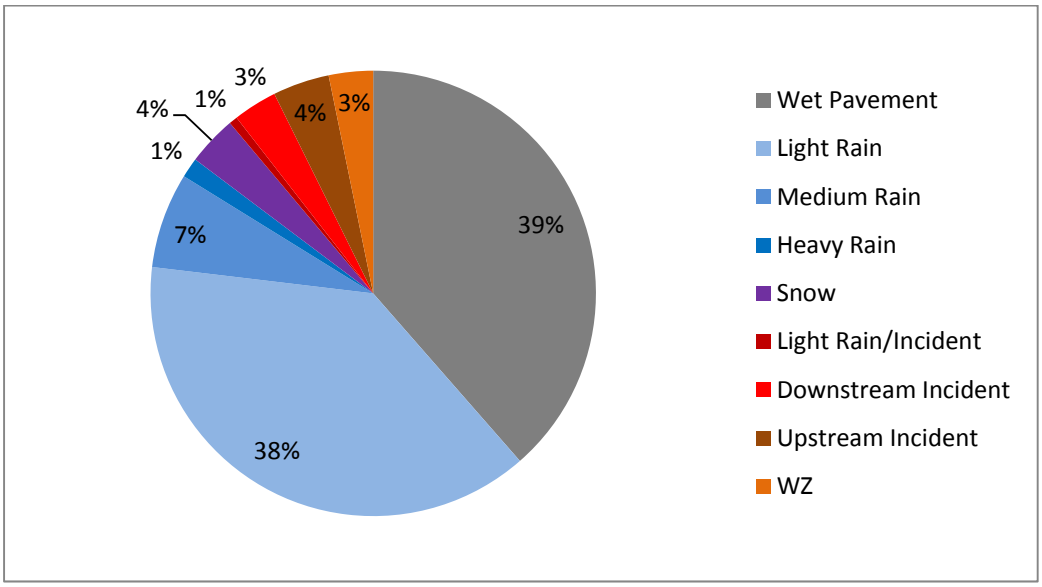

Figure 47 Breakdown of Number of Observation in Each Non-Recurrent Congestion Source

Figure 48 depicts Scenario Average Delay (SAD) per Vehicle for each scenario type. The snow has the highest impact on freeway traffic behavior compared to other traffic sources.

For example, SAD of 0.8 minutes/vehicles (for snow scenario) means that a vehicle will experience 0.8 minutes delay travelling one mile of the facility in the snow condition every 15-min time interval.

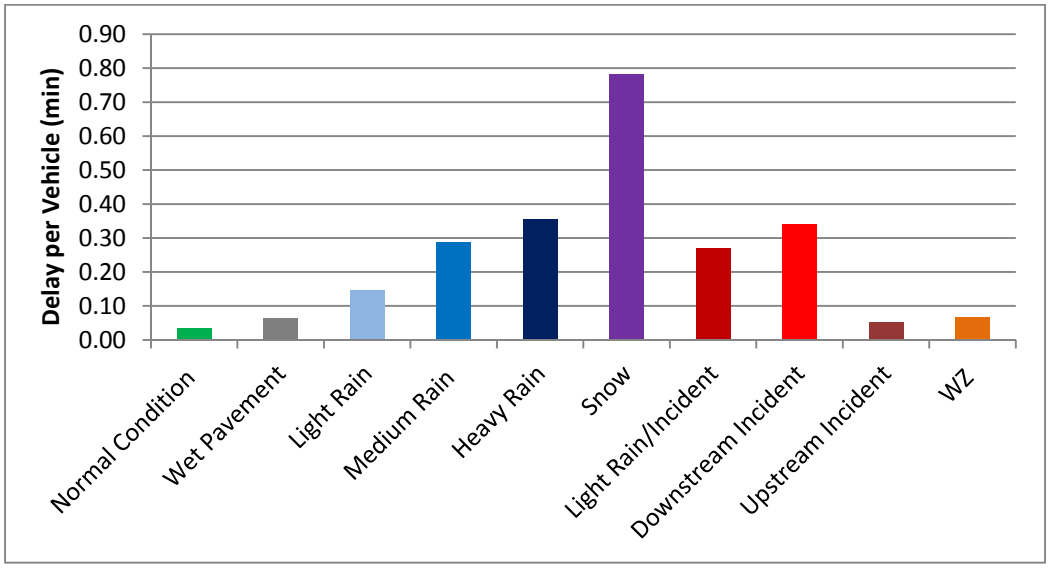

Figure 48 Scenario Average Delay (SAD) per Vehicle for Each Scenario

5.4 Trumpet Impact Analysis

Since all the inclement weather conditions and reported incidents are excluded from the normal scenario data, it was expected to observe low volume observations are centralized around estimated FFS. However, even in the normal scenario. The average reported speed ranges scatters from 45 mph to 75 mph in low volume observations of the speed-flow domain. The variability in speed drops significantly as the volume increases. This phenomenon creates a shape in the speed-flow diagram that resembles a "Trumpet" shape. Thus, this analysis is termed as "Trumpet Impact Analysis". (Figure 49)

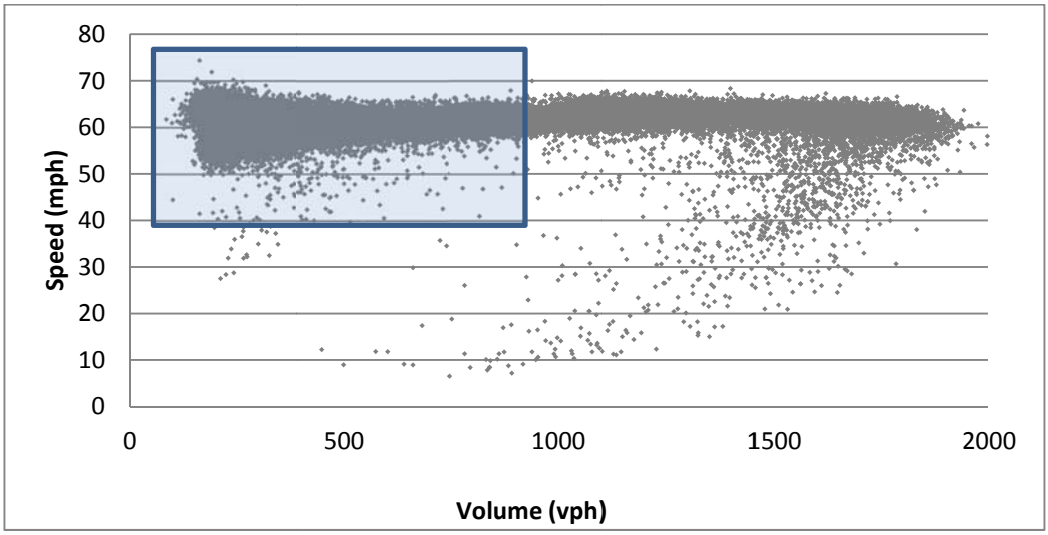

Figure 49 Trumpet Shape in Low Volume Speed Flow Observations

The objective here is to understand this phenomenon. Initial hypothesis is that the low observed speeds could be related to lighting conditions on the freeway. Another possible contributor might be the sample size over which the speed is reported. In order to test these hypotheses, two separate analyses were conducted as follows:

1- Light vs. dark condition: data are divided into two categories of light and dark conditions and the speed-flow scatter diagram for each category is generated. It should be noted that the study site does not have any lighting device at night as confirmed from the street view tool of Google map.(Google Maps,2013)

2- Sample size effect: The number of vehicles passing the sensor in 15-min time interval is actually a sample size of the reported average speed estimation. The reported average speed in the sensor is the average speed of vehicles passing the sensor in 15-min time interval.

The hypothesis is that if the sample size increases the average speed dispersion decreases.

Three separate studies were conducted to test this hypothesis. In the first analysis observations with volumes less than 1,000 vph are divided into 10 categories based on total number of vehicles (in 100 vehicles increment). In the second analysis, in order to make sure that there are equal number of observations in each category, data are sorted and data are categorized into 10 categories with equal number of observations. Since there are 7,900 observations with observed volume less than 1,000 vph, there are 790 observations in each category.

In the third analysis, observations are aggregated such that each speed observation is the average speed of 200 vehicles passing the sensor in 15-min time interval. The base number of 200 has been selected since it represents a condition where the trumpet shape does not exist. Therefore, if observations which are in the low volume area (less than 200 vehicles per 15-min time interval), get aggregated to represent an observation with 200 vehicles per 15-min time interval then the resulted speed-flow diagram is generated by observations with the

same sample size. If the trumpet shape disappears, it can be concluded that the sample size is the variability source of speed in low volume observations. The following section will describe each approach in more details:

5.4.1 Light vs. Dark Condition Analysis

Data are divided into two categories of light and dark conditions in this analysis and the speed-flow diagram is generated for each condition. Information about sunrise, sunset, dawn, and dusk time in Baltimore was acquired using Gaisma.Com website (Gaisma.com, 2013). Figure 50 demonstrates sunrise, sunset, dawn, and dusk times for Baltimore City and the following Table 36 shows the start and end of the light (day) condition for each month.

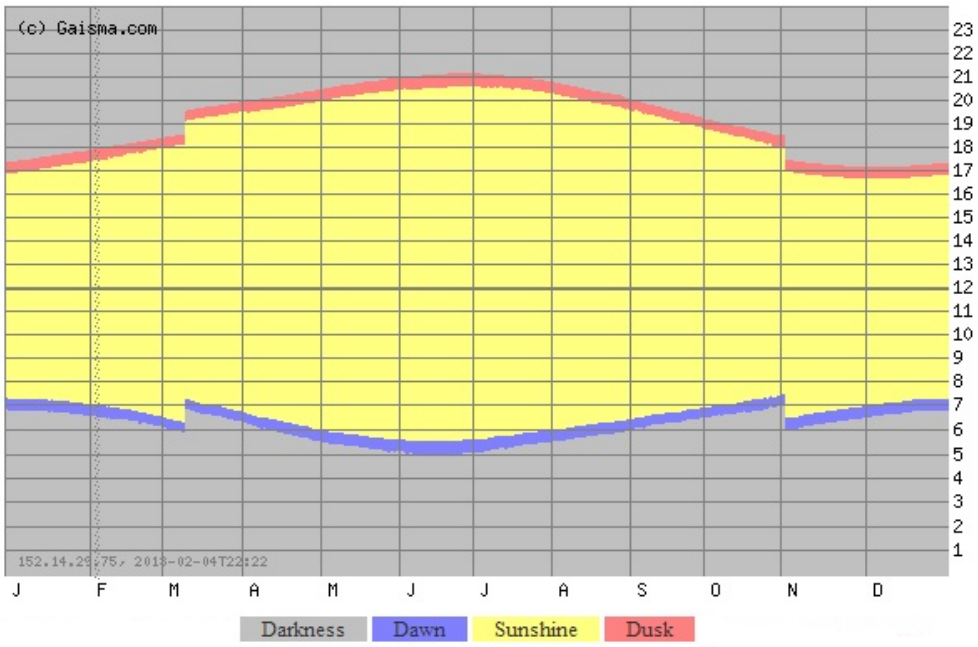

Figure 50 Baltimore City Sunrise, Sunset, Dawn, and Dusk Times. (Source: Gaisma.com 2013).

Table 36 Baltimore Daylight Start and End Times

	Day Light Starts (AM)	Day Light Ends (PM)
January	7:00	5:30
February	6:30	6:00
March	6:30	7:00
April	6:00	8:00
May	5:30	8:30
June	5:30	8:30
July	5:30	8:30
August	6:00	8:00
September	6:30	7:30
October	7:00	6:30
November	6:30	5:00
December	7:00	5:00

(Source Gaisma.com, 2013)

The normal scenario data was divided into 24 bins based on the observation month (12 combinations) and dark vs. light condition (2 combinations). New light and dark conditions were aggregated in order to create two datasets of light and. dark conditions. Figure 4 and Figure 5 illustrate the speed-flow diagram for each of the conditions:

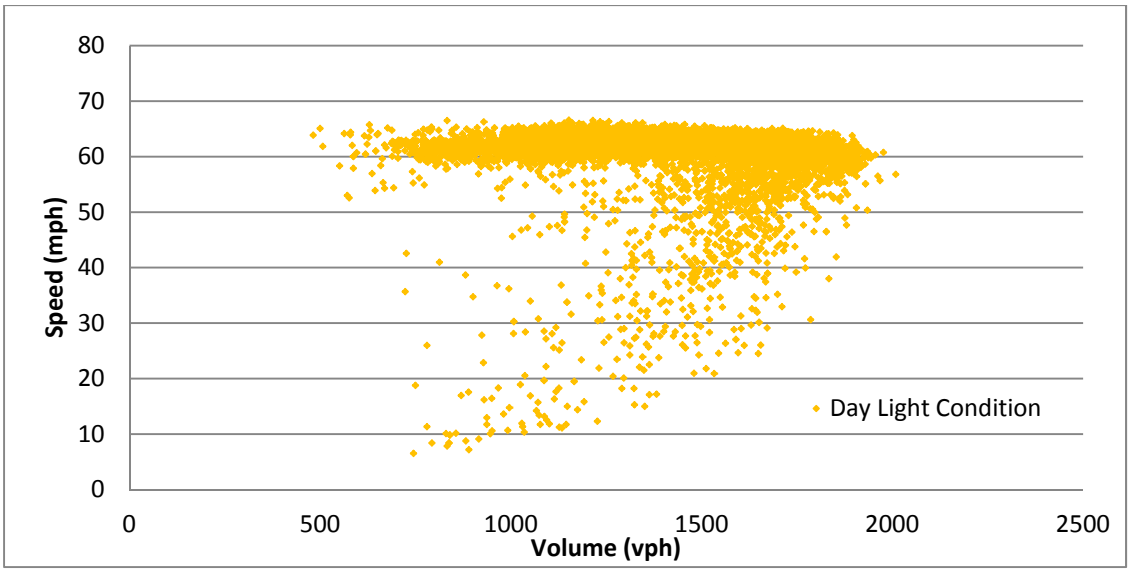

Figure 51 Speed-Flow Diagram under Light Condition

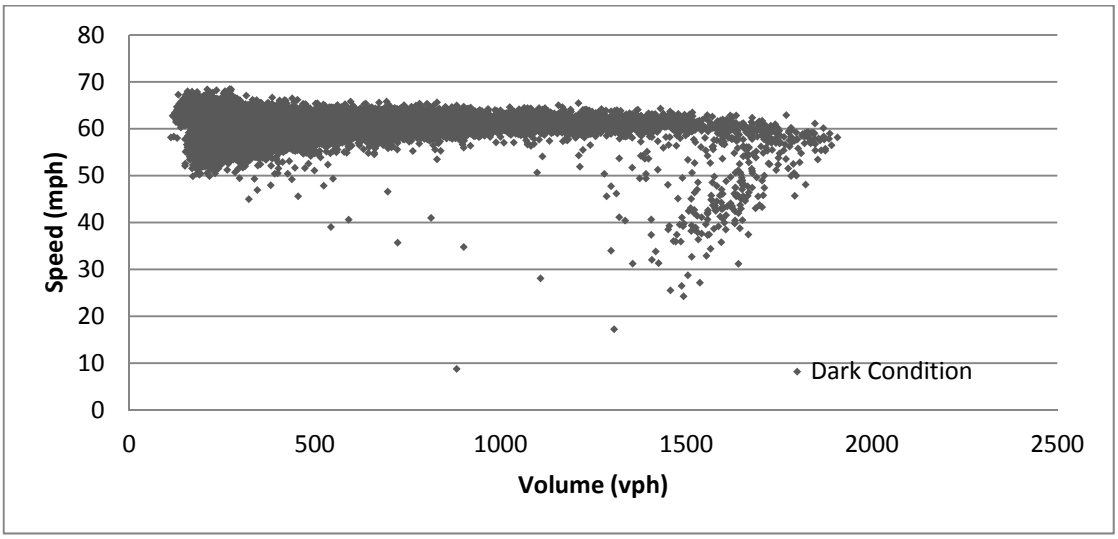

Figure 52 Speed-Flow Diagram under Darkness Condition

Apparently, the speed-flow diagram under darkness condition generates a trumpet shape in low volume observations while in daylight condition, not many observations exist in the low volume area. It seems that the sample size might be a determining factor in trumpet shape of the dark condition.

5.4.2 Sample Size Effect

In the first analysis, the observations in dark (night) conditions with volume less than 1,000 (vph) where divided into 10 categories in 100 (vph) increments. No observation existed in the first category (0-100 mph), therefore, the total number of categories were reduced to 9 groups.

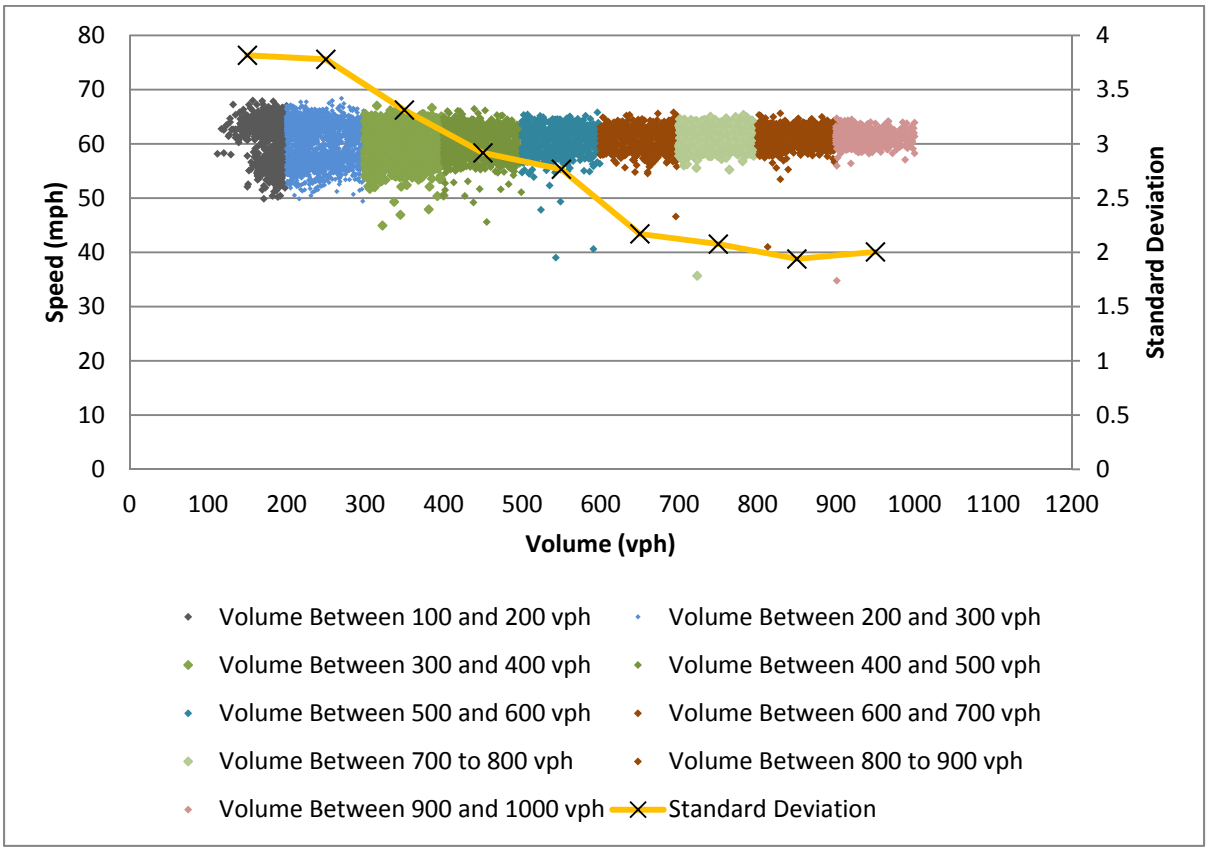

Figure 53 Dark Condition Speed Flow Diagram for Observations with Less than 1000 vph Categorized in Different Groups with 100 vph Increment

Figure 53 illustrates each category its respective standard deviation. The speed dispersion decreases as the sample size (number of observations) increases.

This fact is intuitive, since a speed observation is representing the average speed of vehicles passing the sensor in 15-min time intervals. Thus, when few vehicles pass the sensor in a 15-min interval, highly dispersed speed observations impact the standard deviation more significantly than the situation when the sample size is comparably high.

In the second analysis, data are divided into groups which each group has an identical number of observations. For this reason, the observations volume less than 1,000 (vph) are divided into 10 categories which each category has identical number of observations equal to 790.

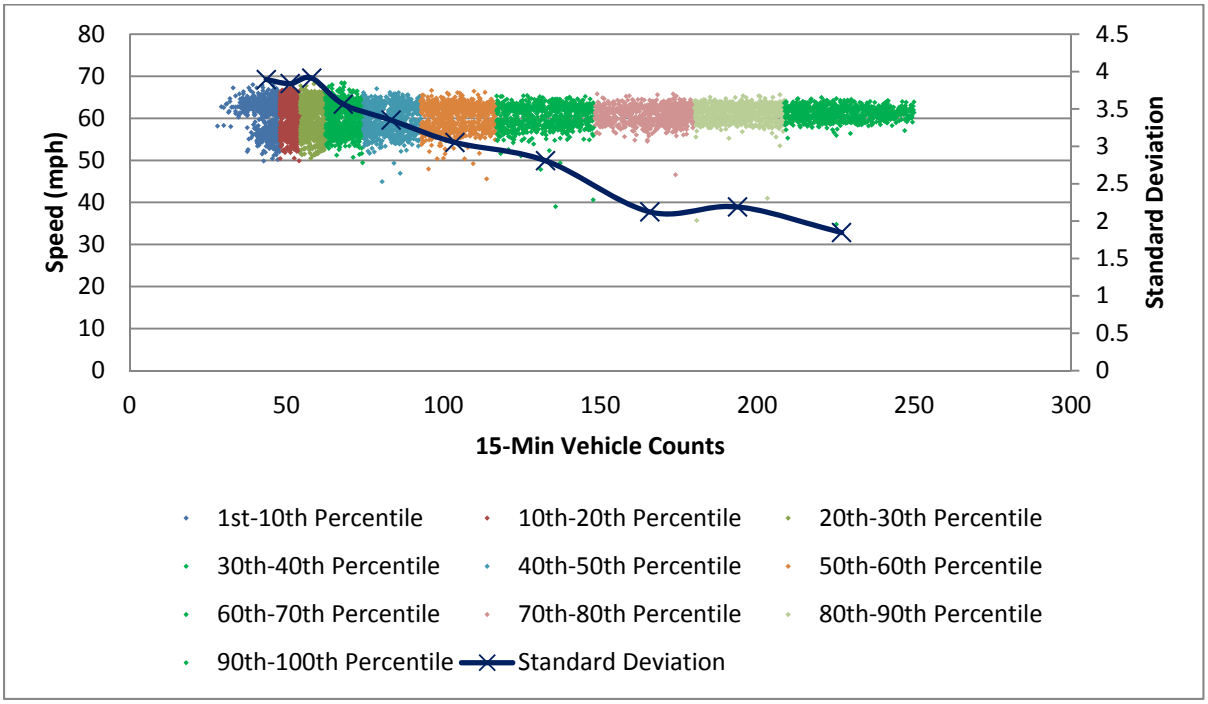

Figure 54 Speed Dispersion Reduction by Increasing Sample Size (Vehicle Counts)

Figure 54 shows that by keeping the total number of observations fixed, the speed dispersion decreases as vehicle counts increase. This finding is intuitive since the reported speed has less variability when sample size increases.

In the third analysis, in order to control for the sample size impact, observations were aggregated together to provide a new set of observations in which each of the observations are representing an average of 200 vehicle counts compared to their original 15-min vehicle counts. The algorithm used to aggregate different observations is explained in the following:

1- Combine (k) observations with vehicle counts (c_i) less than 200 vehicles per 15-min such that

$c_1 + c_2 + \ldots + c_{k-1} + f * c_k \geq 200$

Where (c) is the observation of vehicle count and (f) is a fractional factor which is between 0 and 1.

2. Estimate the combined observations speed and vehicle counts using the following equations:

$\tilde{c} = 200/ (k + f - 1)$

$\tilde{v} = (v_1 c_1 + v_2 c_2 + \ldots + v_{k-1} c_{k-1} + f * v_k c_k) / 200$

Where,

$\tilde{c}$: Represents an estimate of the number of vehicles passing the sensor in 15-min time interval. The unit of ($\tilde{c}$) and (c) are the same.

$\tilde{v}$: is the average speed of combined observation. It is the average speed of 200 vehicles exactly.

3- Eliminate count variables already used for the analysis: (c_1, c_2 , … , c_{k-1}, c_k)

4- Repeat Step 1 to 3 until all the observations are combined.

For example, suppose that:

c_1, c_2, …. to c_4 = 43, 47, 56.5, 57 (veh per 15-min) and

$v_1, v_2, \ldots\ldots to\ v_4$= 55, 62, 57, 62……(mph)

Then:

$c_1 + c_2 + c_3 = 146.5 < 200$ and $c_1 + c_2 + c_3 + c_4 \geq 200$

$f = \frac{200-(43+47+56.5)}{57} = 0.939$

$c_1 + c_2 + c_3 + f * c_4 = 200$

A new combined observation has been created which the average speed is the average speed of exactly 200 vehicles passing the sensor in 15-min time interval. The estimated vehicle count is calculated as:

$\tilde{c}$ = 200/ (k +f-1) = 200/(4+0.939-1) = 50.77 vehicles per 15-min

The estimated average speed of the newly combined observation is calculated as:

$\tilde{v} = (v_1 c_1 + v_2 c_2 + \ldots + v_{k-1} c_{k-1} + f * v_k c_k) / 200$

$\tilde{v}$ = (55*43 + 62*47 + 57*56.5 + 0.939*57*62) / 200 = 59.1 mph

Therefore, four data points were combined to represent an observation with vehicle counts of 50.77 (vehicles per 15-min time interval) and speed of 59.1 mph. Next, the algorithm will select other observations to create new combined observations.

The average speed of the combined observations, are average speed of exactly 200 vehicles which pass the sensor in 15-min time interval. This results in observations which each represent 200 vehicles. The number 200 has been selected as the base number since there is no trumpet shape in observations which approximately have 200 vehicles (Figure 54). Another reason for selecting the number 200 is that this number is dividable by multiple numbers such as (10, 5, 4, and 2) which eases calculation by hand to test the method.

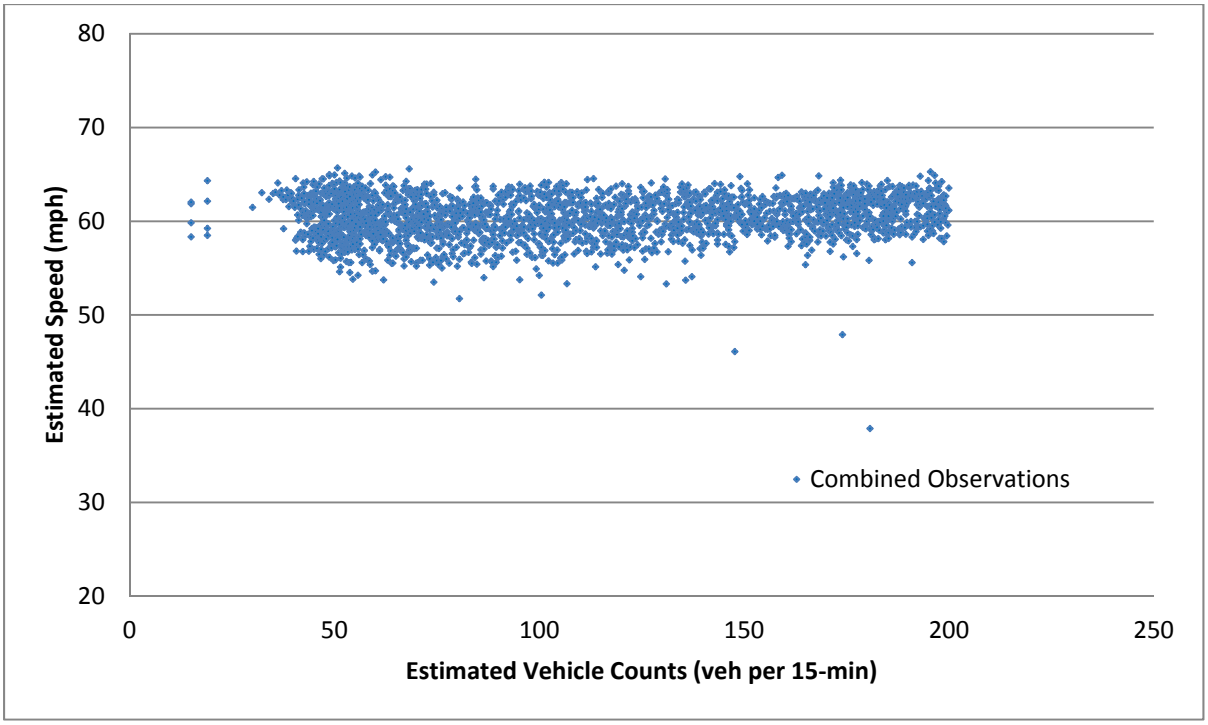

Figure 55 The Visualization of the Combined Observations

Figure 55 demonstrates the speed-flow relationship of the combined observations. The dispersion in the low-vehicle count area of the speed-flow domain has been reduced significantly compared to original speed-flow diagram under dark condition (Figure 52) and the “trumpet shape” does not exist anymore. This visualization analysis supports that the sample size is determining factor in creating the trumpet shape impact. When the impact sample size is removed from the analysis, the trumpet shape in the low volume area of the speed-flow domain vanishes disappears.

6. IMPLEMENTATION

6.1 Overview

This chapter summarizes research efforts to enable HCM methodology with travel time reliability analysis. The chapter starts with the incorporation of SAF and CAF in basic, merge/diverge, and weave segments. Next, the two-capacity phenomenon implementation is described in detail. The chapter ends with introduction of recently added performance measures to the methodology. The recent enhanced performance measures provide better explanation about severely congested scenarios.

6.2 Incorporation of Speed Adjustment Factor (SAF) for Basic Segments

The effects of weather and incidents on freeway facilities are modeled through a CAF in the HCM 2010. However, there is strong evidence in the literature (as it was demonstrated in Chapter 2 of this document) that inclement weather condition also affect the free-flow speed, with especially severe weather events like heavy rain and snow resulting in significant speed drops even at very low volume levels. Therefore, there was a need to incorporate an adjustment factor to account for speed drop. This adjustment factor is Speed Adjustment Factor (SAF).

For basic segments HCM 2010 Equation 25-1 was modified to account for SAF. The equation dates back to the HCM 2000, and uses a CAF to estimate a revised speed-flow relationship for work zones and incidents, using as input the base capacity (C), the free-flow speed (FFS), the CAF, and the prevailing flow rate (v_p). The updated equation is shown below, which adds SAF as a multiplier of the FFS:

$$\boldsymbol{S = (FFS * SAF) + \left[1 - e^{ln\left((FFS*SAF)+1-\frac{C*CAF}{45}\right)*\frac{v_p}{C*CAF}}\right]} \quad (29)$$

Where,

S = segment speed (mi/h);
FFS = segment free-flow speed (mi/h);
SAF =segment speed adjustment factor;
C = original segment capacity (pc/h/ln);
CAF = capacity adjustment factor;
v_p = segment flow rate (pc/h/ln);

With the revised Equation 25-1, the HCM 2010 results remain unchanged for cases with SAF=1.0. The introduction of SAF results in internally consistent results and further provides an additional calibration tool to local conditions and driver culture. The data analysis efforts in this study can provide a good estimate for SAF. It will also provide a framework to estimate local values for incorporation inside HCM methodology.

In order to model the non-recurrent congestion sources appropriate SAF and CAF will be used. In cases when no FFS adjustment is necessary (no recurrent congestion) then SAF equals 1. It should be noted that Equation (29) is only being used when either speed or capacity adjustment is necessary.

An example application of SAF and CAF for different base free flow speeds and weather categories is shown in Figure 56. The graph shows impacts of medium rain (dashed) and heavy snow (dotted), relative to clear weather conditions (solid line) for base free flow speeds of 75 (dark), and 55 (gray) miles per hour. The adjustment factors used in this graph have been acquired from HCM 2010.

It should be noted that CAF and SAF are not independent and the following inequality constraint should hold when selecting the adjustment factors.

$$\boldsymbol{CAF} \leq \frac{\boldsymbol{C-[10*FFS(1-SAF)]}}{\boldsymbol{C}} \qquad (30)$$

Where all the variables have been defined earlier.

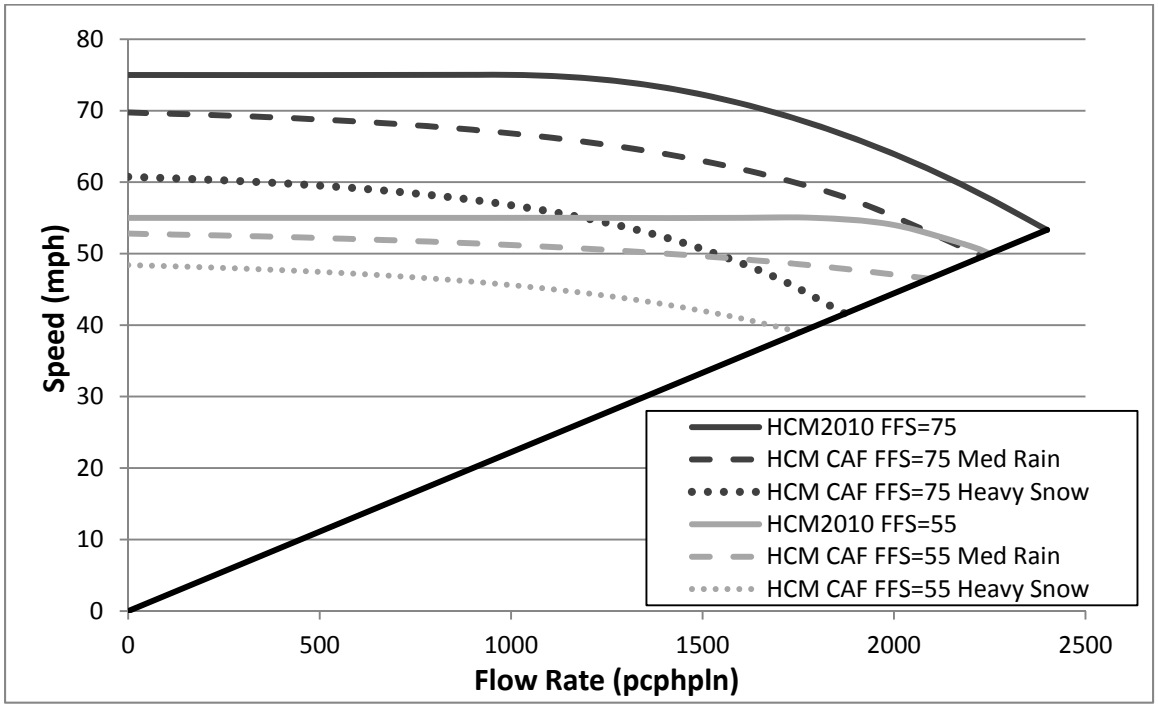

Figure 56 Example Application of SAF and CAF for Different base FFS and Weather Categories.

6.3 Consideration of CAF and SAF for Other Segment Types

6.3.1 Overview

The equation for CAF and SAF described in the previous section is ultimately intended for application to basic freeway segments. However, in HCM 2000 and HCM 2010 it was also applied to the analysis of merge/diverge and weaving segments with a CAF not equal to 1.0. As a further improvement, this section describes the adaptation of CAF and SAF to these other HCM segment types.

A challenge arises in both merge/diverge and weaving methods when considering CAF and SAF (in order to analyze non-recurrent congestion sources like weather, incidents, and work zones), as both methods do not use segment capacity as an input in the speed prediction equation. In essence, those procedures violate the fundamental equation of traffic flow (*speed= flow × density*). Instead, both methods first estimate segment capacity and then perform a check to assure that traffic demands are below that capacity (otherwise, *demand/capacity >1* and the over-saturated module is invoked). If the segment passes the capacity check, the segment speed is estimated from an independent regression equation. The base capacity is adjusted with the appropriate CAF before comparing the demand to capacity check. The following equation shows how the adjusted capacity is calculated:

$$\boldsymbol{Adjusted\ Capacity = Base\ Capacity * CAF} \qquad (31)$$

Where,

$Adjusted\ Capacity$: Capacity used to perform *demand/capacity* check in order to switch to over-saturated procedure (if *demand/capacity>1* then over-saturated procedure is invoked);

$HCM\ Calculated\ Capacity$: Segment capacity estimated from respective HCM 2010 chapter;

CAF: User input capacity adjustment factor;

Given the current structure of the methodology, this study proposes to implement CAF and SAF separately. Specifically, CAF is used as a multiplicative factor of the segment base capacity in the initial checks; and SAF is subsequently used as a multiplier of FFS in the speed prediction equation, which is discussed below for merge/diverge and weaving segment types. Principally, the application of CAF and SAF is consistent with the basic segment procedure, but with the caveat that the factors are applied in two (or more) separate steps.

6.3.2 Merge and Diverge Segments

Exhibit 13-11 in HCM 2010 gives equations for estimating average speed of vehicles within the ramp influence area, and also in outer lanes of the freeway. These equations are updated In SHRP2 L08 to incorporate the SAF. Similar to On-Ramp segments, Exhibit 13-12 in HCM 2010 is used to estimate speed at off-ramp (diverge) junctions. The updated equations for the merge and diverge sections are shown in Table 37.

Table 37 Estimating Speed at Merge and Diverge Junctions with SAF Consideration

Average Speed in:		Equation
Merge	Ramp Influence Area	$S_R = FFS * SAF - (FFS * SAF - 42)M_s$ $M_S = 0.321 + 0.0039\ e^{(v_{R12}/1,000)} - 0.002(L_A S_{FR} * SAF/1,000)$
	Outer Lanes of Freeway	$S_o = FFS * SAF$ $\quad v_{OA} < 500\,pc/h$ $S_o = FFS * SAF - 0.0036\,(v_{OA} - 500)$ $\quad 500\,pc/h \le v_{OA} \le 2300\,pc/h$ $S_o = FFS * SAF - 6.53 - 0.006\,(v_{OA} - 2,300)$ $\quad v_{OA} > 2,300\,pc/h$
Diverge	Ramp Influence Area	$S_R = FFS * SAF - (FFS * SAF - 42)D_s$ $D_S = 0.883 + 0.00009\,v_R - 0.013\,S_{FR} * SAF$
	Outer Lanes of Freeway	$S_o = 1.097\,FFS * SAF$ $\quad v_{OA} < 1,000\,pc/h$ $S_o = 1.097\,FFS * SAF - 0.0039(v_{OA} - 1,000)$ $\quad v_{OA} \ge 1,000\,pc/h$

The variables in Table 37 are defined below:

S_R = average speed of vehicles within the ramp influence area (mi/h); for merge areas this includes all ramp and freeway vehicles in lanes 1 and 2; for diverge areas, this includes all vehicles in lanes 1 and 2;

S_o = average speed of vehicles in outer lanes of the freeway, adjacent to the 1,500-ft ramp influence area (mi/h);

S = average speed of all vehicles in all lanes within the 1,500-ft length covered by the ramp influence area (mi/h);

FFS = free-flow speed of the freeway (mi/h);

SAF = segment speed adjustment factor of the ramp segment;

S_{FR}= free-flow speed of the ramp (mi/h);

L_A = length of acceleration lane (ft.);

v_R = demand flow rate on ramp (pc/h);

v_{12}= demand flow rate in lanes 1 and 2 of the freeway upstream of the ramp influence area

v_{R12} = total demand flow rate entering the on-ramp influence area, including v_{12} and v_R (pc/h);

v_{OA} = average per-lane demand flow in outer lanes adjacent to the ramp influence area (not including flow in lanes 1 and 2) (pc/h/ln);

M_s = speed index for on-ramps (merge areas); this is simply an intermediate computation that simplifies the equations; and

D_s = speed index for off-ramps (diverge areas); this is simply an intermediate computation that simplifies the equations.

Using Exhibit 13-13 in the HCM 2010, average speed for merge and diverge (on-ramp and off-ramp) junctions are calculated.

Similar to basic segments, a sensitivity analysis was performed for a typical merge (on-ramp) segment. The default values used in this analysis are shown in Table 38.

Figure 57 shows the impacts of various weather events including medium rain (dashed) and heavy snow (dotted), relative to normal weather conditions (solid line) for base free flow speeds of 75 (dark) and 55 (gray) miles per hour on a typical merge (on-ramp) segment. Each line in Figure 57 terminates at the capacity for the prevailing adjusted FFS and weather conditions. The flow rate on the x-axis is referenced to the segment immediately downstream of the on-ramp.

Table 38 Default Values Used in Merge (On-Ramp) Segment Analysis

Number	FFS (mph)	S_{FR} (mph)	L_a (ft.)	Normal		Med Rain		Heavy Snow	
				CAF	SAF	SAF	CAF	SAF	CAF
1	75	45	1500	1	1	0.93	0.90	0.81	0.72
2	65	45	1500	1	1	0.94	0.92	0.85	0.76
3	55	45	1500	1	1	0.96	0.94	0.88	0.80

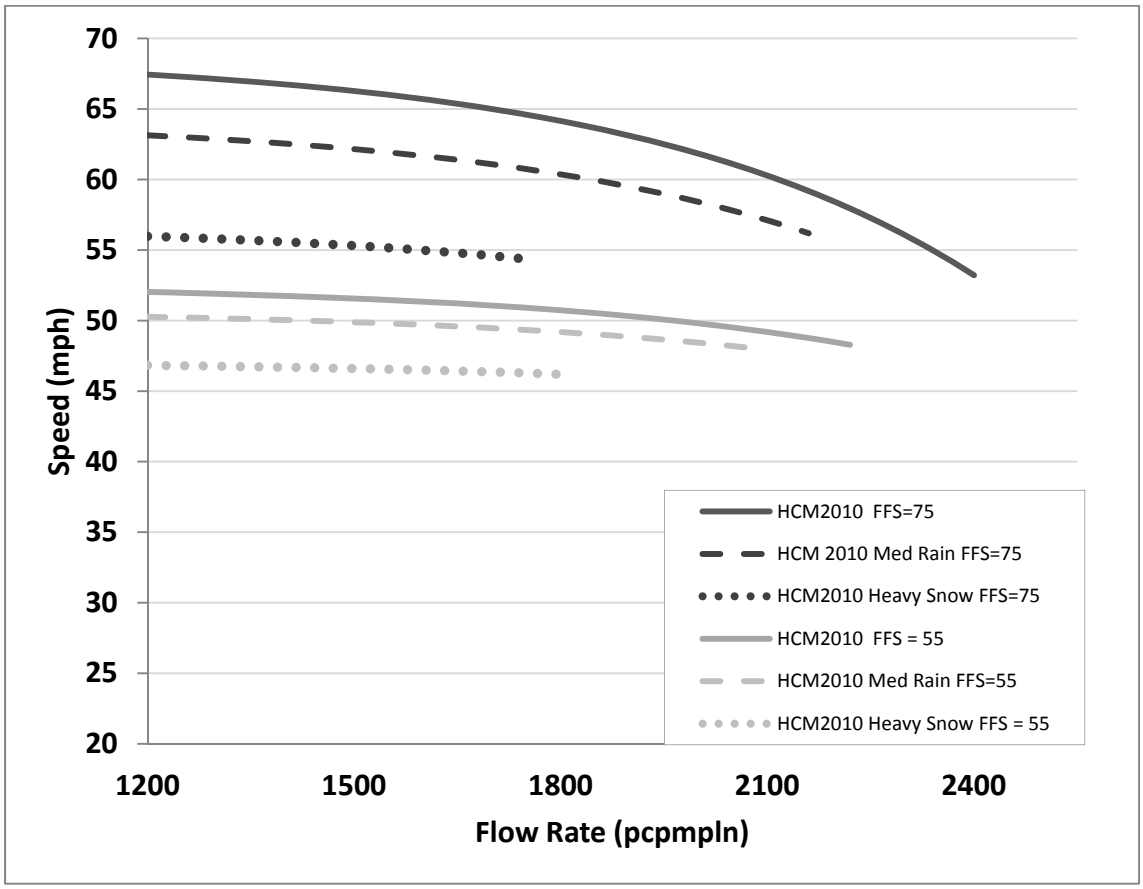

Figure 57 Example Application of SAF and CAF for Different Base FFS and Weather Categories on Merge (on-ramp) Segments

6.3.3 Weaving Segments

The capacity of a weaving segment is calculated using Equation 12-3 in the HCM 2010. In the updated methodology, the weaving segment capacity is further adjusted by the appropriate CAF if necessary (Equation (29)). Also similar to ramp segments, the speed calculation procedure for weave segments is modified to consider weather and incident reduction in free flow speed through the SAF. The method separately estimates the speed of weaving and non-weaving vehicles, which are eventually combined to estimate a space mean speed of all vehicles in the segment. The equations for calculating weaving and non-weaving vehicles (Equations 12-19 and 12-20 in HCM 2010) are modified as follows by multiplying each occurrence of FFS by SAF:

$$\boldsymbol{S_W = 15 + \left(\frac{FFS*SAF-15}{1+W}\right)} \tag{32}$$

$$\boldsymbol{W = 0.226\ (\frac{LC_{ALL}}{L_S})^{0.789}} \tag{33}$$

$$\boldsymbol{S_{NW} = FFS * SAF - (0.0072LC_{MIN}) - \left(0.0048\frac{v}{N}\right)} \tag{34}$$

In the next step, the space mean speed of all vehicles in the weaving segment is computed by Equation 12-20:

$$\boldsymbol{S = \frac{v_W + v_{NW}}{(\frac{v_W}{S_W}) + (\frac{v_{NW}}{S_{NW}})}} \tag{35}$$

The variables used in Equations (32, 33, 34, and 35) are defined here:

S_W = average speed of weaving vehicles within the weaving segment (mi/h);

S_{NW}= average speed of non-weaving vehicles within the weaving segment (mi/h);

FFS = free-flow speed of the weaving segment (mi/h);

SAF = speed adjustment factor of the weaving segment;

W = weaving intensity factor;

L_S = length of the weaving segment, using the short length definition (ft.) (300 ft. is the minimum value);

LC_{ALL} =the total lane-changing rate of all vehicles in the weaving segment, in lane changes per hour, and equals LC_W +LC_{NW}.

LC_{MIN}= minimum rate of lane changing that must exist for *all* weaving vehicles to successfully complete their weaving maneuvers (lc/h), LC_{MIN}= (LC_{RF}×v_{RF}) + (LC_{FR}×v_{FR});

v = total demand flow rate in the weaving segment (pc/h), v = v_W+v_{NW};

N = number of lanes within the weaving section;

Example 1 from the HCM 2010 Chapter 12 was selected to run a speed vs. flow rate sensitivity analysis. The SAF and CAF used in this analysis are the same as in Table 37. It should be noted that under those particular sets of inputs, speed varies linearly with flow. Also note that Figure 58 is truncated for flow rates below 1200 pc/h/ln.

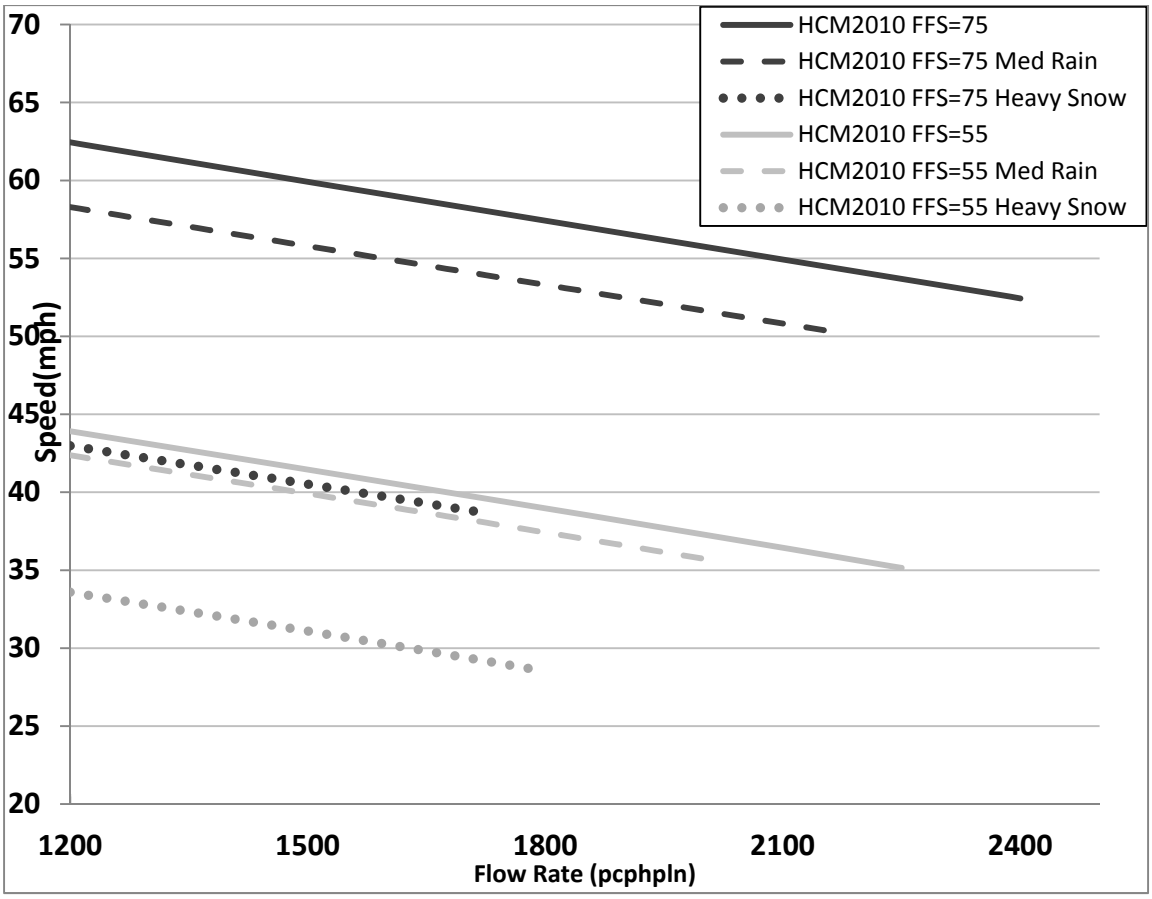

Figure 58 Example Application of SAF and CAF for Different Base FFS and Weather Categories on Weaving Segments.

6.4 Enhanced Performance Measures for Congested Condition

In order to incorporate non-recurring congestion effects onto the HCM method, it is expected that the procedure will be modeling highly over-saturated conditions. To account for such cases, new performance measures are proposed. These measures serve as additional reasonableness checks for the analyst, and are used to derive the travel time distribution, which is expected to be the most critical output from this methodology.

6.4.1 Denied Entry Queue Length (ft.)

A new output variable added in the freeway facilities methodology is the Denied Entry Queue Length (DEQL). The motivation for adding this variable was to identify severely congested scenarios for further analysis. Another advantage of calculating the DEQL is that the analyst gets a sense of the validity of the reliability performance measures. In the other words, the HCM methodology is not designed to handle all congested conditions, and especially has not been validated for very severe congestion scenarios. The procedure therefore may generate unrealistic results under the severely congested scenarios. The DEQL can serve as a flag for these types of scenarios.

The DEQL informs the user of vehicle spillback out of the spatial domain of the coded facility in FREEVAL. The following equation is used to calculate DEQL at each analysis period in the time-space domain:

$$\boldsymbol{Denied\ Entry\ Queue\ Length(ft.)} = \frac{\boldsymbol{UV}}{\boldsymbol{K_Q - K_B}} \times \mathbf{5280} \qquad (36)$$

Where,

$Denied\ Entry\ Queue\ Length\ (ft.)$ = Denied entry queue length at the end of the analysis period;

$UV =$ Number of unserved vehicles which could not enter the first segment of the facility. This value is calculated using the methodology explained in Chapter 25 of the HCM 2010.

K_Q = Queue Density (vehicles/mi/ln): vehicle density in the queue on the first segment of the facility at the end of the analysis period. The queue density is calculated on the basis of a linear density flow relationship in the congested regime inside the computational engine;

K_B = Background Density (veh/mi/ln): first Segment density (veh/mi/ln) over the analysis period assuming there is no queuing on the segment. This density is calculated using the expected demand on the segment in the corresponding under-saturated procedure in Chapters 11–13 of the HCM 2010;

Another advantage of representing denied entry queue length is to give the user a sense on how much he or she should expand spatial scope of the coded facility. For example, it is highly desirable that no DEQL is present for the base scenario, to assure that the spatial extent of base congestion (no weather or incident effect) is fully contained within the facility focus. Similar, the majority of scenarios should preferably result in zero or low denied entry queues, with only rare and very severe scenarios having higher queue estimates.

6.4.2 Travel Time Index (TTI) for Entire Time-Space Domain

The travel times for each segment at each analysis period (time-space domain) are available as output in the original HCM 2010 methodology. Therefore, the facility TTI can simply be calculated by dividing individual travel times by the free-flow travel time. The following equation demonstrates this simple calculation:

$$\boldsymbol{TTI_{ij} = TT_{ij}/FFTT_j} \qquad (37)$$

Where,

TTI_{ij}= travel time index on segment (i) at analysis period (j);

TT_{ij} = travel time on segment (i) at analysis period (j);

$FFTT_j$ = segment (j) free flow travel time;

Also, the facility TTI in each analysis period is calculated simply by dividing facility travel time at a specific time period by its free-flow travel time:

$$\boldsymbol{TTI_i = TT_i / FFTT_i} \qquad (38)$$

Where,

TTI_i = facility travel time index in analysis period (i);

TT_i = facility travel time in analysis period (i);

$FFTT_i$= free flow travel time in analysis period (i);

In the application of the method to multiple scenarios, a separate TTI will be generated for each analysis period (15 minutes) in each scenario. From these calculated TTIs, along with their probability as produced by the freeway scenario generator, a cumulative TTI distribution can be developed. The analyst may further decide to focus on the 50th, 85th, or 95th percentile TTI as a performance measure (see highlights in the Figure 59). The TTI distribution can further be segregated into recurring and non-recurring scenarios, or to compare distributions based on different demand, weather or incident conditions.

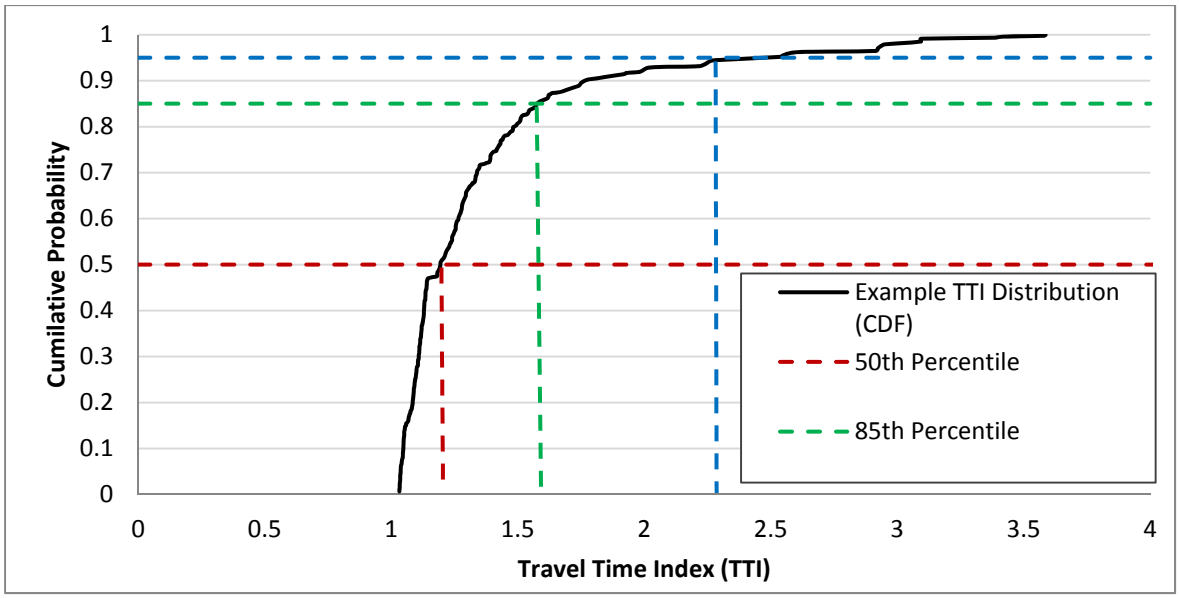

Figure 59 Sample Cumulative TTI Distribution with Key Percentiles

6.5 Incorporation of Two-Capacity Phenomenon

The Freeway Facilities Methodology in the HCM 2010 was limited by its assumption of a fixed capacity threshold between the uncongested and congested regimes. The method did not consider the two-capacity phenomenon which suggests that a drop in the throughput from the theoretical capacity is observed after breakdown has occurred. In other words, in the HCM 2010 methodology, when demand exceeds capacity at a freeway bottleneck, queuing and congestion impacts are estimated, but the bottleneck discharges traffic at the pre-breakdown capacity. As it was highlighted in Chapter 2, there is strong evidence in the literature that the freeway capacity at bottlenecks is measurably reduced after breakdown has occurred. Past research has demonstrated that the incorporation of the freeway two-capacity phenomenon will result in nontrivial impacts on performance measures such as queue lengths, queue formation and dissipation times, speed and travel time, and facility levels of service.

In summary, the effect of capacity drop in queue discharge mode is not limited to just decrease the bottleneck capacity. It also increases queue formation shock wave speed and decreases the queue dissipation speed. The new proposed method is improved such to account for the capacity drop in the queue discharge mode. A simple if statement has been added to the method which states that "If there is a queue on a given segment at a given time interval, the capacity of the next downstream node should be reduced by the default percent capacity drop (α)" The user is given the flexibility to set α within a range of 0% to 10%. It is

also believed that α emerges as a key calibration factor in the methodology, which is described in a separate study by the author.(Sajjadi et. al., 2013)

The two-capacity phenomenon is incorporated into the over-saturated procedure of the HCM 2010 freeway facilities methodology covered in Chapter 25. In the step 17 of the over-saturated procedure if there is a queue on the segment, the segment capacity is reduced by α%. If there is no queue on the segment, the procedure will check if the segment capacity has been reduced in the previous time step and if the answer is true, the segment capacity is retrieved back to the original capacity. (Figure 60)

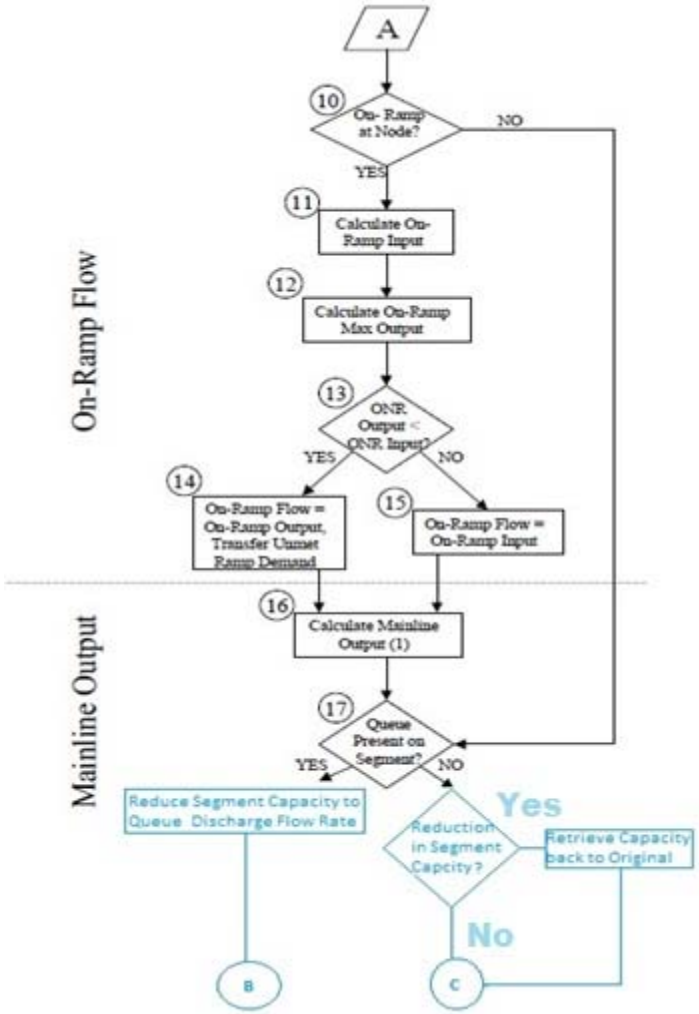

Figure 60 Two-Capacity Phenomenon Implementation in HCM 2010 Over-saturated Procedure

6.6 Discussion

This methodology uses a simplified solution, but it in accordance with current methodology in the HCM 2010. The Equation 25-1 in the HCM 2010 has been validated in multiple research efforts and currently is the vehicle by which users can model weather and incidents for basic segments in the HCM. As such, it was desirable in our effort to retain the existing

HCM 2010 structure to the extent possible, in the absence of additional field data (and resources) that could be used to entirely re-calibrate the speed-flow relationship under the various weather and incident conditions. This is, however, an important topic for future research.

6.7 Implementation Conclusion

Recent enhancements to the Highway Capacity Manual (HCM) freeway facilities methodology are presented in this chapter. These enhancements enable the HCM freeway facilities methodology to perform travel time reliability analysis. These enhancements include: incorporation of capacity drop in queue discharge flow compared to pre-breakdown flow, adding Speed Adjustment Factor (SAF) as a new lever for modeling non-recurrent congestion sources like weather and incidents, modeling improvement of SAF and Capacity Adjustment Factor (CAF) in the merge, diverge, and weaving segments, and adding new congestion performance measures. Also, in order to generate a cumulative travel time distribution, thousands of data points are generated in the new version of the freeway facilities computational engine for travel time reliability analysis. The results of the updated methodology are reasonable based on the results of the analysis.

6.8 Field Verification (I-40 Case Study in NC)

This section aims to deploy the enhanced proposed model described earlier in this chapter along with research findings in Chapter 5 to check how the enhanced model and research findings improve HCM method when it is applied to a real world problem. The objective of this chapter is to tie the research findings and recommendations with a real world example.

6.8.1 Study Site and Data Sources

The calibration methodology was applied to a 12.5 mile freeway facility on Interstate Highway 40 (I-40) in the eastbound direction between mile markers 278.5 and 291 near Raleigh, North Carolina. The facility has a speed limit of 65 mph and a free flow speed of 70 mph. The Reliability Reporting Period (RRP) over which the analysis is carried includes all weekdays of calendar year 2010 in a study period from 2:00 to 8:00 pm. The two-way facility Average Annual Daily Traffic (AADT) was approximately 120,000 in 2010 and the eastbound facility experiences recurring congestion in the PM peak period.

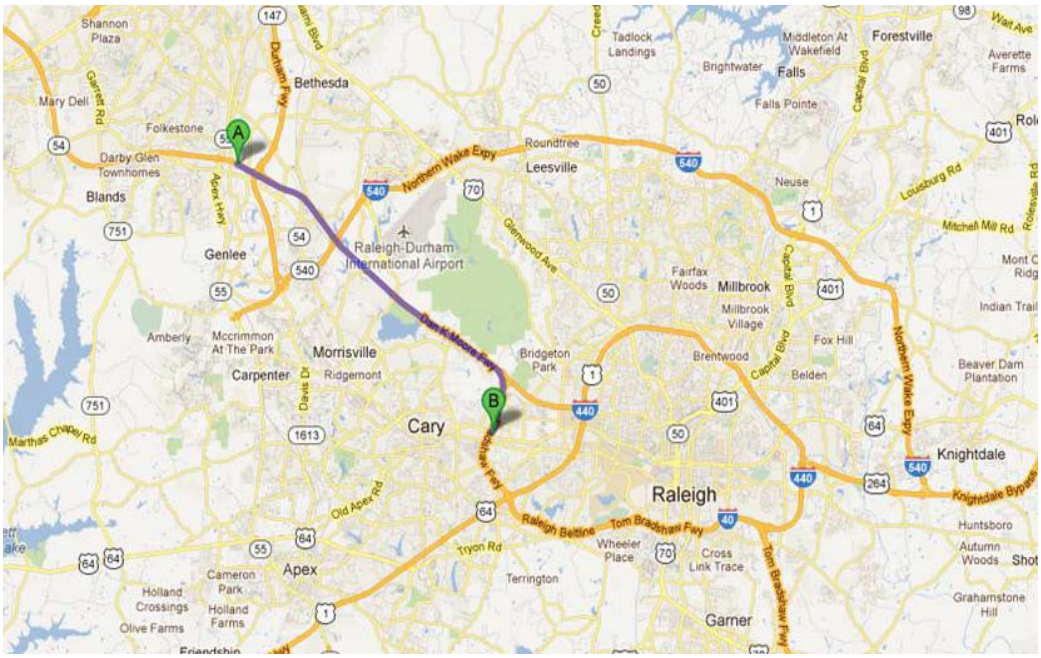

Figure 61 I-40 Facility Location

Traffic demand data were estimated from counts extracted from permanent side-fire radar sensors placed along the mainline of the facility, supplemented with temporary tube counters placed at the on- and off-ramps for a two-week period since there are no permanent sensors on the ramps.

Fifteen minute segment travel times were downloaded from INRIX probe data which were collected across the facility during the RRP from the Regional Integrated Transportation Information System, or RITIS The facility travel time was estimated from the segment travel times using a pseudo-trajectory method based on the concept of "stitching or walking" the travel time (Chase et. al.,2012). Each 15-min traffic data in RRP was fused with local weather and incident data using a similar approach as described in Chapter 3 (Figure 4). The

weather data was collected using weather underground website and the incident data were collected using a NCDOT TIMS online database.

6.8.2 Fused Database Analysis

The INRIX traffic data has about 6,000 observations. When fused with the weather and incident databases, there are about 2,000 observations in normal scenario, 90 observations in light rain scenario and only 4 observations in the medium rain scenario. Therefore, normal and light rain scenarios were selected for this analysis. Please note that time periods when there has been an incident have been excluded from the analysis. Facility Travel Time (TT) was selected as a performance measure in this comparative analysis. The Free-Flow Travel Time (FFTT) of this facility considering 12.5 mile length and FFS of 70 mph is 10.71 minutes. Table 39 demonstrates facility travel times and respective TTIs for normal and light rain scenarios based on the fused INRIX database.

Table 39 Facility Travel Time and Travel Time Index for Normal and Light Rain Scenarios

Scenario	# Observations	TT(mph)		TTI	
		Average	Std. Dev.	.Average	Std. Dev.
Normal	2,334	15.22	6.05	1.42	0.56
Light Rain	90	16.68	6.37	1.55	0.59

6.8.3 HCM 2010 Freeway Facilities Method

In this section, the analysis efforts of modeling the I-40 site using the HCM 2010 freeway facilities method are described. The base HCM file was coded for the I-40 site. The study period starts at 2:00 PM and ends at 8:00 PM. The geometric information was obtained using Google Earth and Google Map. The facility segmentation is done in accordance with HCM 2010 segmentation rules as described in Chapters 10-13.

Figure 60 demonstrates geometrical information of the I-40 site which enters into the computational engine. Since there have been no significant grades on the site the terrain category was set as “level”.

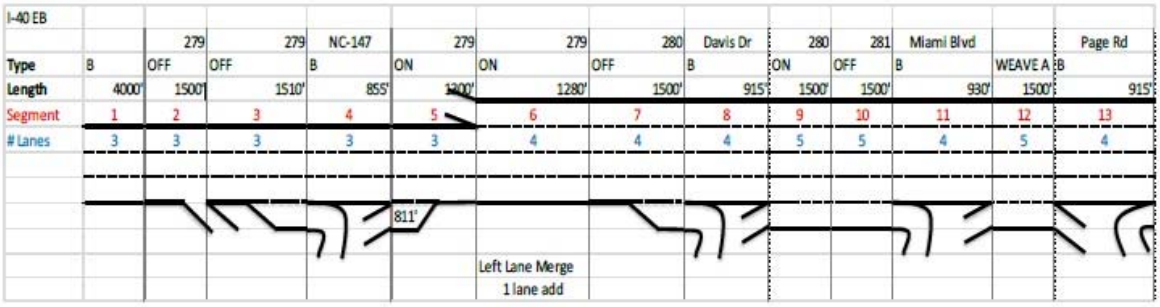

Section A

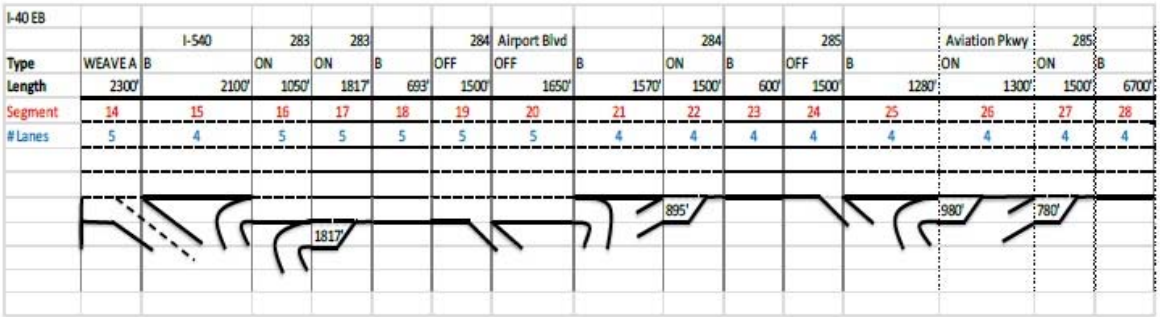

Section B

Section C

Figure 62 I-40 Site Geometrical Information (Source: SHRP2-LO8:HCM2010-Chapter 36)

The FREEVAL computational engine used in this analysis was enhanced based on the Chapter 6 recommendations. The enhanced version was then calibrated for I-40 site using the results of the previous study by the author.

The study suggests increasing the base demand by 3% and using percent capacity drop in the queue discharge mode (α) of 9% to get the best performance of the computational engine in modeling the I-40 site. (*Sajjadi et. al., 2013*)

In order to compare the engine results with the fused database results, the enhanced computational engine was run in five different settings to account for normal and light rain scenarios. These five different runs are summarized in Table 40.

Table 40 Computational Engine Runs Critical Parameters

Scenario	**Run Name**	**DAF**	**α(%)**	**CAF**	**SAF**
Normal	Base	1.0	0.0	1.0	1.0
	Calibrated	1.03	9.0	1.0	1.0
Light Rain (LR)	Base, LR Modeled	1.0	0.0	0.98	1.0
	Calibrated, LR Modeled based on HCM	1.03	9.0	0.98	1.0
	Calibrated, LR Modeled based on Study Findings	1.03	9.0	0.96	0.94

The capacity and speed adjustment factors are applied in for all the segments and all the time periods. In the other words, it is assumed that in the whole study period of 6 hours (24 x 15-min observations), the weather condition is rainy.

Table 41 Computational Engine Run Results

Scenario	Run Name	TT		TTI	
		Avg.	Std Dev.	Avg.	Std. Dev.
Normal	Base	11.35	0.25	1.06	0.02
	Calibrated	13.40	2.45	1.25	0.23
Light Rain (LR)	Base, LR Modeled	11.61	0.35	1.08	0.03
	Calibrated, LR Modeled based on HCM	14.78	3.03	1.38	0.28
	Calibrated, LR Modeled based on Study Findings	16.50	3.85	1.54	0.36

6.8.4 Conclusions

Comparing Table 40 with Table 41 it is concluded that: in the normal scenario the calibrated run, and in the light rain scenario, the calibrated run which uses this study finding (CAF and SAF) to model the light rain condition provide the best overall estimates. It seems that the base run under estimates average facility travel times.

Therefore, the model enhancements and research finding improve the HCM 2010 freeway facilities prediction power. The similar analysis can be implemented for other scenarios based on the data availability.

7. SUMMARY, CONCLUSIONS & RECOMMENDATIONS

7.1 Summary

The need for reliable transportation systems is growing fast as traffic demands increase over time, impacting the travel times for recreational and commercial trips. With capital capacity improvements being increasingly rare, transportation agencies are looking at other method of increasing efficiency and of assuring acceptable throughput on roadways. As agencies are moving towards enhanced efficiency and reliability in traffic operations, there has been a shift in the travel time analysis paradigm that has shifted analysis methods away from the prediction of average travel times, and towards the prediction of travel time reliability. The high user cost of not being able to make a trip in a certain amount of time (successful trip) is an important contributor to this paradigm shift. However, travel time reliability analysis is not a trivial undertaking, and the topic has hence been the focus of a significant amount of research in recent years. As one prominent example, a national level research effort was focused at finding a simplified yet adequate approach to estimate travel time reliability in different facilities. Strategic Highway Research Program Project SHRP2-L08: "Incorporation of Travel Time Reliability into the HCM", tries to determine how data and information on the impact of different causes of nonrecurring congestion (incidents, weather, work zone, special events etc.) can be incorporated into the performance measure estimation procedures contained in the Highway Capacity Manual (HCM 2010).

One of the key challenges of that project and in travel time analysis in general, is the isolation of different factors contributing to unreliable travel. The SHRP2 program generally

identifies seven sources of non-recurring congestion and unreliable travel as: incidents, weather, work zones, special events, fluctuations in demand, inadequate base capacity, and inadequate signal timing. Especially for field observations, it is common to have multiple sources of unreliable traffic confound the observed operations on a facility, making it very challenging to isolate the effects of any individual contributor.

This dissertation developed and implemented an analysis framework for estimating sources of non-recurring congestion from field data, and produced supplementary information for travel time reliability analysis on freeway facilities. Specifically, it pursues three main objectives as follows:

1. Evaluate the operational impacts of non-recurring sources of congestion on freeway operations.
2. Develop or enhance predictive models and tools for estimating freeway performance based on the non-recurrent congestion source impact.
3. Enhance the existing freeway facilities practice with research findings and recommendations.

In order to fulfill the objectives of the study, a new fused database approach is introduced in this study. It uses three databases of traffic, weather and incidents and integrates them using multiple automated procedures developed in this research. The integrated database consists of 15-min traffic observations with detailed information regarding weather and incident conditions associated with them. However, the future use of the proposed framework is not

limited to any fixed time intervals. The method is flexible and can be applied to any type of data with reasonable modifications.

For this study, a pair of sensors in the northbound and southbound directions of a freeway facility near Baltimore, Maryland was selected. Traffic and incident data were acquired from the Regional Integrated Transportation Information System (RITIS) website and weather data were downloaded from the Weather Underground website.

Traffic data were categorized based on the weather and incident information. Multiple scenarios were identified and each scenario was analyzed separately in order to estimate the impact of weather and incidents on traffic stream behavior.

In order to achieve the first objective, two important freeway parameters of Free Flow Speed (FFS) and capacity were estimated under different scenarios. For each scenario, data were grouped into over-saturated and under-saturated conditions, to test for differences in model fit parameters between these commonly-recognized distinct flow regimes.

In the next step, several statistical parameters were estimated for each scenario. These statistical parameters include average and standard deviation of observed speed and volume in different time periods. Each statistical parameter is provided in three different time periods of peak, off-peak, and overall, with traffic data representing an entire year of observations.

Based on the modeling and data analysis findings, several enhancements are proposed to the state of the practice freeway facility analysis method in the HCM 2010. These enhancements enable the HCM freeway facilities methodology to perform travel time reliability analysis by filling key computational gaps associated with modeling the impacts of weather and

incidents. These enhancements include: adding Speed Adjustment Factor (SAF) as a new input parameter for modeling impacts of non-recurrent congestion sources like weather and incidents in undersaturated conditions; implementing model improvements of SAF and Capacity Adjustment Factor (CAF) in merge, diverge, and weaving segments to more adequately represent non-recurring congestion effects for these segment types; adding new congestion performance measures to quantify the operations under severe weather and incident scenarios; and incorporating a capacity drop in queue discharge flow compared to the pre-breakdown flow rate.

The enhanced HCM model is then applied to a real world case study. The study site is a section of the I-40 freeway near Raleigh, NC. The result of the filed comparison indicated that the recent enhancement combined with research findings improve the model performance significantly.

7.2 Conclusions and Findings

This dissertation covered multiple aspects of the impacts of non-recurrent congestion sources on freeway operations. The primary focus in this work was on the impacts of inclement weather and incidents, but the framework could generally be expanded to other effects, like work zones. The conclusions of each analysis are presented in separate sections below.

7.2.1 Modeling Results

Four different models (Northwestern, Van Aerde, Modified Greenshields, and HCM 2010) were tested on five scenarios (Normal, Light Rain, Medium Rain, Heavy Rain, and Snow) for both under-saturated and over-saturated conditions. The following conclusions were drawn:

- Northwestern Model: the estimated FFS reduces as the weather conditions worsen. In the under-saturated mode the model prediction power is acceptable but in the over-saturated condition, the model does not fit the data well. Also, the model overestimates capacity in the normal and light rain scenarios and underestimates the speed in the snow scenario.
- Van Aerde Model: As the weather condition worsens, the estimated FFS is reduced as expected. The model prediction power is in an acceptable range based on selected performance measures for the goodness of fit. The model provides the best fit in the over-saturated condition of the light rain scenario. However, the model tends to underestimate the capacity value when compared to other models.
- Modified Greenshields Model: This model provides the best fit for the entire speed-flow domain for all scenarios. The estimated FFS drops as expected when the weather

conditions worsen. Similar to the Van Aerde model, it seems that the model underestimates capacity values. One drawback of applying this model to different scenario data is that the model requires the full speed-flow domain to be available to provide a good estimate of the freeway facility performance measures.

- HCM 2010 Model: The model yielded the lowest estimated FFS in inclement weather conditions because this approach considers congested observations in FFS estimation. The model fit is generally not adequate for inclement weather scenarios, as the RMSE value almost doubles in the light rain scenario and triples in the medium rain scenario. It seems that the model does not have enough flexibility to fit inclement weather conditions data. A drawback of the model in the under-saturated condition is that it uses a breakpoint of 1800 (pc/h/ln) for comparably low FFS of 55 mph. In scenarios which capacity reduces due to non-recurrent congestion sources, the under-saturated part of the model changes into a straight horizontal line of the estimated FFS. There is a slight difference in using this model compared to the Northwestern, Van Aerde and Modified Greenshields models as the important model parameters like FFS and capacity have been estimated using HCM proposed methods rather than fitting the model to data. The result might have been different if the model variables were fitted to the data (similar to other models), but then it would not have been consistent with the HCM method.
- Empirical Thresholds Approach: the empirical threshold approach proposed for FFS estimation seems to overestimate the observed value. This approach excludes all the

observations in the congested condition. The overestimation phenomenon is more considerable in the snow scenario since the proposed approach filters out all the observations in slightly congested speed-flow domain.

The empirical threshold approach used for capacity estimation provides reasonable results when using the average of the top five percent observed flow rates. The reasonable reduction in capacity exists and the estimated CAFs look reasonable too. However, using the top first percent threshold for estimating the capacity value seems problematic in scenarios with comparably few numbers of observations. For example, the estimated capacity value used in the snow condition is a result of only two observations. This results in unrealistic capacity estimation in the snow scenario.

In conclusion, The Greenshields model is recommended for FFS estimation since the model fits the data better than any other model. The empirical threshold approach with 5% threshold is recommended for capacity estimation, since it provides reasonable predictions in all the scenarios especially with scenarios with few numbers of observations. If all the scenarios possess enough data points (for i.e. more than 1,000), it is recommended to use the average of the highest first percentile observed flow rates as the estimated capacity. If some of the scenarios have comparably lower number of observations. It is recommended to use the five percent threshold in order to alleviate the impact of the statistical outliers.

7.2.2 Scenario Findings

Multiple inclement weather and incident scenarios were analyzed in this dissertation. The inclement weather scenarios analyzed in this study are wet pavement, light rain, medium rain, heavy rain, and snow. The incident scenarios include downstream incident in normal and rain conditions, upstream incident, and opposite direction incident. Multiple analyses were performed on each scenario dataset and the result is compared to the normal condition (clear weather, no incidents).

The result of the analyses showed that both FFS and the capacity are reduced due to effects of inclement weather condition, but that only the capacity is impacted for incident scenarios. The analysis found no evidence of a FFS drop due to the incident scenarios. The following table summarizes the estimated FFS and Capacity and their respective adjustment factors for different scenarios.

Table 42 Summary of Recommended Capacity and FFS Estimation Results for Different Scenarios

Scenario	Capacity (pc/h/ln)	FFS (mph)
Normal Condition	1,935	61.6
Wet Pavement	1,861	57.1
Light Rain	1,860	57.9
Medium Rain	1,838	55.2
Heavy Rain	1,814	58.4
Snow	1,436	43.6
Upstream Incident within a Mile	1,856	61.3

Table 42 demonstrates the estimated FFS and capacity estimates resulting from different scenarios, which were significantly different from the normal scenario values. In addition to FFS and capacity values, multiple statistical performance measure like average speed and volume during the peak and off-peak time periods were estimated for each scenario. Also, the standard deviation of average speed and average volume were estimated to provide a better understanding of the impact of each scenario on the speed and volume dispersion. The peak periods were selected using a moving average approach by using the observed volumes during different times of the day. The efforts to determine the peak periods revealed that the

AM peak period is between 6:30 to 9:30 AM while the PM peak period is between 15:30 to 18:30. A summary of important finding in each scenario is presented in the following:

- Normal Scenario: There are about 42,000 observations in this scenario which is about 88% of all the time of the year. The average speed in the peak and the off-peak time periods are 60.7 and 61.3 mph respectively. It means that the selected facility is not heavily congested. The average volumes are 1,563 and 800 vph during the peak and the off peak time periods.

  The analysis of the observed volume in different weekdays under normal conditions showed that there is no significant change in total demand for different days of the week. Also, the analysis revealed that both directions almost follow the same hourly distribution pattern of volume and speed with two AM and PM peak periods.

- Wet Pavement Scenario: there are 2,227 observations in the wet pavement scenario. The average speed and average volume drop by 4% during the peak period compared to the normal scenario. In the off-peak period, the average volume does not drop significantly, but the average speed drops by 3%. The dispersion in the observed volumes does not change in different time periods but the speed dispersion almost doubles in the peak period. In other words, travel conditions are less uniform and travel times therefore more variable under wet pavement conditions, an effect that is currently not recognized in the 2010 HCM.

- Light Rain Scenario: this scenario consists of 2,212 observations. The impact of the rainy weather on the traffic stream behavior is more considerable during the peak

period compared to the off-peak period. The average speed drops by 10.2% in the peak period compared to 7.5% drop in the off-peak period. The dispersion of the speed increases by 48.4% and 97.2% in the peak and off-peak time periods. Light rain reduces the average volume by 4.3% in the peak period but it has no significant impact in the off-peak time period. Similar to the wet pavement scenario, the higher variability of speeds for this scenario points to very non-homogeneous travel conditions under light rain. Consequently, the error associated with using an average speed value is greater for inclement weather than it is for clear weather days.

- Medium Rain Scenario: There are 400 observations in this scenario. The average speed reduces by 22.1% and 10.4% during the peak and off-peak periods respectively. The average volume during the peak period reduces by 6.8%. The dispersion in the average volume does not change considerably but the dispersion in the average observed speed almost doubles in all the time periods, resulting in greater variability in travel conditions within this weather category.
- Heavy Rain Scenario: There are about 80 observations in this scenario. The average volume drops by 7.0% and the average speed drops by 24.1% during the peak period. The speed dispersion almost doubles in all time periods compared to the normal scenario.

- Snow Analysis: There are total of 208 observations in the snow scenario. The average observed speed and volumes in different time periods reduce significantly compared to the normal scenario. The average observed flow rate volume in the peak hour drops by 36.4% and the average speed drops by 42.2% during peak hour. The dispersion in speed increases significantly in the peak period (160%) and the off peak period (317%).
- Downstream Incident Scenario in Normal Condition: The incident database has recorded 436 events within 1-mile distance of the sensors over one year worth of data. The events cover about 944 observations. The majority of the reported incidents (86%) do not cause lane closure. Shoulder closures occur 6% of the time and less than 8% of the incident scenarios led to the actual lane closure. While the framework is capable of generating detailed incident data, RITIS incident data does not possess enough detailed information such as lane blockage information for the automated module to distinguish between different scenarios. The detail incident analysis depends heavily on the available data resources.

- Downstream Incident Scenario in Rain Condition: One of the new opportunities for researcher in using the proposed framework is that it generates combinatorial scenarios for incident and weather observations. However, data should be available to generate such scenarios. There are about 50 observations in the combinatorial scenario of incident and rain. The scenario data analysis shows that there is a 4.8% reduction in average speed and 9.0% reduction in average observed flow rate volumes compared to "Downstream Incident in Normal Condition" scenario.
- Opposite Direction Incident (Rubbernecking Effect Analysis): An incident in the opposite direction can impact traffic operations in the non-incident direction, when the median which separates two directions is not wide enough, or when adequate visibility allows for rubbernecking behavior. The magnitude of the impact heavily depends on the geometrical characteristics of the freeway facility. This impact is also referred to as the Rubbernecking Impact. The analysis result shows that the average volume reduces by 15.3% during the peak period while the impact on the average volume is not significant during the off-peak period. The average speed during the peak period drops by 2.5% and there is no significant change in the off-peak time period.

- Upstream Incident Scenario: an upstream incident blocks the traffic and creates a special condition on the freeway facility. In this situation, vehicles are queued in the back of the incident and when vehicles pass the incident they speed up. The scenario analysis showed that the average flow rate volume drops by 1.5% in the peak period and the speed almost remains the same. In the off peak period the average observed volume is higher than the normal scenario by 33.1%. The increase in average flow rates is due to backed up vehicles in the queue upstream of the sensor. Another important factor is that incidents are more likely to occur when there are more vehicles on the freeway facility, therefore, the sensor reports higher volume compared to the normal scenario.

7.2.3 Delay Analysis

As another contribution, an incremental delay calculation approach was introduced and applied in this study. The approach estimates the amount of delay attributed to non-recurring sources of congestion by isolating it from the delay experienced on clear weather days. The result of the delay analysis showed that 62% of delays are due to the recurrent congestion sources (demand variability) and that the remaining 38% is due to the non-recurrent congestion sources. The facility performed in the normal condition 87.9% of the time and the remaining time (12.1%) was under non-recurrent congestion conditions. In other words, the 12% of the time of non-recurring congestion is responsible for 38% of the delay on the facility over an entire year.

Within the category of non-recurring congestion, wet pavement conditions contributed to about 10% of the overall delay, which is not currently considered in the HCM. Rain scenarios had the highest contribution, with light rain, medium rain and heavy rain scenarios contributing 38%, 18%, and 4% of the overall non-recurrent delay, respectively. Snow scenarios contributed to 14%, and the incident scenarios contributed to 15% of the overall non-recurrent delay. The remaining 1% of delay is due to construction and maintenance on the road which usually occurred late at night.

The pavement was wet in 4.7% of the total time. Light, medium, and heavy rain scenarios cover 4.6%, 0.8%, and 0.2% of the total observations respectively. The weather was snowy in 0.4% of the time and incident observations cover 1% of the total time. Snow and incident

scenarios rarely happen on the freeway facility, but contribute considerably to the total non-recurrent delay.

The incremental delay analysis is heavily dependent on the site specific characteristics. For example, the amount of delay imposed by the snowy weather varies in different areas based on the driver familiarity with snowy driving condition and local snow removal and road recovery systems. Also, incident management plays an important role in the total amount of delay imposed by incidents.

7.2.4 Trumpet Impact Analysis

Another contribution of this dissertation is a closer examination of the "trumpet effect" in the observed speed-flow data under relatively low traffic conditions. Despite the low volumes, the sensor data show considerable dispersion in the speed observations, even after isolating and removing weather and incident effects. The speed observations in the low volume area of the speed-flow domain for the remaining clear-weather days range from 45 to 75 mph. As the volume increases, the dispersion reduces significantly, suggesting greater reliability of the facility for intermediate volumes (still much below breakdown capacity). This phenomenon is visualized on the speed-flow domain as a "trumpet" shape. The objective of this analysis was to investigate the main cause of "trumpet" shape in the low volume under-saturated portion of the speed-flow relationship.

A possible hypothesis is that this condition might be a result of the impact of lighting conditions on the freeway facilities, with nighttime driving being associated with lower (or at

least more variable) speeds. In order to check that hypothesis, the data were divided into two categories of light vs. dark conditions based on the local sunrise and sunset calendar.

The visual representation of the data showed that the trumpet shape in fact occurred under low volume observations in dark condition and that no trumpet shape exists under daylight condition. The analysis further found, however, that the primary reason for the effect seems to be attributable to low traffic volumes, rather than the lighting effects. This is explained as each 15-min speed observation is estimated by averaging the speed of vehicles which pass the sensor in 15-min time interval. If the number of vehicles which pass the sensor in 15-min time interval reduces, the sample size of the estimated average speed reduces. Consequently, when the sample size reduces, the probability that the sample mean represents the population means reduces. Therefore, it is expected that the speed dispersion in the low volume area of the speed-flow domain is related to its small sample size compared to a high volume area of the speed-flow domain which possess a greater sample size comparably.

In order to further test this second hypothesis, three separate analyses were conducted. In the first analysis, the observations with volume less than 1,000 vph were divided into 10 categories based on the number of vehicles in 100 vph increments. The visualization of the observations revealed that the standard deviation of the observed speed values reduces as the number of vehicles increases. In the second analysis, it was decided to control for total number of observations in each category, and thus the observations with volumes less than 1,000 vph were divided into 10 categories with an identical number of observations. The visualization of the observations in this analysis showed that the speed dispersion (standard

deviation) reduces significantly as the number of vehicles passing the sensor in 15-min time interval increases. In the third analysis, observations were aggregated such that each speed observation is an average of exactly 200 vehicles. In this situation the average speed of each observation is calculated from an identical sample size of 200 vehicles. Therefore the analysis is controlled for the impact of sample size on speed-flow diagram.

After aggregating the observations using an automated module, the visualization of the newly combined observations showed that there is no trumpet shape effect in the updated speed-flow domain anymore, and that any initially-suggested impact of lighting conditions disappeared. It was concluded that the trumpet shape emerges when the sample size (number of vehicles passing the sensor in certain amount of time) is comparably low. Rather than being a "true" effect, it therefore appears to be largely attributable to the method of sensor data collection and aggregation.

7.3 Limitations of the Study

There were certain limitations in conducting this study. Major part of the limitations is related to the available data sources. Some important limitations of the study are summarized as follow:

- The data was acquired from a pair of sensors in one year worth of data in a site near Baltimore, Maryland. All the results and findings of this study represent freeway traffic characteristics of this region.
- The selected study site was a basic segment according to HCM 2010 segmentation rules.
- It was assumed that the weather and incident conditions change spontaneously as represented in the database.
- The RITIS incident database does not possess information about the lane blockage detail of each incident. Therefore, the proposed methodology was not able to generate detail incident scenarios based on the number of lanes closed due to an incident.
- It was assumed that the incidents impact the freeway facility operation if they are in one-mile range of the sensor. However, some severe incidents may impact the traffic even if they are further than 1-mile from the sensor. On the other hand, some less severe incidents which occur in 1-mile distance of the sensor may not impact the traffic operation at all.

- The traffic data used in this study was in 15-min resolution and aggregated over all four lanes. The speed observations are represented as average values of vehicles passing the sensor in 15-min time interval.

7.4 Recommendations for Future Research

The fused database approach provides a rigorous platform for a variety of freeway operational analyses. The potential of the fused database approach reaches beyond the limits and scope of the current study, which was limited by the available sample size and sensor location. In order to use the full potential of the proposed approach, the data should possess adequate detail and quality. The incident data used in this analysis did not possess enough detailed information about the lane blockage information. It is recommended to improve incident data detail especially in terms of the lane blockage information.

Web-based traffic databases are evolving very fast. They provide data in more detail and quality as the time passes. It is recommended to check different web-based data sources and choose the one which provides the best data in terms of quality and accuracy before starting a new study.

The analysis of this study was based on the data acquired from two sensors near Baltimore, Maryland. It is recommended to download more data from multiple sensors and provide comprehensive data platform for the research analysis. It is also possible to select different sensors from different parts of the country and conduct a national level research. There are multiple future paths for extending the results of this dissertation when more sensor data are used for the analyses. Some of the potential future research applications are:

1- Incident Analysis:

This analysis can improve significantly based on the data availability. The proposed framework can generate detailed scenario datasets upon availability of the adequate data.

Special incident cases like incidents occurring in the opposite direction of travel and incidents occurring on the upstream of the sensor location have not been closely explored through research.

2- Delay Analysis:

This analysis can provide a general understanding of the impact of non-recurrent congestion sources on the freeway facility operation, if based on more data points from different sensors located in multiple areas.

3- Inclement Weather Impact Analysis:

It is recommended to collect more data, especially for snow, medium, and heavy rain scenarios. The framework can also be used to conduct site-specific weather analysis.

Other interesting research trends, which were not covered in this dissertation, should also be considered. These research trends are summarized as the following:

1-Two-Capacity Phenomenon Parameter Analysis:

The traffic data in the different weather conditions can be used to calibrate the percent capacity drop during the queue discharge mode under different freeway facility conditions. The research can investigate how inclement weather condition impacts the queue discharge mode throughput.

2-Shock Wave Analysis:

By selecting consecutive traffic sensors, researchers can use traffic data to monitor the shockwaves and conduct a detailed analysis in different weather and incidents conditions.

This analysis will require quite extensive data sources since there should be enough data points in the combinatorial scenarios of weather and incidents.

3-Queuing Analysis:

Similar to the shockwave analysis, downloading data from consecutive sensors on the freeway facilities enables researchers to study queue formation and dissipation patterns in different weather and incident conditions. The researcher can make recommendations on the speed and pattern of a queue forming and dissipation under different prevailing conditions.

4-Impact of Inclement Weather Condition on Non-Basic Segments:

The selected site in this study was a basic segment according to the HCM 2010 segmentation rules. There is a gap in the literature about the impact of the inclement weather conditions on the non-basic freeway segments like weaving, merge, and diverge segments. For this purpose, sensors should be selected in different segment types and data should be downloaded in multiple locations to fully capture the impact of the prevailing condition on non-basic segment types in different conditions.

8. REFERENCES

Agarwal M. T.H. Maze, R. Souleyrette Impact of Weather on Urban Freeway Traffic Flow Characteristics and Facility Capacity [Conference]. - Ames, Iowa : Proceedings of the 2005 Mid-Continent Transportation Research Symposium Iowa State University , August 2005.

Agyemang-Duah K. F. Hall Some Issues Regarding the Numerical Value of Freeway Capacity [Conference]. - [s.l.] : Proceedings of the International Symposium on Highway Capacity and Level of Service, 1991, p1.

Banks J. H. Two-Capacity Phenomenon at Freeway Bottlenecks: A Basis for Ramp Metereing? [Journal] // Transportation Research Record 1320, TRB, National Research Council, Washington, D.C.. - 1991. - pp. 83-91.

Banks J. H. Two-Capacity Phenomenon at Freeway Bottlenecks: A Basis for Ramp Metering? [Journal]. - Washington D.C. : Transportation Research Council, National Research Council, 1991. - Vol. 1320. - pp. 83-90.

Bayyeri M. J. J. O. Berger, German Molina, N. M. Rouphail, and J. Sacks Assessing Uncertainties in Traffic Simulation [Journal]. - Washington D.C. : Transportation Research Record, 2004, pp 32-40. - Vol. 1876.

Board Transportation Research Highway Capacity Manual 2010 [Report]. - Washington D.C. : National Research Council, 2011.

Brilon W. J., Geistefeldt J. and Hendrick Z. Implementing the Concept of Reliability for Highway Capacity Analysis [Journal]. - [s.l.] : Transportation Research Record: Journal of the Transportation Research Board. - pp. 1-8. - 2027.

Brilon W., L. Elefteriadou, A. Kondyli, F. Hall, B. Persaud, S. Washburn Proactive Ramp Metering based on Breakdown Probabilities [Conference]. - Stockholm, Sweden : Presented at the 6th International Symposium for Highway Capacity, Stockholm, Sweden , June 2011, 2011.

Cambridge-Systematics Analytical Procedures for Determining the Impacts of Reliability Mitigation Strategies. [Report] : Final Report / Strategic Highway Research Program 2-L03 (SHRP2-L03). - Washington D.C. : Transportation Research, 2010.

Cambridge-Systematics Providing a Highway System with Reliable Travel Times Study 3-Reliability [Report] : Final Report / Future Strategic Highway Research Program (F-SHRP). - Washington D.C. : Transportation Research Board, 2003.

Cassidy M. J. R. L. Bertini Some Traffic Features at Freeway Bottlenecks [Journal]. - [s.l.] : Transportation Research Part-B, 1999. - Vols. 33 pp. 25-42.

Chase R. T. [et al.] Comparative Evaluation of Reported Speeds from Corresponding Fixed-Point and Probe-Based Detection Systems [Journal] // Transportation Research Record. - Washington, D.C. : [s.n.], In Press.

Chase R. T. Monitoring Freeway Reliability Utilizing Network-Wide Link-Based ITS Data. M.S. Thesis [Book]. - Raleigh : North Carolina State University, 2012.

Chase R.T. A. Hajbabaie, B.J. Schroeder SHRP2 L08 Working Paper: Weather Prediction Methodology for Travel Time Reliability [Report]. - Raleigh, North Carolina : Institute for Transportation Research and Education (ITRE), 2012.

Chung K. J. Rudjanakanoknad, M. Cassidy Relation between Traffic Density and Capacity Drop at Three Freeway Bottlenecks [Journal]. - [s.l.] : Transportation Research Part B, 2007-pp 82-95.

Daniel J. J. Byun, S. (I-Jy) Chien, Paper No. 09-2837 Title: Impact of Adverse Weather on Freeway Speeds and Flows [Conference]. - [s.l.] : 88th Annual Meeting of the Transportation Research Board, 2009. - pp. P.P. 1-25.

Dehman A. EFFECT OF INCLEMENT WEATHER ON TWO CAPACITY FLOWS AT RECURRING FREEWAY BOTTLENECKS [Conference]. - [s.l.] : TRB 2012 Annual Meeting, 2012.

Dowling R. J. Barrios, G. Karkee, S. Ashiabor, and T. Kiattikomol Freeway Free-Flow Speed Adjustment Factors for Weather [Report]. - Oakland, California : SHRP2-L08 Memorandum, 2012.

Eads B.S. N.M. Rouphail, A. D.May, and F. Hall Freeway Facility Methodology in Highway Capacity Manual 2000 [Journal]. - Washington D.C. : National Research Council, 2000. - Vol. 1710.

Elefteriadou L. P. Lertworawanich Defining Measuring and Estimating Freeway Capacity [Conference]. - Washington D.C. : Annual Meeting of Transportation Research Board, 2003.

FHWA NCHRP 03-96 Project, Analysis of Managed Lanes on Freeway Facilities [Report].

FHWA Reducing Non-recurring Congestion [Online] // FHWA. - October 26, 2012. - March 2013. - http://ops.fhwa.dot.gov/program_areas/reduce-non-cong.htm.

GAISMA [Online] // GAISMA. - 2013. - 03 08, 2013. - www.gaisma.com.

Hall F. L., and K. Agyemang-Duah Freeway Capacity Drop and the Definition of Capacity [Journal] // Transportation Research Record, TRB, National Research Council, Washington, D.C.,. - 1991. - Vol. 1320. - pp. 91-98.

Hall F., D. Barrow Effect of Weather on the Relationship Between Flow and Occupancy on Freeways [Journal]. - Washington D.C. : Transporetation Research Record, 1988. - Vol. 1194.

Hall F.L. Loren Bloomberg, Nagui M. Rouphail, Brian Eads, and Adolf D. May Validation Results for Four Models of Oversaturated Freeway Facilities [Journal]. - Washington D.C. : National Research Council, 2000. - Vol. 1710.

Hoel Paul, G. Introduction to Mathematical Statistics [Book]. - Los Angeles, California : John Wiley & Sons, Inc., 1971.

Hu J. B.J. Schroeder, N. M. Rouphail A Rational for Incorporating Queue Discharge Flow in HCM Freeway Facilities Analysis Procedure [Conference]. - Washington D.C. : Annual Meeting of Transportation Research Board, 2012.

Ibrahim A.T. F. Hall Effect of Adverse weather Conditions on Speed-Flow Occupancy Relationships [Journal]. - Washington D.C. : transportation Research Record , 1994. - Vol. 1954.

INRIX I-95 Traffic Monitoring [Online]. - April 19, 2011. - http://i95.inrix.com/I95/Traffic.aspx.

INRIX Traffic Information [Online]. - 2012. - http://inrix.com/trafficinformation.asp.

Institute for Transportation Research and Education (ITRE) Reliability Methodology for Freeway Facilities in the HCM [Report]. - Raleigh, North Carolina : ITRE, 2012.

Institute for Transportation Research and Education (ITRE) SHRP2 L08 Working Paper: Incident Probability Estimation in the Freeway Scenario Generator [Report]. - Raleigh, North Carolina : ITRE, 2012.

Jia A. Williams, B.W., Rouphail N.M. Identification and Calibration of Site-Specific Stochastic Freeway Breakdown and Queue Discharge [Journal] // Transportation Research Record. - 2010. - 2188. - pp. 148-155.

Kim J. H. S. Mahmassani, and J. Dong Likelihood and Duration of Flow Breakdown Modeling the Effect of Weather [Journal] // Transportation Research Record: Journal of the Transportation Research Board. - Washington, D.C. : Transportation Research Board of the National Academies, 2010. - Vol. No. 2188. - pp. pp. 19–28..

Kittleson & Associates Inc. Incorporation of Travel Time Reliability into Highway Capacity Manual [Draf Final Report]. - 2012.

Kittleson & Associates Inc. Incorporation of Travel Time Reliability into Highway Capacity Manual [Proposal] - 2010

Knoop L.,V., S. P. Hoogendoorn, and H. J. van Zuylen Capacity Reduction at Incidents Empirical Data Collected from a Helicopter [Journal]. - Washington D.C. : Transportation Research Record , 2008. - Vol. 2071.

Kwon J. T. Barkley, R. Hranac, K. Petty Decomposition of Travel Time Reliability into Various Sources: Incidents, Weather, Work Zones, Special Events, and Base Capacity [Journal]. - Washington D.C. : Transportation Research Record, 2011. - Vol. 2229.

Masinick J. P. H. Teng An Analysis on the Impact of Rubbernecking on Urban Freeway Traffic [Journal]. - [s.l.] : U.S. DOT University Transportation Center.

Maze T. H. M. Agarwal, and G. Burchett Whether Weather Matters to Traffic Demand, Traffic Safety, and Traffic Operations and Flow [Journal] // Transportation Research Record: Journal of the Transportation Research Board,. - Washington D.C. : Transportation Research Board of the National Academies, 2006. - Vol. No. 1948. - pp. pp. 170–176.

NCHRP 03-107 Work Zone Capacity Methods for the Highway Capacity Manual [Online]. - 2012. - July 2012. - http://apps.trb.org/cmsfeed/TRBNetProjectDisplay.asp?ProjectID=3157.

Rakha H. and Arafeh M. Calibrating Steady-State Traffic Stream and Car-following Models using Loop Detector Data [Journal]. - [s.l.] : Transportation Science, 2009. - DOI: 10.1287/trsc.1090.0297..

Rakha H. and Crowther B Comparison of Greenshields, Pipes, and Van Aerde Car-following and Traffic Stream [Journal]. - [s.l.] : Transportation Research Record: Journal of the Transportation Research Board. - Vol. 1802. - pp. 248-162.

Rakha H. M. Farzaneh, M. Arafeh, and E. Sterzin Inclement Weather Impacts on Freeway Traffic Stream Behavior [Journal] // Transportation Research Record: Journal of the Transportation Research Board. - Washington, D.C. : Transportation Research Board of the National Academies, 2008. - Vol. No. 2071. - pp. pp. 8–18.

RITIS Regional Integrate Transportation Information System [Online]. - 2012. - www.ritis.org.

Sajjad S. B.J. Schroeder, N.M. Rouphail Incorporation of Weather and Incident Events in Highway Capacity Manual Freeway Facilities Methodology [Journal]. - Washington D.C. : National Research Council, In Press 2013.

Sajjadi S. B.J. Schroeder, N.M. Rouphail, T. Fowler A Planning-Level Approach to Estimating User Cost for Freeway Work Zones [Conference]. - Washington D.C. : Transportation Research Board Annual Conference, 2012.

Sajjadi S., A. Hajbabaie, N. M. Rouphail Freeway Facilities Methodology Calibration for Travel Time Reliability Analysis: I-40 Case Study in NC [Conference]. - Washington D.C. : Submitted for Consideration of Presentation and Publication at 92nd Meeting of Transportation Research Board, 2013.

Schroeder B.J. N.M. Rouphail , S.B. Aghdashi A Deterministic Framework and Methodology for Evaluating Travel Time Reliability on Freeway Facilities [Journal] // Transporation Research Record. - In Press 2013.

Schroeder B.J. N.M. Rouphail, S.S. Sajjadi, and T.J. Fowler Corridor-Based Forecasts of Work-Zone Impacts for Freeways [Report]. - Raleigh N.C. : North Carolina Department of Transportation, August 2011. - FHWA/NC/2010-18.

Smith B. L., K.G. Byrne, and R. B. Copperman, S.M. Hennessy, and N.J. Goodall. 7 7 An Investigation into the Impact of Rainfall on Freeway Traffic Flow [Conference]. - Washington, D.C. : Presented at 8 the 83rd Annual Meeting of Transportation Research Board, 2004.

Smith B.L., L. Qin, and R. Venkatanarayana Characterization of Freeway Capacity Reduction Resulting From Traffic Accidents [Journal] // Journal of Transportation Engineering. - 2003. - Vol. 129. - pp. p. 362-368..

TRAFFIC.COM [Online]. - ITIP Stakeholder Applications. - www.stakehodler.traffic.com.

Transportation Research Board Highway Capacity Manual 2000 [Report]. - Washington D.C. : National Research Council, 2000.

TRB Highway Capacity Manual [Book]. - Washington, D.C. : National Research Council, 2010. - Vol. 2 : pp. 10-39.

Tu H. I. F. Viti, H. J. van Zuylen Impacts of Traffic Accidents on Travel Time Reliability of Freeways Corridors [Conference]. - Washington D.C. : Presented at 87th Meeting of the Transportation Research Board, 2008.

Tu H. J. van Lint, H.J. van Zuylen The Impact of Traffic Flow on Travel Time Variability of Freeway Corridors [Journal]. - Washington D.C. : Transportation Research Board, 2007.

Van Aerde M. H. Rakha Multivariate Calibration of Single-Regime Speed-FlowDensity Relationships [Journal] // Vehicle Navigation and Information Conference (VNIS)-IEEE. - Piscataway N.J. : [s.n.], 1995. - Vol. USA 95CH35776. - pp. 334-341.

Van Lint H. O. Miete, H. Taale A Systematic Framework for the Assessment of Traffic Measures and Policies on the Reliability of Traffic Operations and Travel Time [Journal]. - Washington D.C. : TRansportation Research Board, Natioanl Science Council, 2012.

WeatherUnderground Weather History [Online]. - April 2012. - http://www.wunderground.com/history/.

Zhang L. D. Levinson Some Properties of Flows at Freeway Bottlenecks [Journal]. - Washington D.C. : Transportation Research Record, National Research Council, 2004. - Vols. 1883 pp. 122-131.

APPENDICES

APPENDIX A

The data fusion related codes in Excel VBA platform:

```
Private Const C_RADIUS_EARTH_KM As Double = 6370.97327862
Private Const C_RADIUS_EARTH_MI As Double = 3958.73926185
Private Const C_PI As Double = 3.14159265358979
'Public trafficData() As varaint
'Public weatherData() As Variant
'Public incidentData() As Variant

Function GreatCircleDistance(Latitude1 As Double, Longitude1 As Double, _
        Latitude2 As Double, Longitude2 As Double, _
        ValuesAsDecimalDegrees As Boolean, _
        ResultAsMiles As Boolean) As Double

Dim Lat1 As Double
Dim Lat2 As Double
Dim Long1 As Double
Dim Long2 As Double
Dim X As Long
Dim Delta As Double

If ValuesAsDecimalDegrees = True Then
   X = 1
Else
   X = 24
End If

' convert to decimal degrees
Lat1 = Latitude1 * X
Long1 = Longitude1 * X
Lat2 = Latitude2 * X
Long2 = Longitude2 * X

' convert to radians: radians = (degrees/180) * PI
Lat1 = (Lat1 / 180) * C_PI
Lat2 = (Lat2 / 180) * C_PI
Long1 = (Long1 / 180) * C_PI
Long2 = (Long2 / 180) * C_PI

' get the central spherical angle
Delta = ((2 * ArcSin(Sqr((Sin((Lat1 - Lat2) / 2) ^ 2) + _
   Cos(Lat1) * Cos(Lat2) * (Sin((Long1 - Long2) / 2) ^ 2)))))

If ResultAsMiles = True Then
   GreatCircleDistance = Delta * C_RADIUS_EARTH_MI
```

```
Else
   GreatCircleDistance = Delta * C_RADIUS_EARTH_KM
End If

End Function

Function ArcSin(X As Double) As Double
   ' VBA doesn't have an ArcSin function. Improvise.
   ArcSin = Atn(X / Sqr(-X * X + 1))
End Function

Public Function TimeSerial(serialNumber As Long) As Long

Dim YY, MM, DD, HH, QQ As Double

YY = Right(Str(Year(serialNumber)), 2)

MM = Month(serialNumber)
DD = Day(serialNumber)
HH = Hour(serialNumber)
QQ = Minute(serialNumber)

TimeSerial = YY * 100000000 + MM * 1000000 + DD * 10000 + HH * 100 + QQ

End Function

Public Sub InsertIncidentData()

Dim numberTraffic, numberWeather, numberIncident As Single

Dim startIncident, endIncident, currentTime  As Long
Dim durationIncident, typeIncident As String
Dim distanceIncident As Double
Dim ifUpstream As Boolean
Dim vehiclesInvolved As Integer
Dim maxLanesClosed As Integer

Sheets("all").Activate

numberTraffic = ActiveSheet.Cells(3, 1)
numberWeather = ActiveSheet.Cells(3, 7)
numberIncident = ActiveSheet.Cells(3, 14)

For i = 2 To numberIncident

   Sheets("all").Activate
   startIncident = ActiveSheet.Cells(i + 1, 16)
   endIncident = ActiveSheet.Cells(i + 1, 17)
```

```
    durationIncident = ActiveSheet.Cells(i + 1, 18)
    distanceIncident = ActiveSheet.Cells(i + 1, 19)
    typeIncident = ActiveSheet.Cells(i + 1, 20)
    ifUpstream = ActiveSheet.Cells(i + 1, 21)
    vehcilesInvolved = ActiveSheet.Cells(i + 1, 22)
    maxLanesClosed = ActiveSheet.Cells(i + 1, 23)

    Sheets("result").Activate

    With ActiveSheet
        For j = 1 To numberTraffic

        currentTime = .Cells(j + 1, 2)

        If currentTime >= startIncident And currentTime < endIncident Then

            .Cells(j + 1, 6) = startIncident
            .Cells(j + 1, 7) = endIncident
            .Cells(j + 1, 8) = durationIncident
            .Cells(j + 1, 9) = distanceIncident
            .Cells(j + 1, 10) = typeIncident
            .Cells(j + 1, 11) = ifUpstream
            .Cells(j + 1, 12) = vehiclesInvolved
            .Cells(j + 1, 13) = maxLanesClosed

        'ElseIf startIncident < .Cells(j + 1, 2) And endIncident < .Cells(j + 1, 2) Then Exit For

        End If
      Next j

    End With

  Next i
  End Sub


Public Sub insertWeatherData()

Dim numberTraffic, numberWeather, numberIncident As Single

numberTraffic = Sheets("all").Cells(3, 1)
numberWeather = Sheets("all").Cells(3, 7)
numberIncident = Sheets("all").Cells(3, 14)

Dim startWeather, endWeather, currentTime As Long
Dim Percipitation, Visibility, Temprature As Integer
Dim Condition As String
Dim lastVisited, i, j  As Long
```

```
lastVisited = 1

For i = 1 To numberWeather

   Sheets("All").Activate

   With ActiveSheet
         startWeather = .Cells(i + 2, 9)
         endWeather = .Cells(i + 3, 9)
         Percipitation = .Cells(i + 2, 10)
         Condition = .Cells(i + 3, 11)
         Visibility = .Cells(i + 2, 12)
         Temprature = .Cells(i + 2, 13)
   End With

   Sheets("Result").Activate

   For j = lastVisited To numberTraffic

      With ActiveSheet

     currentTime = .Cells(j + 1, 2)

        If currentTime >= startWeather And currentTime < endWeather Then

          .Cells(j + 1, 15) = startWeather
          .Cells(j + 1, 16) = endWeather
          .Cells(j + 1, 17) = Percipitation
          .Cells(j + 1, 18) = Condition
          .Cells(j + 1, 19) = Visibility
          .Cells(j + 1, 20) = Temprature
        End If
      End With
      If currentTime > endWeather Then

        lastVisited = j
        GoTo exitFor

        Exit For

      End If


   Next j

exitFor:
```

```
Next i
End Sub



Public Sub GroupObs()

' This Procedure Groups Observations to observations which each of them have 200 vehicles.


Dim oldVolume(6884) As Double
Dim oldSpeed(6884) As Double
Dim newVolume(5000) As Double
Dim newSpeed(5000) As Double
Dim currentOldVolume As Double
Dim currentNewVolume As Double
Dim currentOldSpeed As Double
Dim currentNewSpeed As Double
Dim currentVolumeSum, currentSpeedSum As Double
Dim currentOldIndex As Integer
Dim currentNewIndex As Integer
Dim currentSum As Double
Dim speedSum As Double
Dim counter As Integer

Sheets("Analysis").Activate


For i = 1 To 6884

   oldVolume(i) = ActiveSheet.Cells(1 + i, 5)
   oldSpeed(i) = ActiveSheet.Cells(1 + i, 3)

Next i


currentOldIndex = 1
currentNewIndex = 1
counter = 0

Do While currentOldIndex <= 6884

   currentOldVolume = oldVolume(currentOldIndex)
   currentOldSpeed = oldSpeed(currentOldIndex)

   currentVolumeSum = currentVolumeSum + currentOldVolume
```

```
    currentSpeedSum = currentSpeedSum + (currentOldVolume * currentOldSpeed)

    counter = counter + 1

    If currentVolumeSum >= 200 Then

        'Calculate f

        f = (currentOldVolume - (currentVolumeSum - 200)) / currentOldVolume

        'Calculate Adjusted Vehciel Counts

        newVolume(currentNewIndex) = 200 / (counter + f - 1)

        'Calculate Adjusted Speed

        newSpeed(currentNewIndex) = (currentSpeedSum - ((1 - f) * currentOldSpeed * currentOldVolume)) / 200

        counter = 0
        currentVolumeSum = 0
        currentSpeedSum = 0
        f = 0

        currentOldIndex = currentOldIndex + 1
        currentNewIndex = currentNewIndex + 1

      Else

       currentOldIndex = currentOldIndex + 1

     End If


Loop


'Printing The Output


For i = 1 To currentNewIndex

    ActiveSheet.Cells(1 + i, 7) = newSpeed(i)
    ActiveSheet.Cells(1 + i, 8) = newVolume(i)

Next i
End Sub
```

APPENDIX B

B1. RITIS Data

Four major data sources used in this process are listed below. Each of these data sources will be explained in more details in the following section.

1-Traffic Data (RITIS)

2-Incident Data (RITIS)

3-Weather Data (Weather Underground)

4-Facility Geometry Information (Google Map and Google Earth ®)

B1.1 RITIS Traffic Data

Regional Integrated Transportation Information System (RITIS) archives data from Traffic Management Centers (TMC). The database also has a user friendly online interface which provides detail information. As interest of this study, it archives incidents and work zones event logs. The detail of each incident and work zone is accessible via detector tool under data archive menu. User can request a query using detector tool. When the query process is finished a notification email will be send to the user. The notification email also includes the direct link for data download.

Traffic data in RITIS are captured from more than 100 sensors across DC, Maryland, and Northern Virginia. This database is the principal database which will be updated at the end of the process. All the fields in this database will be kept and more explanatory fields of weather and incident are added accordingly.

A sample traffic data file (provided in ".csv" format) may include up to 9 fields as follow:

1- Date and Time: Date and time of when the sensor recorded traffic information.

2- Sensor Location: This filed identifies sensor location in sentence format. It usually comes up with a mile post describing the location of the incident.

3- Direction: The direction of which data was collected like (South/North) or (East/West)

4- Sensor Latitude: Latitude position of the sensor in decimal format.

5- Sensor Longitude: Longitude position of the sensor in decimal format

6- Vehicle Count (in specific time interval): Total number of vehicles passing the sensor in a specific time interval. The observation is aggregated for all lanes. The data collection interval is fixed to 15-minute period..

7- Vehicles per Hour: Total number of vehicles converted to hourly rate. This value is integrated for all lanes of the facility at the sensor location.

8- Speed (mph): Speed of vehicle passing the sensor in mile per hour.

9- Occupancy (%): Occupancy percentage of the sensor.

B1.2 RITIS Incident Data

Similar to traffic data incident data is provided in ".csv" format. The incident database usually has 15 fields as follow:

1-System: This field corresponds to the agency which provided the data. It can be Northern Virginia (Open TMS), VaTraffic, or Maryland (CHART ATMS)

2-Standardized Type: This field depicts the type of incident or event. It is called "Standard" because it is similar between different agencies. There are 10 predefined categories for event

type as follow: 1-Accident, 2-Construction Work, 3-Debris on Roadway, 4-Disabled Vehicle, 5- Road Maintenance Operations, 6-Road Marking Operations, 7-Road Widening, 8-Incidents, 9-Obstructionsrain, 10-Traffic Congestion. The standardized incident type may vary from site to site and sensor to sensor.

3- Agency Specific Type: This field is similar to "Standardized Type" field but it varies by different agencies and thus is not useful for research purposes.

4-Location: Estimated location of an event is named in string format. Some example of this field value are "SB 395 SO PENTAGON 9MM" and "I-395N north".

5-Time Opened: start time of an incident

6-Time Closed: end time of an incident

7-Duration: duration of an incident

8-Latitude: latitude position of the start point of an incident

9-Longititude: longitude position of the start point of an incident

10-County: the county which incident has occurred in. For example "Wake County"

11-Vehicles Involved: number of vehicles involved in an incident.

12-Max Lanes Closed: maximum number of lanes closed in blockage duration of an incident. If maximum number of lanes closed equals to 1 then the shoulder has been closed. It should be noted that a limitation of the incident data is that it only shows maximum number of blocked lanes and does not depict the full characteristics of incidents. It should be noted that there are three more fields of "Operator Notes", "Notification Sent", and "On-Scene Responders" which do not contain value for research purposes.

B1.3 Weather Data

The weather data are extracted from a web-based database named Weather Underground. Weather Underground website provides weather data for Almost 2,000 Automated Surface Observation System (ASOS) stations located at airports throughout the country. These are maintained by the Federal Aviation Administration (FAA) and observations are updated hourly or more frequently when adverse weather affecting aviation occurs (low visibility, precipitation, and etc.). The website also covers over 14,000 Personal Weather Stations (PWS's). However, PWS's are not certified by an official agency. In this regard the selected data collection sites should be close to an airport to assure weather accuracy

The weather data (presented in ".csv" format) contains the following fields:

1- Date and Time: the weather condition recording time intervals are varied based on the change in weather but no longer than 1 hour. In other words, if the weather status changes sooner than an hour, a new record will be added to the database, otherwise, regular hourly observation will be recorded.

2- Temperature: temperature at the time of data recording provided both in Fahrenheit and Celsius degrees.

3- Precipitation: the amount of precipitation in inches/hour at the observation interval.

4- Weather Category: the Weather Underground website uses different weather categories to classify the weather condition for every record in the database. These weather categories are presented in alphabetic order here:

    a. Blowing Snow
    b. Clear

c. Drizzle
d. Fog
e. Funnel Cloud
f. Hail
g. Haze
h. Heavy Drizzle
i. Heavy Freezing Rain
j. Heavy Ice Pellets
k. Heavy Rain
l. Heavy Snow
m. Heavy Thunderstorms and Rain
n. Heavy Thunderstorms with Small Hail
o. Ice Pellets
p. Light Drizzle
q. Light Freezing Drizzle
r. Light Freezing Fog
s. Light Freezing Rain
t. Light Ice Pellets
u. Light Rain
v. Light Rain Showers
w. Light Snow
x. Light Thunderstorms and Rain
y. Light Thunderstorms and Snow
z. Mist
aa. Mostly Cloudy
bb. Overcast
cc. Partly Cloudy
dd. Patches of Fog
ee. Rain
ff. Scattered Clouds
gg. Shallow Fog
hh. Smoke
ii. Snow
jj. Squalls
kk. Thunderstorm
mm.Thunderstorm and Ice Pellets
nn. Thunderstorm and Rain
oo. Thunderstorms with Hail
pp. Thunderstorm with Small Hail
qq. Unknown
rr. Widespread Dust
ss. Visibility

5- Visibility: the visibility condition is reported in numeric format from 1 to 10. The value of 1 represents low visibility and 10 represents the highest level of visibility.

11. Humidity: humidity percentage at the observation period in percentage format.
12. Wind Direction: the direction of wind at the recording time.
13. Wind Speed: the speed of wind at the observation period in miles per hour.
14. Sea Level Pressure: the observed sea level pressure in inches.

The weather data are extracted from sensors in airports since these sensor are certified by Federal Aviation Association (FAA). The latitude and longitude of the sensors are not provided in the data file but they are available from the airport website.

B1.4 Google Map and Google Earth

All the information explained above are meaningful in a limited spatial scope. In order to analyze the impact of weather and incident on freeway traffic stream, a section of the freeway should be selected. This section of the freeway is referred to as the facility under study. For further analysis on facility under study, basic information regarding the facility under study like geometry, segmentation, ramp locations, and number of lanes at each segment can be gathered using Google Map or Google Earth applications.

B2. Selected Study Site

The selected site is a section of I-95 near Baltimore in Maryland State. The data have been extracted from two pairs of sensors for year 2011.

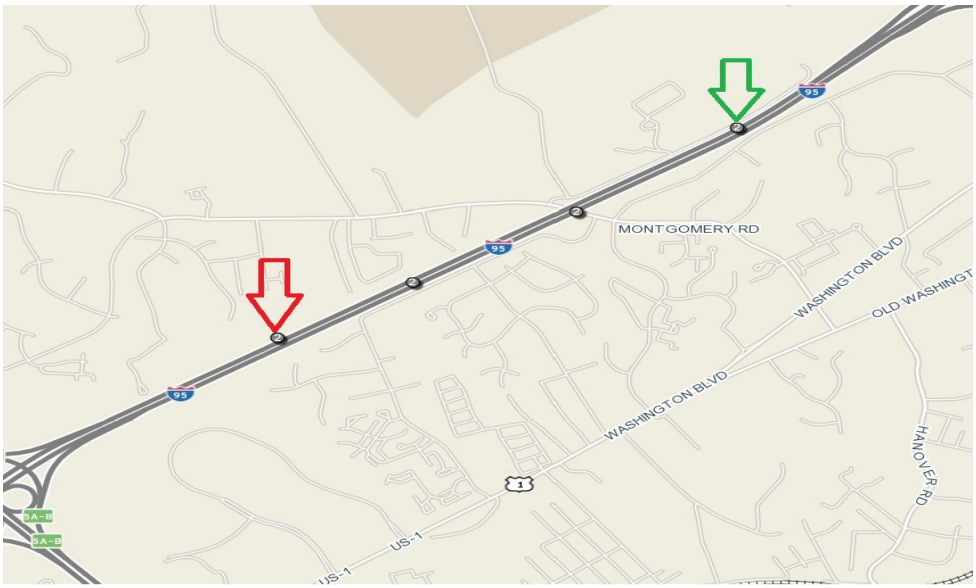

Figure 63 Selected Study Site near Baltimore (Source: www.ritis.org)

The site is close to Baltimore-Washington airport, which means accurate weather data, can be extracted using weather underground website. Also both sensors are located at basic segments since the nearest ramp is almost 2500 ft. in distance (upstream and downstream). The location of sensors is provided in latitude and longitude thus a relative distance to the incidents can be measured. The following table summarizes sensor information:

Table 43 Sensors Identification

Zone ID	Name	Direction	Detector Type	Latitude	Longitude
0_3267	I-95@0.92 Mile South of River Rd.	North	Microwave	39.21603	-76.73084
0_3266	I-95@0.92 Mile South of River Rd.	South	Acoustic	39.21603	-76.73084
0_3344	I-95 @ 0.86 Mile South of Montgomery Rd	North	Microwave	39.20529	-76.7526
0_3343	I-95 @ 0.86 Mile South of Montgomery Rd	South	Acoustic	39.20529	-76.7526

The facility has four lanes at each direction. It also includes two shoulder lanes at each side. The median is a grass median about 30 ft. in length which is protected by a wire barrier. Figure 63 and Figure 64 demonstrate Google Earth view of the study site.

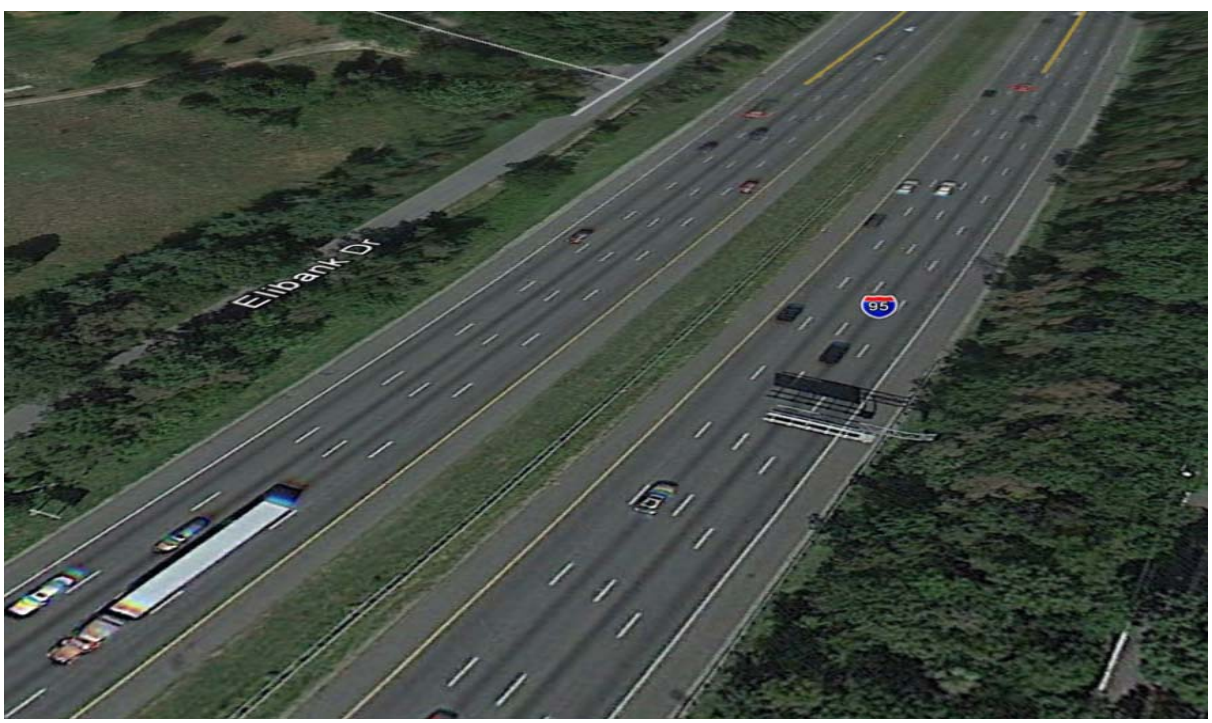

Figure 64 Google Earth Image of the Study Site (Source: Google Earth)

The Montgomery Rd. crosses the I-95 freeway with a bridge. The distance between the sensors to the nearest ramp is greater than 2,000 ft. and there is a 7,329 ft. distance between the sensors.